CHARACTERIZATION OF RAN-BINDING PROTEIN 6 AS A NOVEL REGULATOR OF THE EPIDERMAL GROWTH FACTOR RECEPTOR

A Dissertation

Presented to the Faculty of the Weill Cornell Graduate School

of Medical Sciences

In Partial Fulfillment of the Requirements for the Degree of

Doctor of Philosophy

by

Wan-Ying Hsieh

May 2018

CHARACTERIZATION OF RAN-BINDING PROTEIN 6 AS A NOVEL REGULATOR OF THE EPIDERMAL GROWTH FACTOR RECEPTOR

Wan-Ying Hsieh, Ph.D.

Cornell University 2018

The epidermal growth factor receptor (EGFR) regulates many key biological processes including cell proliferation, survival and differentiation. It is frequently altered or amplified in cancers. Regulation of physiological EGFR function occurs at multiple levels, such as negative feedback regulation. We previously identified RAN-Binding Protein 6 (RanBP6), a protein of unknown functions, as a candidate EGFR interactor from an EGFR interactome study. Here, we validated that RanBP6, a member of the importin β superfamily, interacts with EGFR and the proteins involved in nucleo-cytoplasmic transport. In addition, depletion of RanBP6 raised EGFR mRNA and protein levels, and upregulated EGFR promoter activity. Further studies revealed that RanBP6 represses EGFR transcription by modulating the subcellular localization of Signal transducer and activator of transcription 3 (STAT3). Focal deletions of the *RANBP6* locus on chromosome 9p were found in a subset of glioblastoma (GBM). Silencing of RanBP6 promoted glioma growth *in vivo* and conferred resistance to EGFR tyrosine kinase inhibitors. Lastly, examination of RanBP6 substrates suggested RanBP6 is an importin for many tumor suppressors or oncoproteins. Our results demonstrated that RanBP6 functions as a novel EGFR feedback regulator to maintain EGFR homeostasis, and an importin for cancer-associated cargoes.

BIOGRAPHICAL SKETCH

Wan-Ying Hsieh was born in Taipei, Taiwan and was raised by her parents Henry Hsieh and Jenny Huang, with an older brother, Steven. She went to Taipei First Girls' High School, where she first became passionate about science. She then joined National Sun Yat-sen University in Taiwan, and graduated with a Bachelor's degree in Biological Sciences with a focus on molecular biology. She then studied abroad and earned a Master's degree in Biotechnology at Columbia University, New York, where she investigated the molecular pathogenesis of diffuse large B cell lymphoma in Dr. Owen O'Connor's laboratory. To further advance her understanding in biomedical sciences, she joined a vascular biology lab as a research assistant, where she studied tumor angiogenesis and vascular inflammation in Dr. Timothy Hla's laboratory at Weill Cornell Medical College. With her strong research interest in understanding the biochemical mechanisms of Receptor Tyrosine Kinase signaling and its impact on cancer cells, she applied to the Ph.D. program in Pharmacology at Weill Cornell, and joined Dr. Ingo Mellinghoff's laboratory to work on dissecting signaling pathways of the epidermal growth factor receptor in cancer.

During her graduate study, she was awarded the best presenter prize of the year from a school-wide symposium at her Graduate School (2013, Vincent du Vigneaud Award of Excellence), won two travel awards from the American Society for Cell Biology (2015 and 2017) and received a Scholar-in-Training Award from the American Association of Cancer Research (2017). Furthermore, she applied and was awarded a research grant from the U.S. Department of Defense (FY15 Horizon Award) as a principal investigator to fund her recent Ph.D. work. She was featured on the Cornell Website for this prestigious honor.

In her leisure time, she enjoys travelling across the U.S. She has been to 35 National Parks, including 29 in the U.S. and 6 in Canada[*]. She enjoys planning the itineraries, hiking, wildlife viewing/bird watching, stargazing, and photography[#].

[*] (U.S.) Acadia, Arches, Big Bend, Bryce Canyon, Canyonlands, Capitol Reef, Carlsbad Caverns, Channel Islands, Death Valley, Denali, Everglades, Grand Canyon, Grand Teton, Great Sand Dunes, Great Smoky Mountains, Guadalupe Mountains, Joshua Tree, Katmai, Kenai Fjords, Kings Canyon, Mount Rainier, Olympic, Rocky Mountain, Sequoia, Shenandoah, Wrangell-St. Elias, Yellowstone, Yosemite, Zion
(Canadian) Banff, Glacier, Jasper, Kootenay, Revelstoke, Yoho

[#] Mainly landscape, partially wildlife, no astrophotography, definitely no portrait

To my parents

ACKNOWLEDGMENTS

I would like to thank my mentor Dr. Ingo Mellinghoff for his constant support, guidance, enthusiasm and encouragement. Dr. Mellinghoff trained me how to think critically about my experimental design and how to interpret my data as a scientist. He advanced my education by helping me improve my skills in grant writing and literature critiques. I am very grateful that he provided an excellent research environment with numerous resources, where I could pursue any interesting question with a legitimate proposal.

I would also like to thank my thesis committee members, Dr. John Blenis, Dr. Neal Rosen, and Dr. Alan Hall (deceased) for their guidance and suggestions on my thesis project over the years. In addition, I would like to thank Dr. Yueming Li and Dr. Emily Cheng, for being on my exam committee and their critical review on my work. I am truly grateful because they have spent substantial efforts and time on improving the quality of my research, as well as giving me career advice.

I would like to thank my former PI, Dr. Timothy Hla, for teaching me how to purify recombinant protein and the basics of protein biochemistry, which were instrumental for my Ph.D. study. I also want to thank my collaborators, Dr. Barbara Oldrini and Dr. Hediye Erdjument-Bromage for their contributions to perform the initial screen of the EGFR interactome, Dr. Massimo Squatrito for his contributions in computational analyses of cancer cell lines from Cancer Cell Line Encyclopedia, and the *in vivo* glioma mouse model, Dr. Nicolas Lecomte for teaching me how to 3D culture pancreatic organoids, Dr. Steven Leach for generously sharing their murine pancreatic organoids with us, Craig Bielski and Dr. Barry Taylor for assisting our genomic

analysis of *RANBP6*, Dr. Yueming Li for sharing his AKTA purifier with us, and Dr. Eitan (Wan Fung) Wong for his assistance in setting up FPLC columns and problem-solving. Furthermore, I am very grateful to collaborate with Dr. Henrik Molina and Caitlin Steckler from the Mass Spectrometric Core Facility in Rockefeller University for screening the RanBP6 interactome and substrates.

I would like to thank my current and past lab members, and Pharmacology fellow graduate students. I specifically want to thank our lab manager Carl Campos. Carl is always there to give me extra help for both *in vitro* and *in vivo* work, weekdays or weekends. He assisted me to collect 5 billion HeLa cells for a proteomic study I set up (Chapter 6). Without his assistance, I would have worked 18 hours instead of 13 hours on that day. I would also like to thank Dr. Paolo Codega for his assistance in immunofluorescence staining, Dr. Daniel Rohle for teaching me how to do 3D soft agar assays, Dr. Igor Vivanco and Dr. Donna Nichol for answering my scientific questions, and our former and current lab assistants Bridget King and Susan Zhen. I would especially like to thank Sarah Tang. She's always there to share my happiness and sorrow, my success and setbacks, and my scientific thoughts and personal life.

I would like to thank my family and friends, who were extremely supportive during my graduate study. I would not be able to achieve this much without their infinite love. Although my family and I usually have 12-13 hours time difference, I never felt distant from them. My brother Steven always had time to listen to me, encouraged me and gave me advice. I am truly thankful to have someone I can always speak with. I would like to express my special thanks to Zhen Chen, who always challenged me with difficult scientific questions and enlightened me from the first day we met. I have noticed my growth over time with him, and I'm truly grateful to have him in my life.

Lastly, I would like to thank our funding agencies, including National Brain Tumor Society, National Institutes of Health, the U.S. Department of Defense, MSKCC Core Grant, the Geoffrey Beene Cancer Research Foundation, and the Cycle for Survival Grant. This work would not be possible without these generous funds.

TABLE OF CONTENTS

LIST OF FIGURES

LIST OF TABLES

CHAPTER 1

INTRODUCTION

1.1 Overview of EGFR signaling

The epidermal growth factor receptor (EGFR) is a receptor tyrosine kinase (RTK) that belongs to the ERBB family, which includes three other members (ERBB2/HER-2, ERBB3/HER-3 and ERBB4/HER-4) (Hynes and Lane, 2005). These receptors are localized on the cell membrane, and share a similar domain architecture comprised of an extracellular ligand-binding domain, a hydrophobic transmembrane region, and an intracellular tyrosine kinase domain. These receptors are expressed in various tissues of epithelial, mesenchymal and neuronal origins. Under normal physiological conditions, activation of these receptors is regulated by spatial and temporal expression of their ligands. Known EGFR ligands include epidermal growth factor (EGF), transforming growth factor-α (TGF-α), amphiregulin (ARG), epigen (EGN), heparin-binding EGF-like growth factor (HB-EGF), epiregulin (EPR) and batacellulin (BTC). The latter three are known as bi-specific ligands that regulate both EGFR and ERBB4 (Yarden and Sliwkowski, 2001).

The extracellular region of EGFR is composed of four domains: Domain I (amino acids 1-165), domain II (amino acids 165-310), domain III (amino acids 310-480), and domain IV (amino acids 480-620) (Lemmon et al., 2014). Domains I and III share high sequence homology and are the interfaces responsible for bivalent ligand binding. Domain II and IV also share high sequence homology. Domain II is the dimerization arm. It is buried by intramolecular autoinhibitory interaction with Domain IV under steady state but induces a dramatic conformational change in response to ligand binding. With the domain II dimerization arm exposed to the ligands, the extracellular

region of EGFR then dimerizes (Burgess et al., 2003). This further brings the intracellular tyrosine kinase domains into close proximity to form the asymmetric dimer that leads to kinase activation (Zhang et al., 2006). For the asymmetric dimer, one monomer serves as an "activator" and the other serves as a "receiver" to allosterically activate and trans-phosphorylate tyrosines in the tail of the activator. This creates docking sites for cytoplasmic proteins containing Src homology 2 (SH2) domain or phosphotyrosine-binding (PTB) domain (Wagner et al., 2013). These adaptor proteins bind to specific phosphotyrosine residues and activate the downstream signaling, including mitogen-activated protein kinase (MAPK), phosphatidylinositol 3-kinase (PI3K), the guanine nucleotide exchange factor of Ras-related Ral proteins (RalGDS), and phospholipase Cγ (PLC γ) (Fig. 1-1).

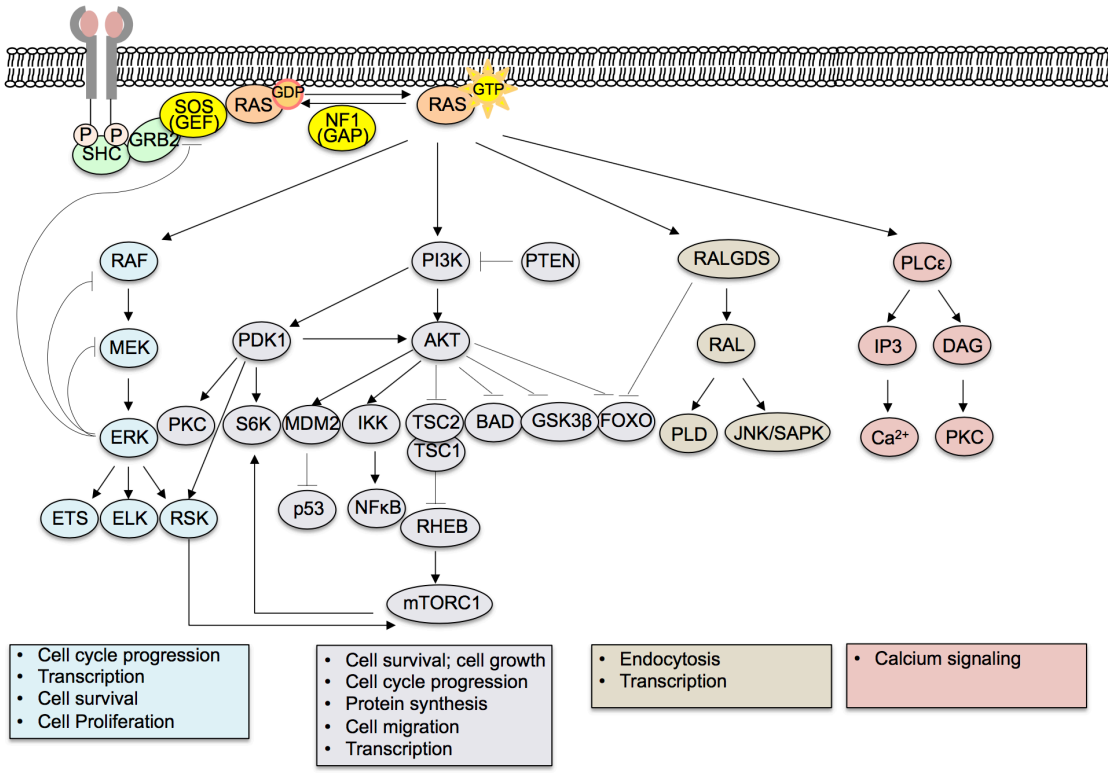

Figure 1-1. Cartoon illustrates EGFR signaling.
Ligand-induced activation of EGFR activates downstream signaling through the adaptor proteins that contain the SH2 or PTB domains (shown in green). Recruitment of RAS to the membrane further activates the signaling cascades, including MAPK (shown in blue), PI3K (shown in purple), RalGDC (shown in olive), and PLC γ (shown in pink).

The RAS-RAF-MEK-ERK cascade

Following autophosphorylation at Y1068 or Y1086, EGFR kinase recruits the SH2-containing protein GRB2 to the cell membrane, where it directly binds to SOS, a guanine nucleotide exchange factor (GEF) of RAS that charges RAS with GTP (Hynes and Lane, 2005). In addition, autophosphorylation at Y1148 and Y1173 of EGFR kinase binds to the PTB domain via the adaptor protein SHC, which recruits GRB2/SOS complex and activates the RAS-MAPK pathway through the GTP-loaded RAS. The farnesylated membrane-bound RAS directly interacts with the RAF kinase, resulting in the relocalization of RAF from the cytoplasm to the plasma membrane

(Moodie et al., 1993; Stokoe et al., 1994; Vojtek et al., 1993; Warne et al., 1993; Zhang et al., 1993), where it promotes the phosphorylation and activation of mitogen-activated protein kinase kinases 1 and 2 (MEK1/2). These kinases are capable of phosphorylating and activating the mitogen-activated protein kinases, MAPKs, also known as extracellular signal regulated kinases 1 and 2 (ERK1/2) (Leevers and Marshall, 1992). The known substrates for ERK1/2 include cytoplasmic proteins such as p90 ribosomal S6 kinase (RSK) (Wood et al., 1992), and transcription factors such as E26 transformation-specific (ETS) and ETS domain-containing protein (ELK) (Yordy and Muise-Helmericks, 2000). In addition to the linear activation of RAS-ERK, ERK also negatively regulates MEK (Lito et al., 2012), RAF (Dougherty et al., 2005), and SOS (Douville and Downward, 1997). Taken together, the RAS-ERK cascade is crucial in promoting cell cycle progression, cell survival and proliferation.

The PI3K-AKT-mTORC cascade

RAS-GTP directly binds and allosterically activates the lipid kinase, phosphatidylinositol 3-kinase (PI3K) (Rodriguez-Viciana et al., 1994). PI3K can be recruited to the growth factor receptors directly or indirectly through other docking proteins, including insulin receptor substrate (IRS) or GRB2-associated binder (GAB) in a RAS-independent manner. PI3K is composed of a regulatory p85 subunit that is responsible for the anchorage to EGFR docking sites and a catalytic p110 subunit for generating the second messenger phosphatidylinositol 3,4,5-trisphosphate (PIP3) (Hiles et al., 1992; Whitman et al., 1988). The enzymatic activity of PI3K is reversed by the tumor suppressor- Phosphatase and tensin homolog (PTEN), which de-phosphorylates PIP3 to phosphatidylinositol 4,5-bisphosphate (PIP2) (Maehama and Dixon, 1998). The membrane-bound PIP3 recruits many proteins by binding to their pleckstrin homology (PH) domain. These proteins include the serine/threonine kinases

AKT, also known as protein kinase B, 3-phosphoinositide-dependent kinase 1 (PDK1), and the phosphatase PH domain and leucine rich repeat protein phosphatase (PHLPP). The membrane-bound AKT is fully activated through phosphorylation by PDK1 on T308 residue, and by the rapamycin-insensitive mammalian target of rapamycin (mTOR) complex (mTORC2) on S473 residue. Activated AKT is dephosphorylated by PHLPP (Manning and Cantley, 2007).

The activated AKT phosphorylates a wide range of substrates that are important for cell growth, proliferation and survival though various mechanisms. Known AKT substrates include tuberous sclerosis complex 1 and 2 (TSC1/2), a heterodimeric complex and an important tumor suppressor. TSC2 contains a GTPase activating (GAP) domain, which is important for inactivating the small GTPase Ras homolog enriched in brain (RHEB). Phosphorylation of TSC complex by AKT releases its inhibition on RHEB and subsequently allows RHEB to activate mTORC1 (Sengupta et al., 2010). Phosphorylation of mTORC1 activates the serine/threonine kinase p70-S6 kinase (S6K) and eukaryotic initiation factor 4E binding protein 1 (4EBP1), which are crucial for translation initiation and elongation through phosphorylating multiple substrates (Ma and Blenis, 2009). In addition, activated AKT has inhibitory effects on the serine/threonine kinase Glycogen Synthase Kinase-3 (GSK3β) that modulates glucose metabolism and cell cycle regulatory proteins (Cross et al., 1995), the transcription factor FOXO family which promotes apoptosis (Matsuzaki et al., 2003), and the pro-apoptotic protein BAD (Datta et al., 1997). Furthermore, activated AKT also has stimulatory effects on IKKα, which drives the nuclear localization of NFκB in promoting the transcription of pro-survival genes (Dan et al., 2008). Moreover, phosphorylation of MDM2 by AKT enhances its E3 ligase-mediated ubiquitylation and degradation of p53 (Ogawara et al., 2002), a tumor suppressor that promotes

apoptosis. Taken together, the RAS-PI3K-AKT pathway is important for cell growth, survival, and proliferation.

Ligand-induced EGFR endocytosis

Signaling from activated EGFR, including the cascades, occurs mostly from the plasma membrane, and receptor endocytosis is thought to terminate the activated receptor from cytosolic organelles (Brankatschk et al., 2012; Sousa et al., 2012). Adaptor proteins such as AP-2, which contains a PIP2-binding domain, mediate the binding of clathrin to plasma membranes (Abe et al., 2008; Sun et al., 2007). This multimeric protein is crucial for the formation of clathrin-coated pits at the plasma membrane and for the endocytosis of EGFR. Ligand binding to EGFR induces receptor dimerization and autophosphorylation of the kinase domains, allowing the SH2-containing protein E3 ubiquitin ligase CBL to bind to Y1045 of EGFR directly (Jiang and Sorkin, 2003), or indirectly through GRB2 (Jiang et al., 2003). Recruitment of CBL results in mono- and polyubiquitylation (polyUb) of the EGFR tail (Huang et al., 2006), and the polyUb-attached tails interact with Ub-interaction motifs-containing proteins epsin-1 and Eps15 (Hofmann and Falquet, 2001). Given that Eps15 is localized at the rim of clathrin-coated pits, and that epsin-1 is localized along the clathrin coat, it has been demonstrated that Eps15 is responsible for initial contact of ubiquitylated EGFR while epsin-1 recruits EGFR into the central region of clathrin-coated pit (Stang et al., 2004; Tebar et al., 1996). The clathrin-coated membrane EGFR is then invaginated and released into the cytosol as a clathrin-coated vesicle.

These internalized receptors are further delivered to a compartment known as the early or sorting endosome. Upon sequential interaction with the endosomal sorting complex

required for transport (ESCRT) complex at the membrane of early endosomes, EGFR is then deubiquitylated and translocated to inner vesicles of endosomes (Hanson et al., 2009). The endocytosed receptors can either be recycled back to the plasma membrane or selected for lysosomal sorting by incorporation into small vesicles called the lumen of multivesicular bodies (MVBs) (Longva et al., 2002). By segregating the cytosolic substrates from EGFR kinase and promoting receptor degradation, lysosomal sorting is crucial for negatively regulating the anti-apoptotic signal mediated by EGFR (Hofmann and Falquet, 2001) (Fig. 1-2).

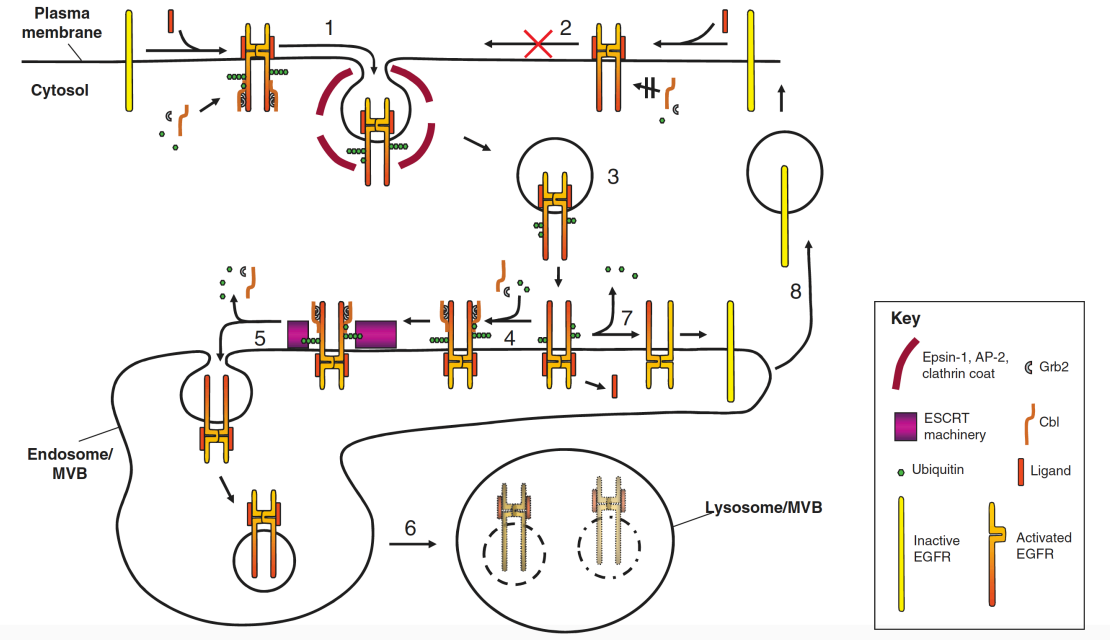

Figure 1-2. Cartoon illustrates EGFR endocytic trafficking.
Ligand-binding induced EGFR activation, ubiquitylation and recruitment into clathrin-coated pits (1). This process is inhibited when blocking ubiquitylation of activated EGFR (2). Once the activated EGFR is internalized (3), it is delivered to early endosomes (4). Through sequential interactions with the ESCRT complex on the early endosomes, EGFR is incorporated to inner vesicles of endosomes (5) and to the MVBs for lysosomal-mediated degradation (6). However, if the EGFR ligand dissociates at low pH, then EGFR is deactivated and deubiquitylated (7). As a result, EGFR is recycled back to the plasma membrane (8). Figure is adapted from (Madshus and Stang, 2009).

Alternative fates for endocytosed EGFR

Although sorting of activated EGFR for lysosomal degradation or recycling to the plasma membrane is fundamental to the regulation of EGFR signaling, alternative fates for activated EGFR emerged, including EGFR traffic to either the nucleus or the mitochondria (Liao and Carpenter, 2007). It has been shown that the full-length EGFR translocates to the nucleus from the endosomes and through Sec61β, a translocon on the ER upon EGF stimulation (Wang et al., 2010). Nuclear EGFR functions as a co-transcription factor of oncogenic Cyclin D1 (Lin et al., 2001), and it is associated with poor prognosis in breast cancer (Lo et al., 2006). It has been shown that EGFR enters to the nucleus through its nuclear localization sequence, with an association of the importin complex, proteins that are involved in the nucleo-cytoplasmic transport of macromolecules (Hsu and Hung, 2007). However, the mechanism for nuclear translocation of EGFR remains unclear. For instance, whether a chaperone or clathrin-mediated endocytosis is involved in the translocation of full-length EGFR to the nucleus is uncertain. In addition, EGFR transport to the mitochondria has been reported (Demory et al., 2009). Mitochondrial EGFR was discovered to play a role in regulating apoptosis by reducing cytochrome c oxidase subunit II (CoxII) activity and cellular ATP. However, the mechanism of how EGFR translocates to the mitochondria remains not fully defined.

EGFR signaling in cancer

Among these four members in the ERBB family, EGFR and ERBB2 are frequently involved in development of numerous types of human cancer (Hynes and Lane, 2005). Amplification and overexpression of EGFR through ligand-dependent or ligand-independent mechanisms have been described in multiple human cancers. In gliomas, EGFR overexpression is often accompanied by structural rearrangements that cause

in-frame deletions in the extracellular domain of the receptor, also known as EGFRvIII variant. This variant is unable to bind to ligands and results in constitutive activation of EGFR (Ekstrand et al., 1992). Mutations within the tyrosine-kinase domain of EGFR have been identified in non-small-cell lung cancer (NSCLC) patients. These NSCLC-associated EGFR mutants appear to disrupt their interactions with CBL, which results in a defect in ubiquitylation and degradation (Scaltriti and Baselga, 2006). In addition to glioma and NSCLC, mutations or amplifications of EGFR are also implicated in colorectal cancer, head and heck squamous-cell cancer, and renal-cell cancer (Hynes and Lane, 2005).

1.2 Inhibition of EGFR signaling

EGFR inhibitors

There are two types of anti-EGFR agents that have shown clinical activity and achieved regulatory approval for cancer therapies: monoclonal antibodies (mAbs) that target the extracellular domain of the receptor and small molecule ATP-competitive tyrosine kinase inhibitors (TKIs) that target the intracellular kinase domain (Vivanco and Mellinghoff, 2010). Currently, two mAbs (cetuximab and panitumumab) are approved by the FDA for the treatment of colorectal carcinoma (CRC) and squamous cell carcinoma of head and neck. Cetuximab is a chimeric mAb that recognizes an epitope in extracellular domain III of EGFR and blocks the ligand binding directly, while panitumumab is a fully humanized EGFR mAb that also binds to domain III.

For EGFR TKIs, there are three EGFR TKIs in clinical use today, including erlotinib, gefitinib, and lapatinib. All three of these compounds contain a 4-anilinoquinazoline scaffold and reversibly inhibit EGFR through ATP competition. Erlotinib have been approved for the treatment of advanced non-small cell lung cancer (NSCLC) and

pancreatic carcinoma (Yewale et al., 2013), while lapatinib is a dual ErbB2/EGFR inhibitor and is used for the treatment of HER2-positive breast cancer patients.

Feedback regulation of EGFR

There are two different types of negative regulators of EGFR, depending on their requirement for novel protein synthesis (Anastasi et al., 2016). Protein synthesis-independent feedback regulators are constantly present and bind to the receptor readily upon the activation of the RTKs (Waterman and Yarden, 2001). For example, the E3 ligase CBL binds to activated EGFR immediately upon ligand stimulation, which results in EGFR ubiquitylation and subsequent protein downregulation. However, protein synthesis-dependent feedback regulators require transcriptional activation that is regulated by EGFR signaling. These inducible feedback regulators of EGFR include ERBB receptor feedback inhibitor 1 (ERRFI1, also known as RALT or MIG6), Leucine-rich repeats and immunoglobulin-like domains protein 1 (LRIG1), and Suppressor of cytokine signaling 4/5 (SOCS4/5) (Anastasi et al., 2016). As many studies have provided compelling evidence to show that MIG6 negatively regulates EGFR by directly binding (Park et al., 2015; Zhang et al., 2007a), and MIG6 has a tumor suppressor function in different cancers (Maity et al., 2015; Zhang et al., 2007a; Zhang et al., 2007b), I will focus my subsequent discussions of negative regulator of EGFR on MIG6.

MIG6 interacts with ligand-activated ErbB RTKs directly through an evolutionarily conserved domain ErbB binding region (EBR) (Zhang et al., 2007a). The EBR interacts with the catalytically active ErbB receptors through the tyrosine kinase domain. Given that ERBB3 does not have a functional kinase domain, MIG6 does not

bind to ERBB3, but it can bind to ligand-driven ERBB2 and ERBB3 heterodimers, through the kinase domain of ERBB2.

Structural studies have shown that EBR consists of two modules, named segments 1 and 2 (hereafter referred to as S1 and S2) (Park et al., 2015). S1 binds to the C lobe of the EGFR tyrosine kinase domain (TKD) monomer after phosphorylation of Y395 of MIG6 by Src, while S2 contacts the peptide-substrate binding site of the EGFR TKD and is phosphorylated on Y394 by EGFR itself. Tyrosine phosphorylated S2 remains bound to the TKD active site, which prevents substrate phosphorylation and stabilizes the EBR and EGFR interaction. In summary, recruitment of MIG6 to EGFR TKD causes immediate termination of EGFR catalytic activity via peptide-substrate competition through S2 and prevents further allosteric activation of kinase dimers via S1 (Fig. 1-3).

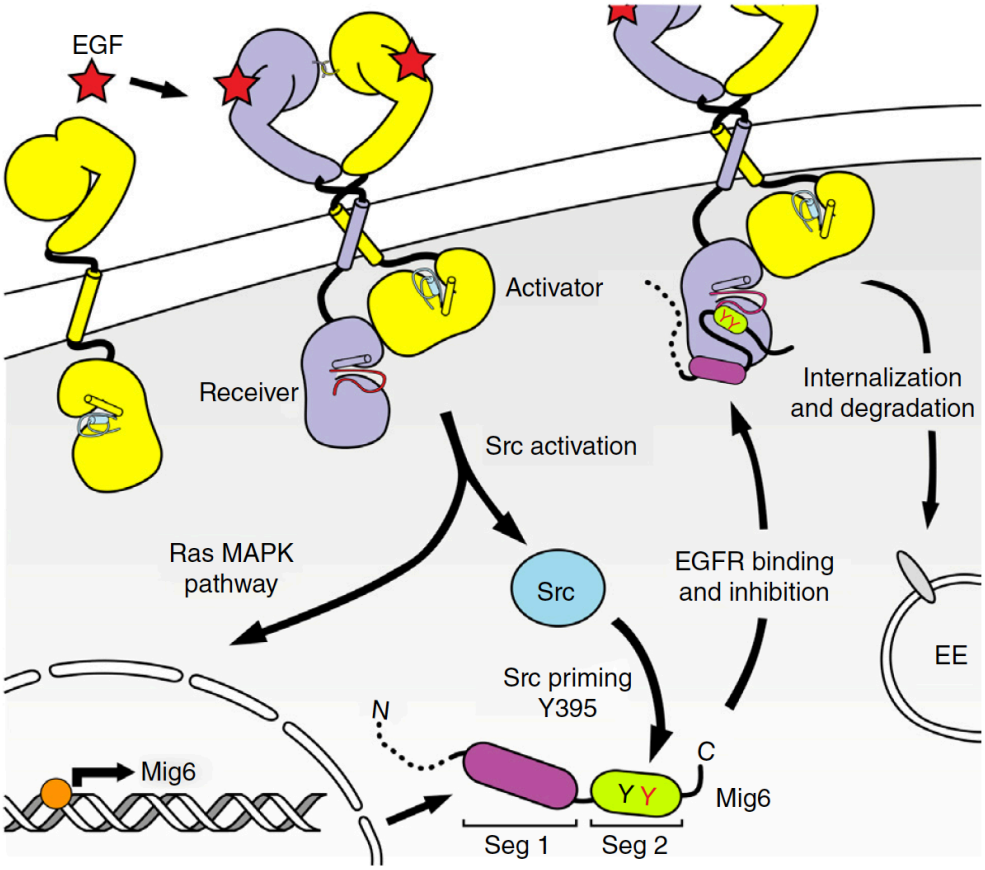

Figure 1-3 The feedback inhibition of EGFR by MIG6.
Ligand-binding activates EGFR signaling and induces expression of MIG6 through RAS-MAPK cascade. The binding of MIG6 to EGFR are mediated by two phosphorylation events, with the primary phosphorylation of Y395 by Src and the secondary phosphorylation of Y394 by EGFR kinase. The first phosphorylation results in MIG6 binding to EGFR kinase, while the second one triggers segment 2 reaarangements and blocks the peptide substrate-binding cleft. Figure is adapted from (Park et al., 2015).

In summary, recent studies have challenged the traditional view of EGFR regulation. Structural studies have characterized a distinctive receptor-mediated dimerization mechanism and identified allosteric changes that govern the regulation of the intracellular kinase domain. The study of EGFR and its coreceptors at the systems level identified additional EGFR-binding partners, dynamic patterns of pathway activation, and further layers of EGFR regulation through feedback inhibitors and

intracellular signal compartmentalization. Taken together, these findings highlight the need for a deeper understanding of EGFR regulation through other signaling pathways.

1.3 Nucleo-cytoplasmic transport machinery

The nuclear membrane divides cells into two compartments, and this physical separation of the nucleoplasm and cytoplasm provides an additional level of spatial regulation of protein activity. Movement of macromolecules between these two compartments occurs via channels that are composed of nuclear pore complexes (NPCs) in the nuclear envelope. The macromolecules, known as cargoes, include proteins, RNAs, or larger complexes such as ribosomal subunits. In summary, there are four important elements for macromolecular nucleo-cytoplasmic transport: transport receptors including importins and exportins (also known as karyopherins), the RanGTPase, and the NPC (also known as nucleoporins) (Chook and Blobel, 2001).

Ran (Ras-related nuclear protein) is a 25-kDa member of the Ras superfamily of small GTPases and modulates several cellular functions including nucleocytoplasmic transport (Gorlich, 1997), mitotic spindle assembly (Kalab et al., 1999), and nuclear envelope assembly (Hetzer et al., 2000; Zhang and Clarke, 2000). .

Known Ran-binding proteins can be classified into three protein families: (i) Those that contain a well-characterized Ran Binding Domain and do not physically translocate to the other side of the nuclear membrane. For instance, RanBP1 and RanBP2 are localized in the cytoplasm to facilitate RanGTPase-activating protein (RanGAP)- induced GTP hydrolysis. On the other hand, RanBP3 is localized in the

nucleus to facilitate the nuclear guanine nucleotide exchange factor (RanGEF, also known as RCC1)-mediated nucleotide exchange. (ii) Those that have ~150 amino acid residues in the N-terminus that allow interaction with RanGTP, including importin β1, RanBP4 (importin-4), RanBP5 (importin-5), RanBP7 (importin-7), RanBP8 (importin-8), RanBP11 (importin-11), RanBP13 (importin-13) and RanBP16 (exportin-7), RanBP20 (exportin-6), Crm1/XPO1, and exportin-4. Proteins of family (ii) are known as importin β superfamily members. (iii) Those that lack any Ran-binding sequence identity such as importin α1/2/3 (Strom and Weis, 2001). Proteins of families (ii) and (iii) can translocate to the other side of the nuclear membrane, by either directly interacting with their cargoes, or indirectly through the adapter proteins such as importin α (Cingolani et al., 1999).

The transport is a process highly regulated by karyopherins and the RanGTP gradient through multiple steps: First, an import cargo that contains nuclear localization sequence (NLS) is recognized by importin α, forming an import complex with importin α-β in the cytoplasm. Then the cargo-loaded importin translocates through the nuclear pore complex (NPC) into the nucleus. Next, upon entering into the nucleus, the cargo is competed out from the importin by RanGTP binding to the importin. Lastly, the exportin-RanGTP forms a trimeric complex with an export cargo in the nucleus and translocates to the cytoplasm, where RanGTP hydrolysis is stimulated by RanGAP and RanBP1/RanBP2, which release the transport receptors for the next round of import (Chook and Blobel, 2001; Gorlich, 1997). The directionality of this process is controlled by RanGTP/GDP gradient across the nuclear membrane. This asymmetrical distribution of the different nucleotide-bound forms of Ran drives transport by the loading and unloading of cargoes in their correct compartments. (Gorlich and Kutay, 1999).

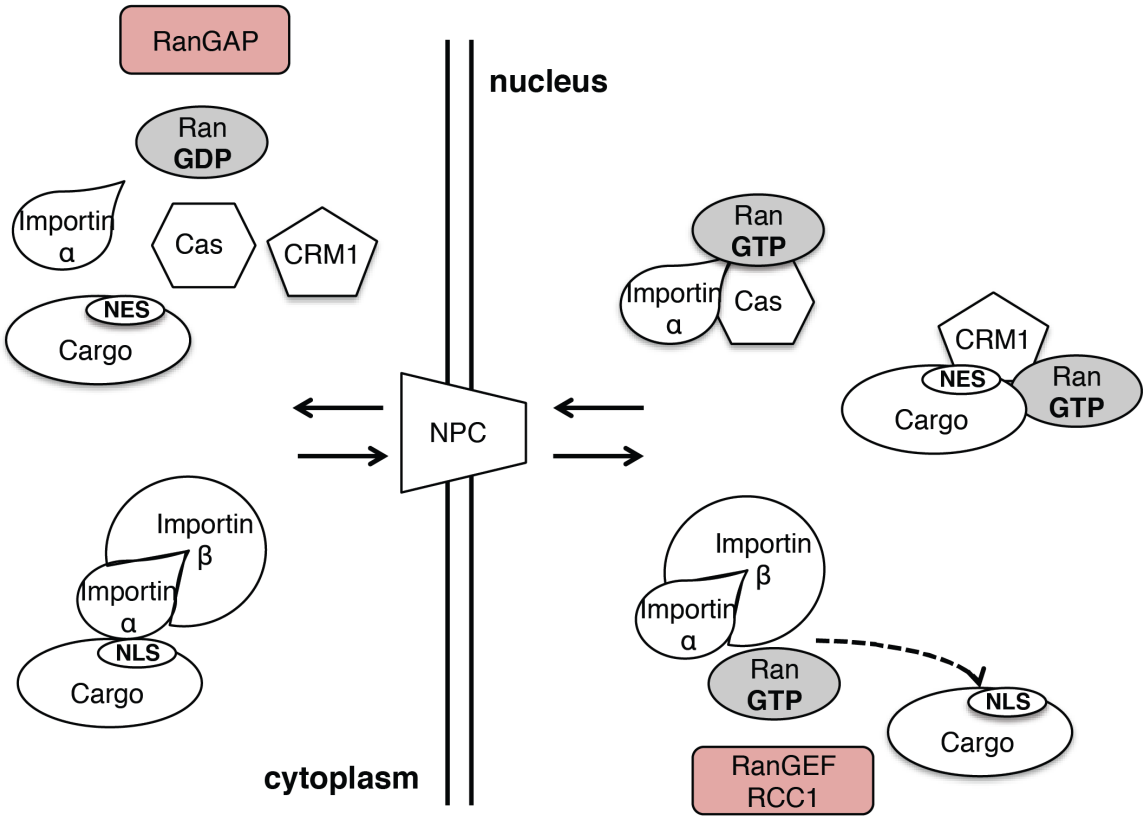

Figure 1-4. The nucleo-cytoplasmic transport machinery for macromolecules. Cartoon depicts a canonical nucleo-cytoplasmic transport system. The importin β forms a complex with the cargo that contains nuclear localization sequence (NLS) through the adaptor protein importin α. Through the interaction with nucleoporins, the whole complex translocates to the nucleus through the nuclear pore complex (NPC). Upon the complex arrives in the nucleus, the cargo was release through a competition binding of RanGTP (shown in grey) to importin β. The high gradient of RanGTP is mediated by the nucleotide exchange factor RanGEF (RCC1) in the nucleus (shown in red). To complete a cycle, the exportin CRM1/XPO1 recognizes a cargo containing nuclear export sequence (NES) and forms a trimeric complex with RanGTP. The export complex shuttles back to the cytoplasm through NPC. Upon it arrives in the cytoplasm, RanGAP (shown in red) immediately hydrolyzes RanGTP to RanGDP (shown in grey). The exportin complex then dissociates in the cytoplasm for the next round of the transport. Of note, importin α and β shuttle back to the cytoplasm through an exportin named CAS, and Ran is imported to the nucleus through nuclear transport factor 2 (NTF2) (Ribbeck et al., 1998), which is not shown here.

Members of importin β superfamily are required for the translocation of certain nuclear proteins, and they are capable of responding to the Ran-GTP gradients (Gorlich and Mattaj, 1996). Such proteins were initially discovered as nucleoporin-binding proteins, and their sequence homology with importin β suggested a function in nuclear transport. These proteins can be further classified as either importins or exportins based on their transport directions (Flores and Seger, 2013).

To date, there are 20 species of Importin β family members that have been identified in humans. Ten are nuclear import receptors, including Imp- β, transportin (Trn)-1, Trn-2, Trn-SR(-3), Imp-4, Imp-5 (RanBP5), Imp-7, Imp-8, Imp-9, and Imp-11. Seven are export receptors, including exportin (Exp-1/CRM1), -2(CAS/CSE1L), -5, -6, -7, -t and RanBP17. Two are bi-directional receptors (Imp-13 and Exp-4), while the function of RanBP6 is undetermined (Kimura et al., 2017). Although numerous studies have contributed to the identification of different cargoes/substrates for these nuclear transport receptors, the number of specific cargoes of these transport receptors that have been reported is surprisingly small.

One of the β-like importins that has a better-characterized repertoire of cargoes is Imp-7, which exploits several mechanisms and distinct NLSs to shuttle its diverse cargoes (Flores and Seger, 2013). For example, under steady state, Imp-7 can complex with Imp-β, or in parallel with Imp-2, Imp-4, and Imp-8 for nuclear translocation (Jakel et al., 1999). Imp-7 can also function as an import receptor for nuclear translocation by itself. It has been discovered to mediate the nuclear translocation of ERK1/2 and MEK1 by binding to the nuclear translocation signal (NTS) sequences of these cargoes (Chuderland et al., 2008; Yao et al., 2008). In addition, Imp-7 was also found to shuttle glucocorticoid receptor (GR) to the nucleus through binding to a canonical

NLS sequence on GR under hormonal stimulation (Freedman and Yamamoto, 2004). Moreover, Imp-7 has been reported to shuttle other signaling molecules or transcription factors/regulators including HIF-1α, c-JUN, SMAD proteins, SOX-2, EGR-1, and the oncogenic ALK (Flores and Seger, 2013). Interestingly, certain cargoes can also be shuttled by different import receptors under different stimuli. For example, c-JUN was reported to be transported by different importins (e.g., importin 2, 5, 7, 9, and 13) under different stimuli (Waldmann et al., 2007). Taken together, these data demonstrate the importance of karyopherins in mediating the subcellular localizations of a variety of cargoes.

1.4 Disruptions of nucleo-cytoplasmic transport in cancer cells

Altered expression of these karyopherins have been implicated in multiple tumors (Kau et al., 2004). Furthermore, modifications to the cargoes, changes in the nuclear transport machinery and alterations in the NPC/nucleoporins can also promote tumorigenesis. Mislocalization of a tumor suppressor or oncoprotein can result in uncontrolled cell growth and subsequent tumorigenesis. For instance, the transcriptional activator nuclear factor κB (NF-κB) has been shown to be involved in tumorigenesis mainly as an active form in the nucleus by increasing cell proliferation and inhibiting apoptosis (Perkins, 2000), in addition to its role in inflammation and immune response. In normal cells, NF-κB is bound to its inhibitor IκB in the cytoplasm, which in turn masks the NLS of NF-κB and prevents it from localizing to the nucleus (Beg et al., 1992; Ganchi et al., 1992; Henkel et al., 1992). However, once IκB is phosphorylated by IKK complex and degraded by the 26S proteasome, the NLS is unmasked and NF-κB is translocated to the nucleus.

It has been shown that in many cancer cells or tumors such as Hodgkin's lymphoma and childhood acute lymphoblastic leukemia (C-ALL), NF-κB is predominantly localized to the nucleus, and this mislocalization is due to hyperactivation of upstream kinases that result in IκB phosphorylation and degradation, or improper acetylation of NF-κB by p300 (Chen and Greene, 2003; Rayet and Gelinas, 1999). In addition, predominantly nuclear NF-κB has also been implicated in breast, ovary, colon, pancreas and thyroid tumor cells (Rayet and Gelinas, 1999).

Similarly, mislocalization of potent tumor suppressors could also result in tumorigenesis. For instance, the function of p53 is tightly regulated by its localization (Ryan et al., 2001). In response to cell stress such as DNA damage, p53 translocates to the nucleus to activate the transcription of its target genes. Mislocalization of wild type p53 to the cytoplasm has been reported in some cancer cells, including inflammatory breast carcinomas and neuroblastomas (Horak et al., 1991; Isaacs et al., 1998; Moll et al., 1995; Moll et al., 1992). As a result, these cancer cells do not undergo p53-mediated G1 cell-cycle arrest when exposed to DNA damaging agents. Although the detailed mechanisms of how p53 localizes to the cytoplasm remains unclear, it has been demonstrated one possible mechanism is through hyperactivated nuclear export of MDM2 by CRM1 (Lu et al., 2000).

Karyopherins that are heavily involved in nucleo-cytoplasmic transport of oncogenes or tumor suppressors are potential targets for corrections of cargo mislocalization. Since the structures of several different importins or exportins have been solved (Fahrenkrog and Aebi, 2003; Vetter et al., 1999), the transport receptors have become attractive therapeutic targets in many cancers. For instance, inhibition of XPO1/CRM1-mediated nuclear export of multiple tumor suppressor proteins has been

proposed as a novel cancer therapeutic strategy to fine tune oncogenic signals and regain tumor suppression (Kau et al., 2004). The natural product Leptomycin B (LMB) was the first XPO1/CRM1 inhibitor, and it covalently and irreversibly binds to C528 of CRM1 (Kudo et al., 1999). Unfortunately, LMB failed in the clinical trials for cancer therapies due to its toxicities to the cells (Newlands et al., 1996). More recent studies have shown that LMB-treated cells have permanently blocked nuclear export, which is lethal not only for cancer cells, but also for normal cells (Sun et al., 2013).

The second generation of XPO1/CRM1 inhibitor is named selective inhibitor of nuclear export (SINE). Like LMB, the SINEs exploit a mechanism by forming a covalent bond with C528 of CRM1 (Sun et al., 2016). However, these small molecules are more compact compared with LMB, and the binding of SINEs to CRM1 is found to be slowly reversible (Sun et al., 2013). This explains the fact that SINEs are significantly less toxic than LMB when entering clinical trials. In addition, SINEs but not LMB treatment promotes CRM1 degradation, while CRM1 is re-synthesized after drug removal (Breit et al., 2014).

CRM1 levels are shown to be elevated in many different types of cancer (Parikh et al., 2014). Since many tumor suppressors including p53, p21, p73, RB1, APC, FOXO and STAT3 are exported by CRM1, targeting CRM1 with SINEs should restore the proper subcellular localizations and functions of these tumor suppressors. Indeed, SINEs have shown promising results in early clinical trials in both solid tumors and hematological malignancies.

In summary, the nuclear transport machinery is tightly regulated and can be disrupted in cancer through mutations or altered expression of nuclear transport components or

disruption of the RanGTP/GDP gradient. Since it has been reported that a small pool of EGF receptors localize to the nucleus through association with the importin α-β complex, we wondered whether there is a protein complex that links the cancer signaling pathways with Ran-mediated nucleo-cytoplasmic transport. This further motivates us to examine the EGFR interactome and identify novel regulators of EGFR signaling.

CHAPTER 2

IDENTIFICATION OF RANBP6 FROM EGFR INTERACTOME

2.1 Introduction

Recent discoveries have revealed the extra complexity of EGFR regulation. The inducible feedback regulator Mitogen-inducible gene 6 (MIG6) exploits a dual-phosphorylation mechanism for direct binding and inhibition of tyrosine kinase domain of EGFR (Zhang et al., 2007b), and promotes EGFR internalization and down-regulation (Park et al., 2015).

We sought to further advance our understanding of EGFR regulation by characterizing the EGFR "interactome" through EGFR-immunoaffinity purification. We immunoprecipitated endogenous EGFR using EGFR antibody Cetuximab from A431 whole cell extracts (human epidermoid carcinoma), which has been serum-starved overnight and then stimulated for 5 minutes with EGF (100 ng/ml), and subjected trypsin digests of EGFR-associated proteins to Liquid Chromatography-Tandem Mass Spectrometry (LC-MS/MS).

In summary, we identified 431 EGFR-associated proteins in three independent biological replicates. Among these EGFR interactors, about 40% of the proteins (175/431) associating with EGFR were listed as EGFR interactors in the Biological General Repository for Interaction Datasets (BioGRID), including components of the adaptor protein complex 2 (AP-2), members of the CBL family of E3 ubiquitin-protein ligases, growth factor receptor-bound protein (GRB2), SHC-transforming protein 1 (SHC1), son of sevenless homolog 1 (SOS1), the phosphatidylinositol 4,5-bisphosphate 3-kinase catalytic subunit α and β isoforms (PIK3CA and PIK3CB),

phosphatidylinositol 3-kinase regulatory subunit α (PIK3R1), 1-phosphatidylinositol 4,5-biphosphate phosphodiesterase gamma-1 (PLCG1), and ERBB receptor feedback inhibitor 1 (ERRFI; also known as MIG6 protein).

In addition to these proteins with well-documented roles in EGFR signaling, gene ontology analysis (www.geneontology.org) showed an enrichment of proteins involved in protein import into nucleus (Fig. 2-1). In line with a prior examination of the EGFR-interactome in A431 cells (Foerster et al., 2013), the most highly enriched pathway (GO:0006610) members included Importin subunit β-1, Importin-5, Transportin-2, Importin-4, 60S ribosomal protein L23, Transportin-1, and Ran-binding protein 6 (RanBP6). Among this group of proteins, only RanBP6 had not yet been identified as an EGFR interactor, and the biological functions of RanBP6 remained unknown. Therefore, we focus our subsequent study on RanBP6, but not other proteins known to be involved in EGFR signaling or regulation.

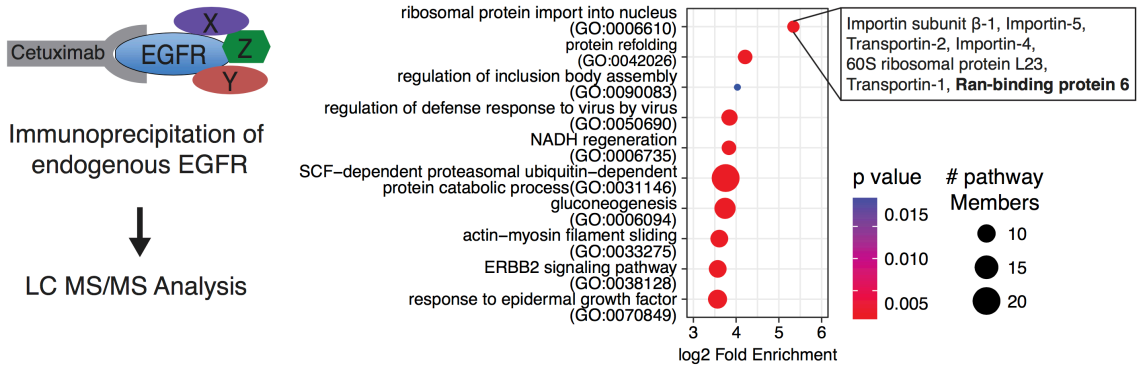

Figure 2-1. Identification of Ran-binding protein 6 from EGFR interactome study. Left panel, schematic representation of EGFR immunoaffinity purification and LC-MS/MS analysis in A431. Right panel, plot showing the top ten categories of the gene ontology enrichment analysis of the EGFR-associated proteins.

2.2 Validation of RanBP6 as a novel EGFR interactor

To validate RanBP6 as an EGFR-associating protein from our EGFR interactome study, two different methods- co-immunoprecipitation and Glutathione S-transferase (GST)-pulldown assays were exploited in multiple cell lines. We first generated a construct by cloning RanBP6 cDNA to a doxycycline (Dox)-inducible V5-tagged vector, and expressed it in A431 cells. Immunoprecipitation with a V5 antibody confirmed the interaction between RanBP6 and EGFR (Fig. 2-2).

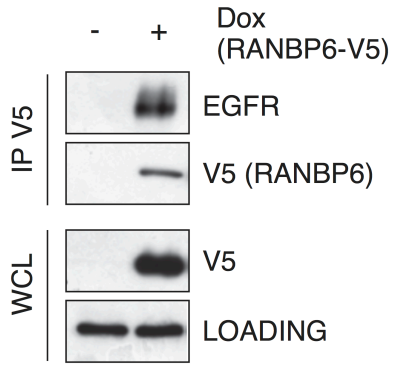

Figure 2-2. Validation of RanBP6-EGFR interaction by co-immunoprecipitation. Top panel, IP using V5 antibody; bottom panel, immunoblot of whole-cell lysates (WCL) from A431 cells. Data provided by Dr. Oldrini.

We next examined the interaction between RanBP6 and EGFR in cells that do not overexpress EGFR. We further generated a GST and human RanBP6 cDNA fusion construct (pGEX6p-RanBP6), expressed it and optimized the protein production with isopropyl β-D-1-thiogalactopyranoside (IPTG) in *E.coli*. The optimal culture condition for producing RanBP6 fusion protein is at 20°C overnight (Fig. 2-3a). SDS-PAGE analysis revealed that RanBP6 is the dominant species after GST fusion protein purification (Fig. 2-3b). Similarly, GRB2, the cytosolic bona-fide EGFR interactor is also the dominant species after purification. These data suggest that we can obtain biochemically pure GST fusion proteins for our downstream pulldown assays.

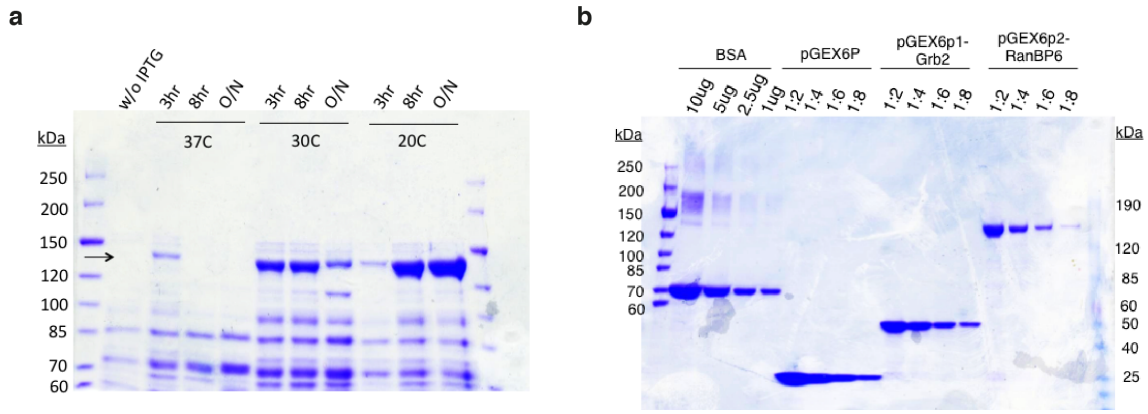

Figure 2-3. Expression and purification of pGEX6p-RanBP6 from *E. coli*. a, The soluble fraction from bacterial lysates after inducing with 0.5 mM isopropyl β-D-1-thiogalactopyranoside (IPTG) indicated that overnight culture at 20C has the most optimal protein expression of pGEX6p-RanBP6. **b,** Shown are GST protein purifications of pGEX6p, pGEX6p1-Grb2 (an EGFR bona fide interactor), and pGEX6p2-RanBP6. The concentrations of each fusion protein were compared to BSA concentration. Proteins were aliquot and snap frozen with liquid nitrogen after purification. Of note, pGEX-RanBP6 has a M.W. ~146 kDa.

To perform GST pulldown assays, 30 µg of purified pGEX or pGEX-RanBP6 proteins were further incubated with cell extracts from HEK293T, mouse embryonic fibroblasts (MEFs), and LN18 glioblastoma cells. We confirmed the interaction between RanBP6 and EGFR in all three different cell lines (Fig. 2-4).

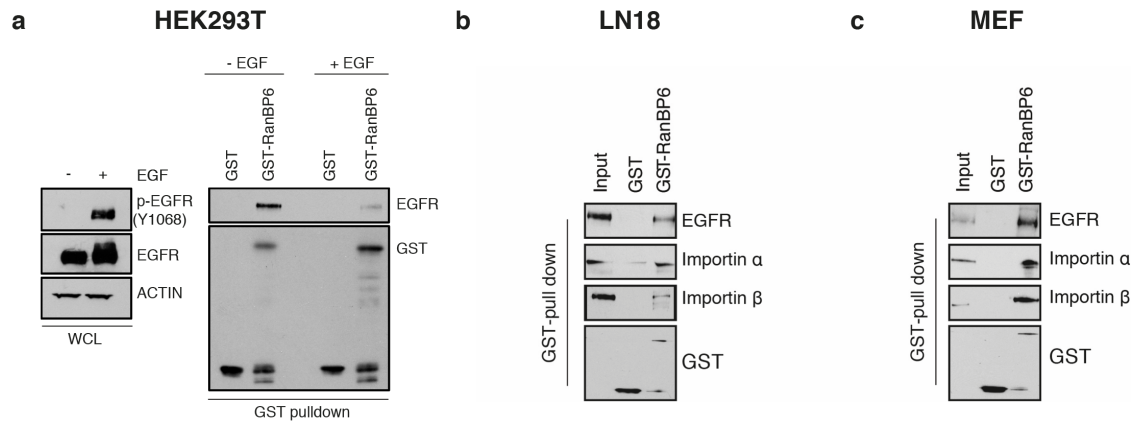

Figure 2-4. Validation of RanBP6-EGFR interaction by GST-pulldown assays. a, Left panel, immunoblot of HEK293T whole-cell lysates (WCL); right panel, GST-pulldown assay. Of note, pretreatment of cells with 100 ng/ml of EGF for 5 minutes dissociates the RanBP6-EGFR complex, which will be further discussed in Chapter 4. **b,** GST-RanBP6 interacts with EGFR and importin α-β complex with the lysates from LN18, and MEF **(c).**

2.3 RanBP6 is an importin-β-like protein

RanBP6 is a protein that has no known biological function. It contains a putative importin N-terminal RanGTP binding domain (Imp. N-ter) (Fig 2-5a), suggesting it is a member of the importin β superfamily (Strom and Weis, 2001). By sharing high amino acid sequence homology (~85%) with RanBP5, which has been reported as an importin for cargoes involved in spindle organization or microtubule-based processes (Kimura et al., 2017). RanBP6 also contains several HEAT (huntingtin, elongation factor 3, the PR65/A subunit of protein phosphatase 2A, and the lipid kinase Tor) repeats, which have been identified in importins and exportins for substrate binding, and a putative Ran-binding domain (RBD). Sequence alignments of the putative RBDs of RanBP6, RanBP5, and importin β1 showed a high sequence homology across different species (Fig 2-5b).

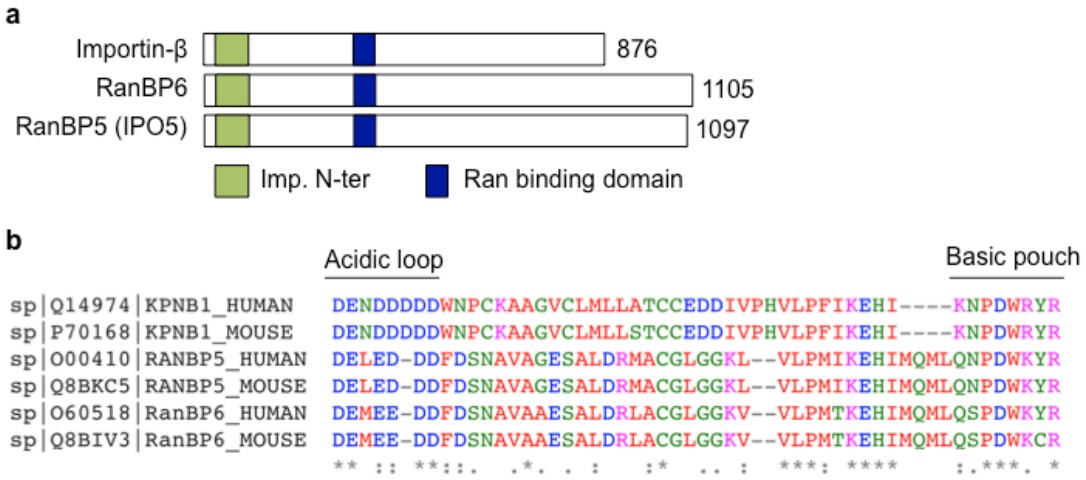

Figure 2-5. Domain structures of members in the importin β superfamily members. a, RanBP6 belongs to importin β superfamily because it includes an importin β-like N-terminal domain (Imp. N-ter) and a putative Ran-binding domain (RBD). Ran binds to both these two domains of importin β. RBD is also important for cargo binding. The number to the right of each protein shows the total number of amino acids. **b,** Sequence alignment of the RBD of RanBP5, RanBP6 and importin β showed high sequence homology across different species. The acidic loop of importin β has been shown to be important for cargo binding.

2.4 RanBP6-EGFR interaction is decreased by the acidic loop mutations of RanBP6

To further identify the region of RanBP6 that is essential for EGFR binding, we hypothesized that the acidic loop region of RanBP6 is important for EGFR binding because 1) the loop region has been shown to be important for cargo binding (Vetter et al., 1999), and 2) multiple sequence alignment with importin β and RanBP5 showed high sequence homology at this region (Fig. 2-5b and 2-6a). We mutated DExEEDD of RanBP6 to either alanine residues AAxAAAA (hereafter named mutant #1), or NQxQQNN (hereafter named mutant #2). The latter one is a more conservative mutant form.

For expressing and purifying these two mutants with GST-fusion protein system from *E.coli*, we optimized IPTG induction of each mutant, purified RanBP6 wildtype with these two mutants, and ran a small fraction of the purified protein on the SDS-PAGE (Fig. 2-6b). Both mutants are soluble, with comparable quality and quantity to wildtype RanBP6. We further performed GST pulldown assays of GST-RanBP6 wt, mt#1, mt#2 with EGFR from HEK293T lysates that were either pretreated or not with 100 ng/ml EGF for 5 minutes. GST was used as a negative control while GRB2 was used as a positive control for this assay.

RanBP6 and EGFR interaction was impaired with either mt#1 or mt#2, with a more profound decrease with the alanine mutants (mt#1) (Fig. 2-6c). Interestingly, addition of EGF increases EGFR-GRB2 association, while decreases EGFR-RanBP6 association, as we previously shown in Fig. 2-4a. We will further discuss this phenotype in Chapter 4. Taken together, these data suggest that the acidic loop region is essential for EGFR and RanBP6 interaction, albeit the interaction could be either direct or indirect.

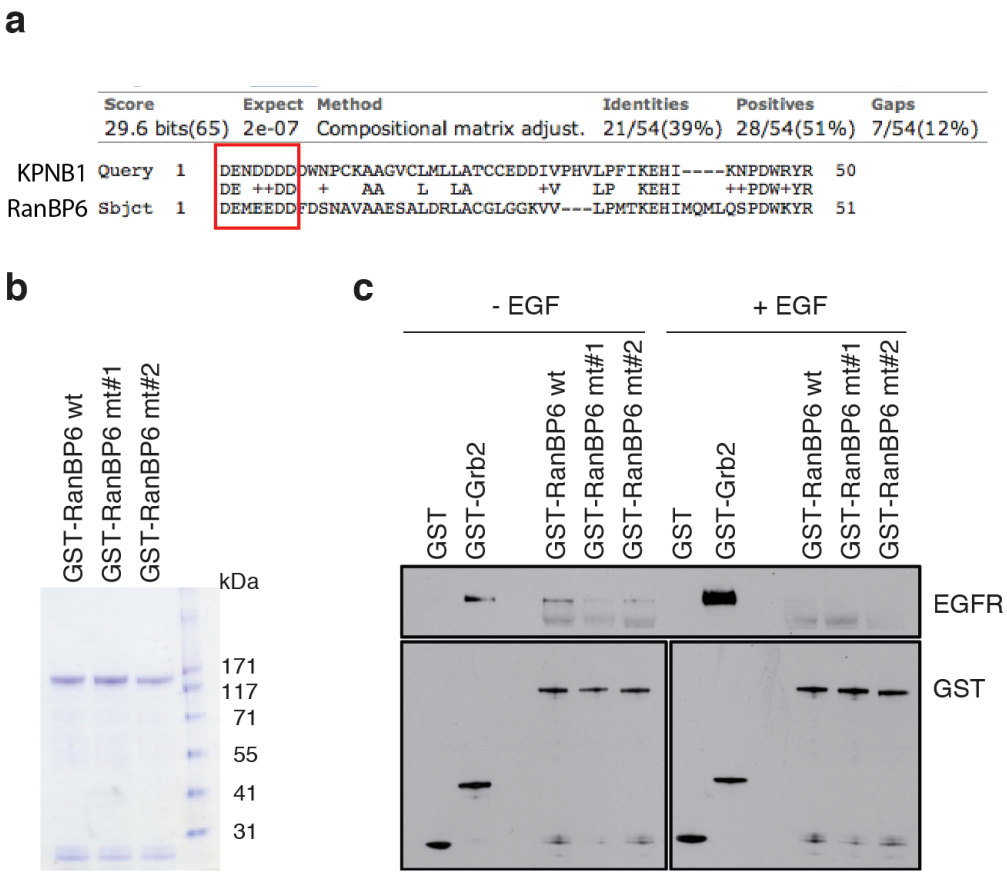

Figure 2-6. Mutations of the acidic loop of RanBP6 decrease its binding to EGFR. **a,** Sequence homology of the acidic loop of Importin β (DExDDDD) with RanBP6 (DExEEDD). **b,** GST-fusion protein expression and purification of GST-RanBP6 wt, mt#1 (AAxAAAA) and mt#2 (NQxQQNN) on CBB-stained gel. **c,** the association of EGFR and RanBP6 was impaired in both mutant forms. While acute EGF (100 ng/ml, 5 minutes) stimulation increases EGFR-Grb2 association, we observed a dissociation of RanBP6-EGFR complex.

2.5 RanBP6 interacts with proteins involved in RanGTP-mediated nucleo-cytoplasmic transport

Since RanBP6 has the specific motifs related to nucleo-cytoplasmic transport, we therefore examined interaction of RanBP6 with other members of the Ran-GTPase

pathway. To further understand whether RanBP6 indeed binds to Ran, we fractionated the HEK293T cells and incubated either the cytoplasmic or nuclear extracts with purified GST-RanBP6. Interestingly, GST pulldown assays showed a differential association between RanBP6 and Ran. RanBP6 only interacts with nuclear but not cytoplasmic Ran, suggesting that it predominately associates with RanGTP (95% of Ran is GTP-bound in the nucleus) (Fig 2-7a). Along with RanGTP, we also pulled down RCC1, a guanine nucleotide exchange factor that mediates the conversion of RanGDP to RanGTP in the nucleus (Bischoff and Ponstingl, 1991).

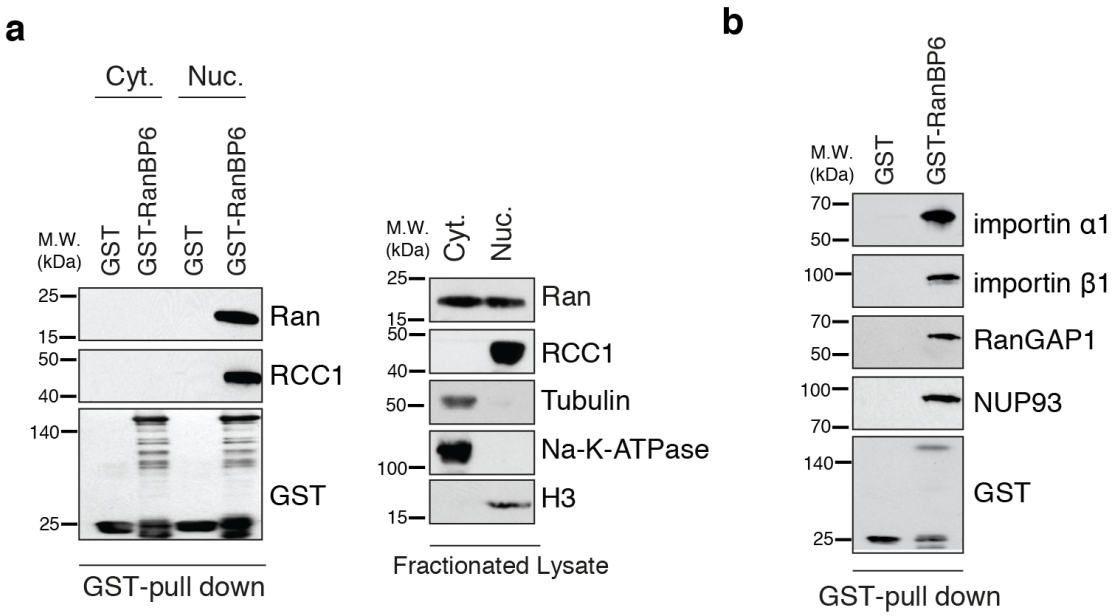

Figure 2-7. RanBP6 interacts with nuclear RanGTPase and members involved in nucleo-cytoplasmic transport. a, Subcellular fractionation of HEK-293T cells (right panel) shows that Ran is present in both nuclear and cytoplasmic compartments, but only interacts with RanBP6 in the nuclear fraction (left panel). **b,** GST pulldown assays show that RanBP6 interacts with importin α-β complex, RanGAP1 and nuclear pore complex 93 (Nup93) in HEK-293T whole-cell lysates.

We next examined the interaction between RanBP6 and the proteins involved in nucleo-cytoplasmic transport that were also immunoprecipitated with EGFR. GST

pulldown assays with extracts from HEK293T showed that RanBP6 interacts with nuclear pore complex 93 (Nup93), importin α1, importin β1, the GTPase-activating protein RanGAP1, which hydrolyzes RanGTP into RanGDP in the cytoplasm (Fig 2-7b, also see Fig. 2-4b and Fig. 2-4c for cell lines LN18 and MEF), and SEC61α, a subunit of the translocon SEC61 complex on the endoplasmic reticulum (ER), which has been shown to route EGFR from cytoplasm toward the nucleus (Liao and Carpenter, 2007). Taken together, these data suggest that RanBP6 not only associates with EGFR, but also interacts with the proteins that are involved in nucleo-cytoplasmic transport.

2.4 Discussion

In this Chapter, our EGFR interactome study identified RanBP6, a protein with currently unknown functions, as EGFR-interacting protein and a member of the Ran-GTPase nuclear transport pathway. Since we used an EGFR monoclonal antibody Cetuximab that binds to the ectodomain of EGFR, we were aware that the interactors from our study were mainly cytoplasmic bound. The validations of EGFR-RanBP6 association were performed using an EGFR antibody that recognized the cytoplasmic domain of EGFR.

Furthermore, we showed that by mutating the acidic loop of RanBP6, the binding of EGFR to RanBP6 was decreased. EGFR has been reported to localize to the nucleus through a process that involves trafficking of EGFR from the plasma membrane to the ER, binding to the Sec61 translocon, and shuttling toward the nucleus. Of note, the importin α-β complex has been shown to co-localize with nuclear EGFR. In addition, nuclear EGFR has been shown to function as a transcriptional co-activator for Cyclin

D1 (Lin et al., 2001). However, the observation of nuclear EGFR is controversial because many laboratories including ours could not detect nuclear EGFR either at the steady-state or after EGF stimulation (Itzhak et al., 2016; Lin et al., 2015; Thul et al., 2017). We did observe peri-nuclear localization of EGFR with EGF stimulation, but we did not detect nucleolus EGFR localization. Therefore, we hypothesized that RanBP6 plays a role in EGFR regulation through its interaction with EGFR, but it does not serve as a transport receptor for routing EGFR toward the nucleus.

CHAPTER 3

RANBP6 REPRESSES EGFR TRANSCRIPTION THROUGH STAT3

3.1 Introduction

Several feedback proteins that bind to EGFR, such as CBL family members or ERBB receptor feedback inhibitor 1 (also known as MIG6), play critical roles in EGFR negative regulation. Recent studies have shown that MIG6 inhibits EGFR kinase activity and promote degradation of wild-type EGFR (Maity et al., 2015). Our EGFR interactome study suggested that RanBP6 binds to EGFR intracellular domain, we therefore wondered whether RanBP6 has a function in regulating EGFR signaling, in a similar manner as the inducible feedback regulator MIG6.

3.2 Depletion of RanBP6 increases EGFR transcription and promoter activity

To determine whether RanBP6 plays a role in regulating EGFR levels, we generated HEK-293T sublines expressing two different DOX-inducible RanBP6-short hairpin RNAs (shRNAs). RanBP6 knockdown (KD) with either hairpin increased EGFR protein levels (Fig 3-1a). We next evaluated the effects of RanBP6 on EGFR mRNA levels. Dox-induced knockdown of RanBP6 raised EGFR mRNA levels, typically about 2-fold (Fig. 3-1b).

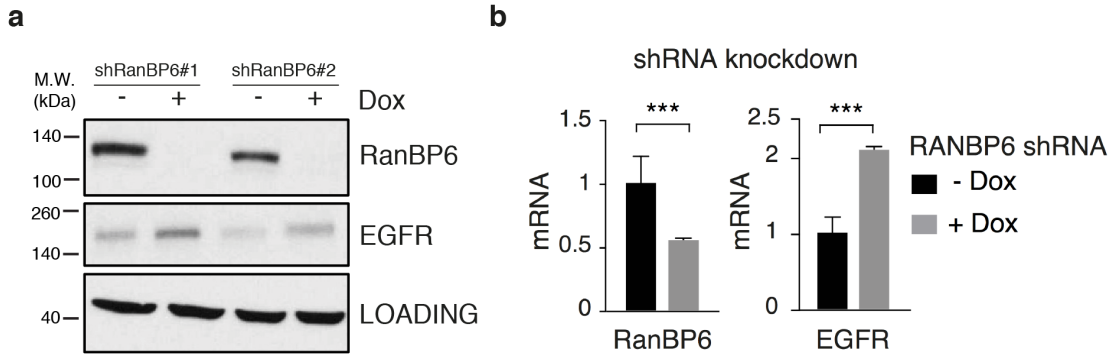

Figure 3-1. RanBP6 regulates EGFR at both protein and mRNA levels. a, Dox-induced shRNA-mediated RanBP6 knockdown raises EGFR protein levels with two different RanBP6 hairpins in HEK293T cells. **b,** RanBP6 KD increases EGFR mRNA levels in HEK-293T cells. Shown are RT-qPCR results.

To further confirm the effect of RanBP6 KD on EGFR, we depleted RanBP6 using the Clustered Regularly Interspaced Short Palindromic Repeats (CRISPR)/Cas9 system (Fig. 3-2a and 3-2b). Complete RanBP6 depletion resulted in a more pronounced elevation of EGFR mRNA and protein levels (Fig. 3-2c and 3-2d).

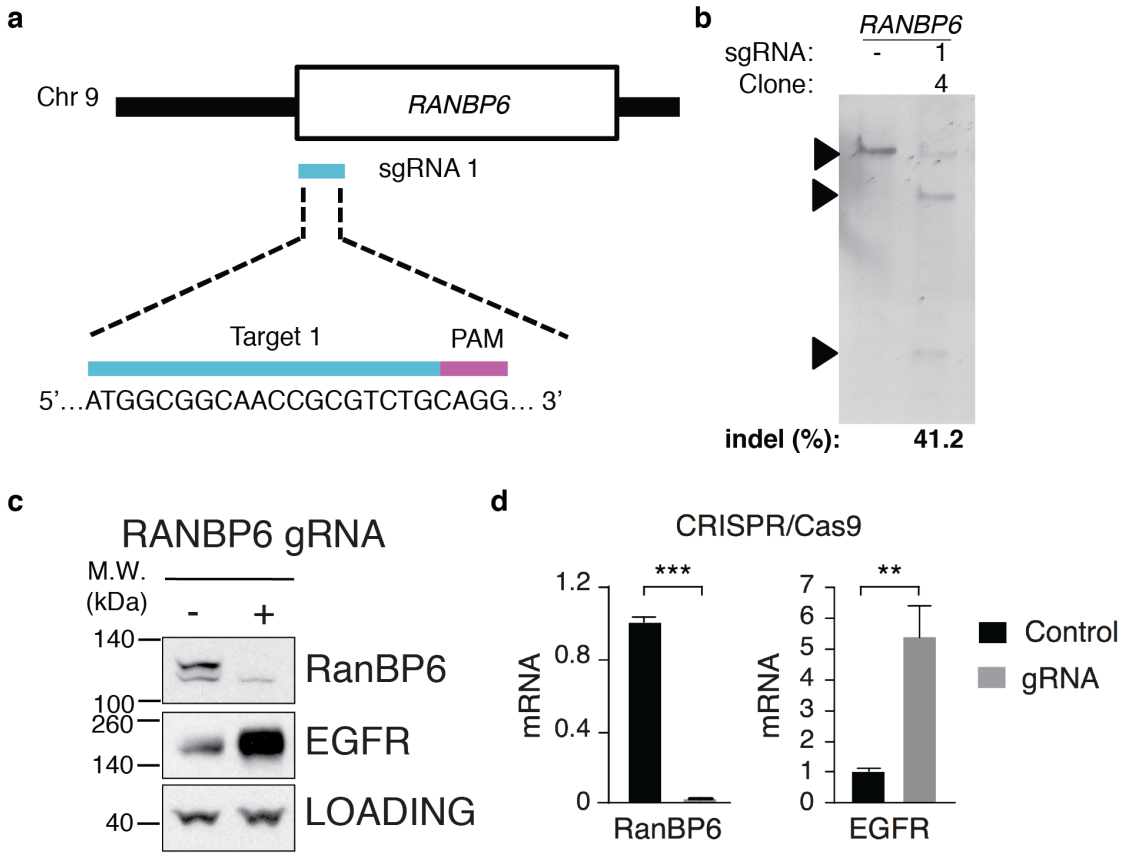

Figure 3-2. CRISPR/Cas9-mediated knockout of RanBP6 increases EGFR mRNA and protein levels in HEK293T. a, Shown is the single-guided RNA target sequence on *RANBP6* gene locus. **b,** Shown is the SURVEYOR (endonuclease digestion) assay result confirms the indel rate of a specific single clone. Overall, 196 clones were screened and 6/196 have good indel rate (>20%). Please see the Appendix A: materials and methods for more details. **c and d,** complete RanBP6 depletion raises EGFR protein and mRNA levels in a more dramatic manner.

We further examined the promoter activity of EGFR, RanBP6 KD also increased the expression of a luciferase reporter cloned downstream of the EGFR promoter sequence, but had no effect on a control β-actin luciferase reporter (Fig. 3-3), suggesting that RanBP6 regulates *EGFR* mRNA levels through effects on *EGFR* promoter activity.

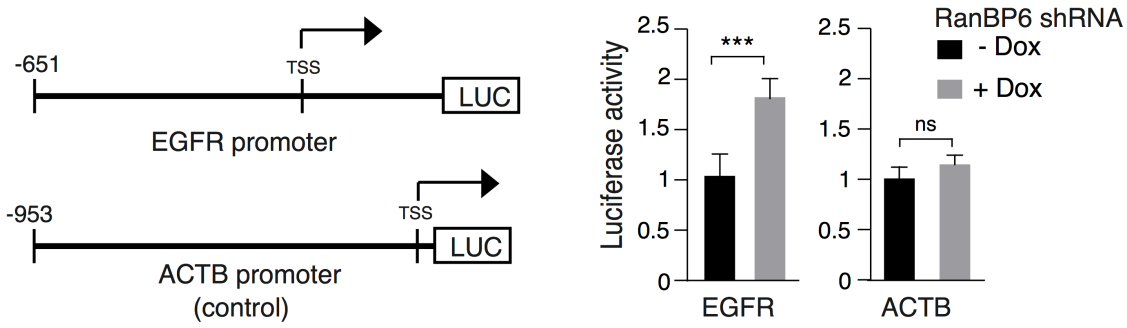

Figure 3-3. RanBP6 KD increases transcription of a luciferase reporter gene from *EGFR* promoter in HEK293T. Left panel, Cartoon depicts the luciferase reporter gene was cloned to the downstream of either EGFR promoter or β-actin (ACTB) promoter. Right panel, KD of RanBP6 with Dox-inducible hairpin increases EGFR luciferase activity but not ACTB.

3.3 Depletion of RanBP6 activates EGFR downstream signaling pathways

Lastly, we examined whether the increase in EGFR levels associated with RanBP6 depletion resulted in increased EGFR pathway output. This was indeed the case, as demonstrated by increased phosphorylation of EGFR (Y1068), phosphorylation of the adapter protein Gab1 (Y627), and downstream EGFR pathway members phosphorylated ERK1/2 (Y202/204), phosphorylated Akt (S473), and phosphorylated S6 kinase (S240/244) following a time-course EGF stimulation (Fig. 3-4). Of note, the rate of EGF-induced EGFR protein degradation was comparable in the absence and presence of doxycycline, further supporting the conclusion that increased EGFR protein levels in RanBP6 knockdown cells were not the result of impaired EGFR protein degradation.

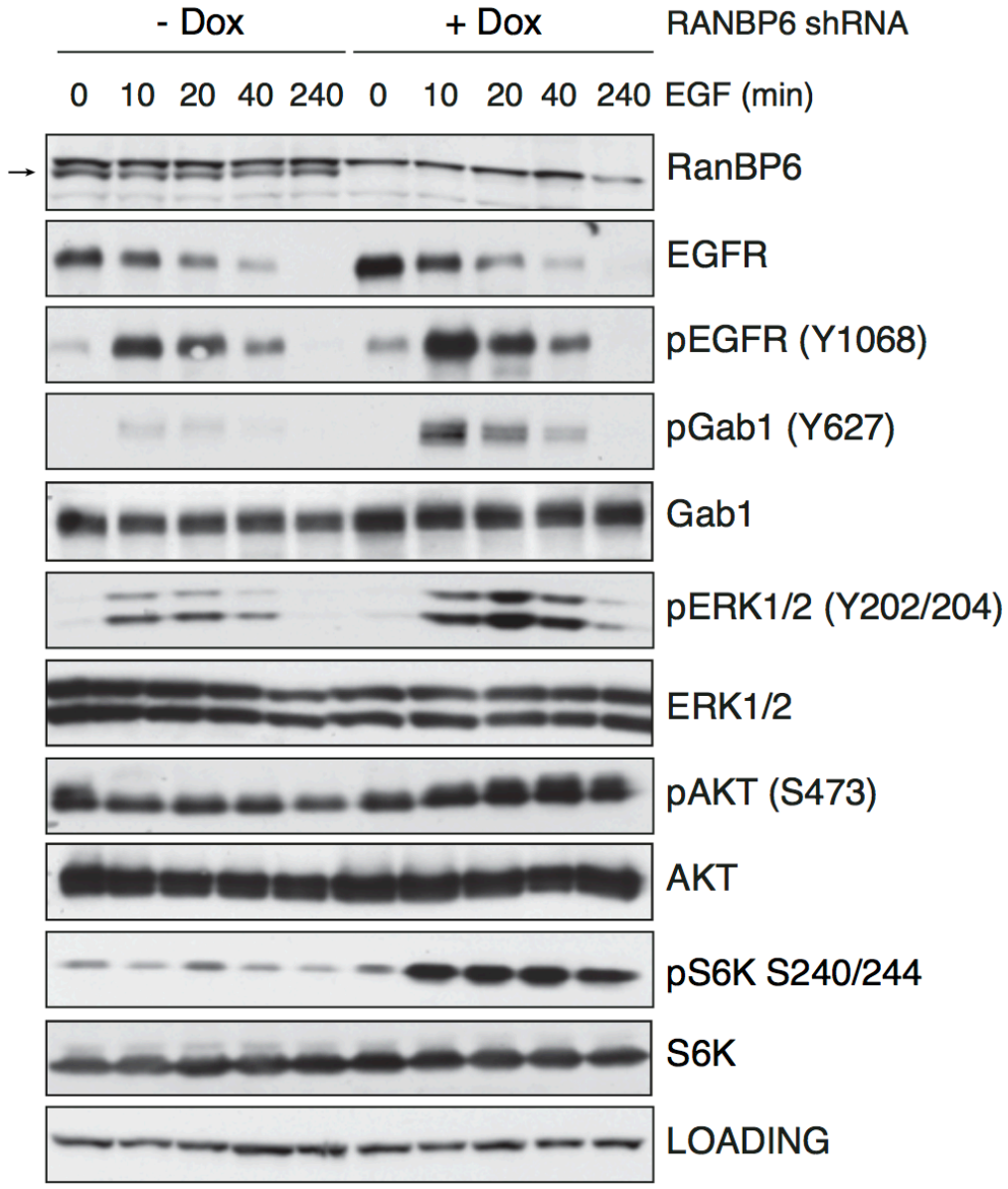

Figure 3-4. RanBP6 KD increases activation of the EGFR downstream signaling pathways but does not impair EGF-induced EGFR degradation in HEK-29T cells. Immunoblot of whole-cell lysates serum starved for 16 hr and then stimulated with EGF (100 ng/ml) for the indicated time points. Data provided by Dr. Oldrini.

3.4 RanBP6 promotes nuclear translocation of the transcription factor STAT3

Given that 1) members of the β-importin-like protein superfamily transport a variety of cargoes, including transcription factors, and 2) we do not observe RanBP6 shuttles EGFR into the nucleus (see Chapter 2.4), we hypothesized that RanBP6 might facilitate the nuclear transport of a transcription factor that regulates *EGFR* promoter activity (Yarden and Sliwkowski, 2001). We therefore examined the subcellular localization of several transcription factors that regulate EGFR transcription.

We performed subcellular fractionation with HEK293T sublines transfected with either the vector (wildtype- sgCtrl) or single-guided RanBP6 RNA (knockout-sgRanBP6) (Fig 3-3c). In a panel of transcription factors that have been selected for examination by western blot, STAT3 was decreased in the nuclear portion while increased in cytoplasmic compartments (Fig. 3-5). In contrast, we observed no changes in the subcellular localization of other transcription factors that regulate EGFR transcription, including Elk, C-Jun, and phosphorylated c-Jun (S73). Interestingly, we observed a decrease of nuclear c-Myc and p-ERK (Y202/204), and an increase of sp1 (predominantly localized in the nucleus) upon RanBP6 KO (see 3.7 Discussion).

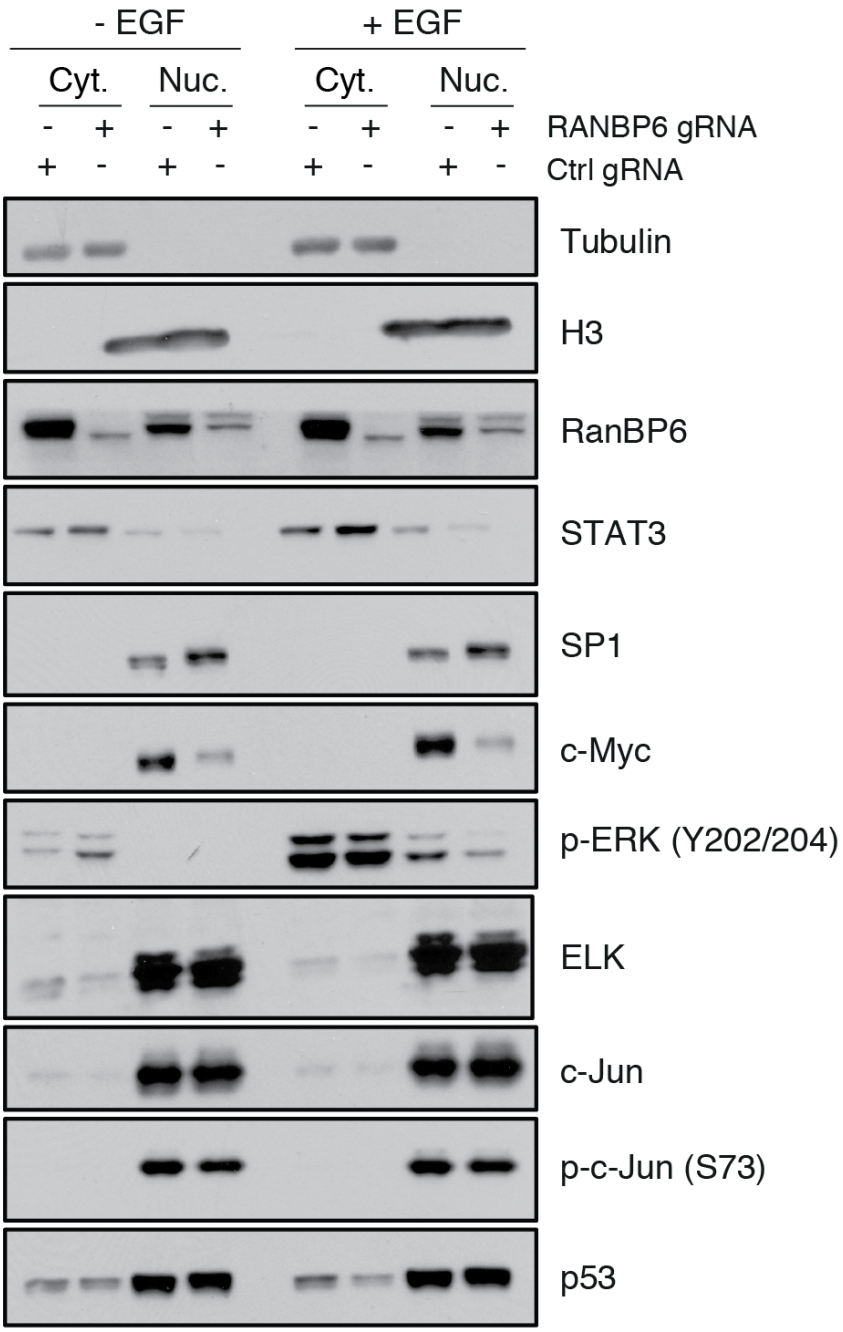

Figure 3-5. RanBP6 knockout (KO) affects the subcellular localization of several transcription factors that regulate EGFR transcription. Shown are immunoblots of subcellular fractionations with HEK293T cells with either control gRNA or RanBP6 gRNA. Cytoplasmic (Cyt.) and nuclear (Nuc.) fractions were immunoblotted with the indicated antibodies. RanBP6 KO accumulates cytoplasmic STAT3 while decreases its nuclear entry.

Furthermore, we expanded our analyses to examine the subcellular localizations of several other cancer-related proteins, including the transcription factors p53, Retinoblastoma-associated protein (RB), $p27^{Kip1}$, Forkhead box protein O3 (FOXO3), and Survivin (Fig. 3-6). None of these proteins altered their subcellular localization upon RanBP6 KO.

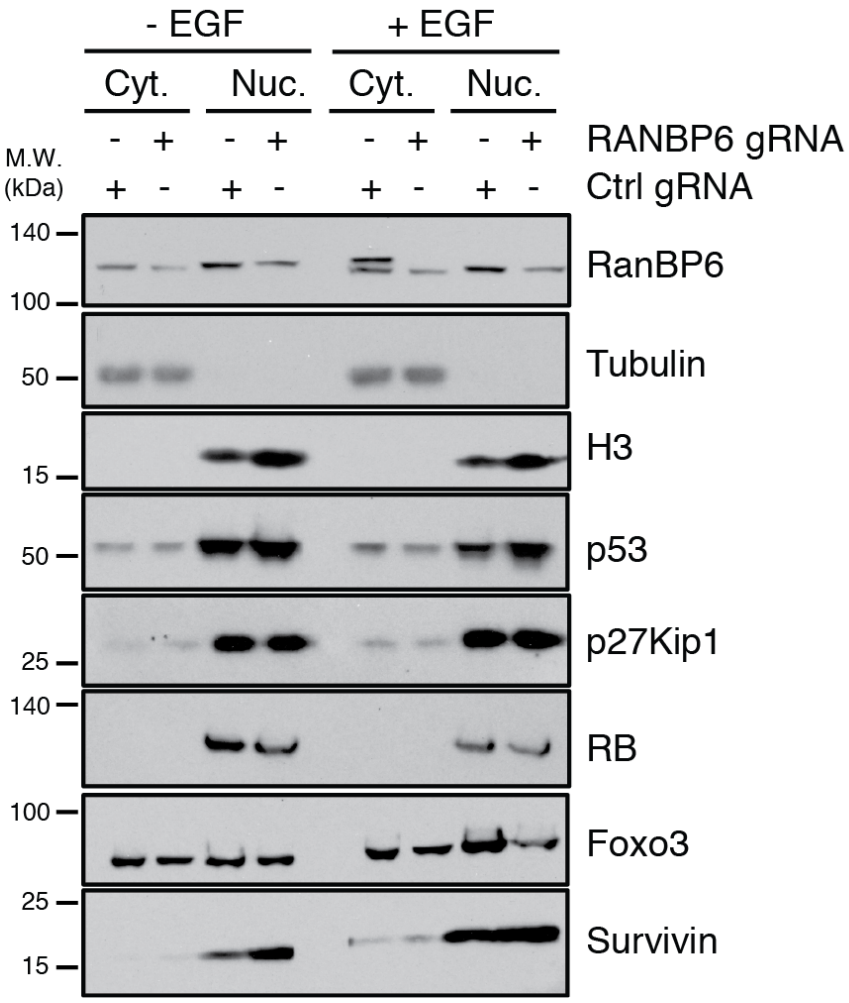

Figure 3-6. RanBP6 depletion does not change the subcellular localization of several tumor suppressors. Shown are immunoblots of subcellular fractionations with HEK293T cells with either control gRNA or RanBP6 gRNA. Cytoplasmic (Cyt.) and nuclear (Nuc.) fractions were immunoblotted with the indicated antibodies. While Survivin is an oncoprotein, p53, p27, RB, and Foxo3 are known tumor suppressors. Note that addition of EGF (100 ng/ml, 5 minutes) does not change nuclear localization of these proteins.

We selected the transcription factor STAT3 for further analysis because it associated with EGFR in our mass spectrometric analysis, had previously been shown to associate with EGFR (Bild et al., 2002; Fan et al., 2013; Lo et al., 2005) and has been proposed to enter the nucleus through an importin-mediated transport mechanism (Cimica et al., 2011). Therefore, we hypothesized that RanBP6 shuttles STAT3 to the nucleus, which further regulates EGFR transcription.

To test this hypothesis, we first examined the effects of RanBP6 on nuclear translocation of STAT3 by immunofluorescence. RanBP6 knockdown impaired interleukin 6 (IL-6)-induced nuclear translocation of STAT3, similar to the ATP-competitive Janus Kinases (JAK) inhibitor ruxolitinib in HEK293T cells (Fig 3-7).

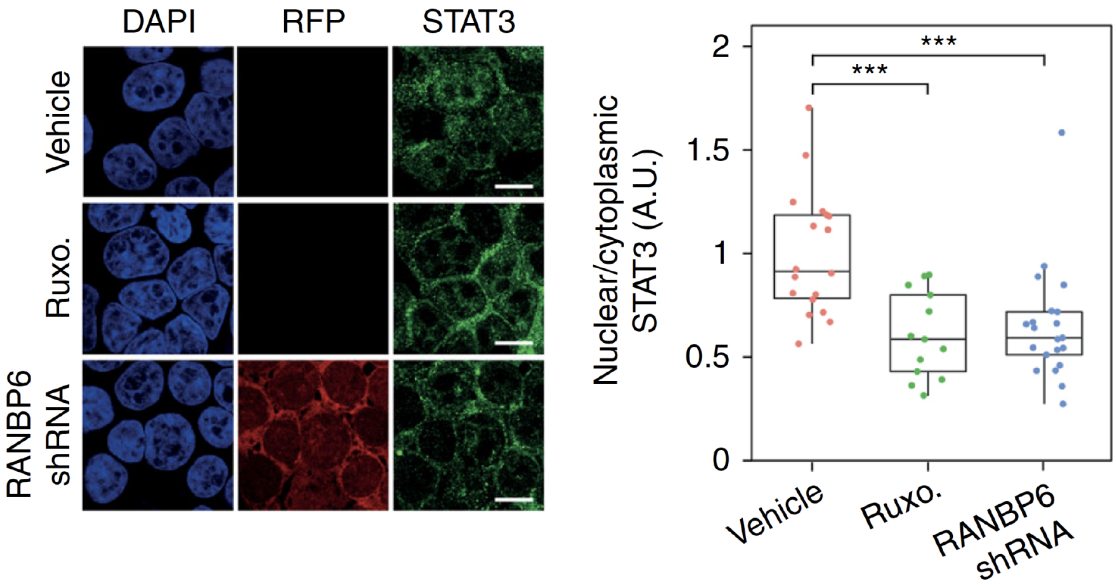

Figure 3-7. RanBP6 KD impairs IL-6-induced nuclear STAT3 translocation. Left panel, confocal immunfoulorescence. RFP is used as a reporter for shRNA expression. Right panel, ratios of nuclear/cytoplasmic STAT3 staining (field of views: vehicle, n=18; ruxolitinib, n=13; RANBP6-shRNA, n=21). The janus kinase (JAK) inhibitor ruxolitinib was included as a positive control. Scale bar = 10 μm.

We also examined this phenotype by performing subcellular fractionations of HEK293T sublines expressing Dox-inducible RanBP6 shRNA (Fig 3-8). Consistent with our observation with immunofluorescent staining, KD of RanBP6 decreases nuclear STAT3, as well as phosphorylated STAT3 (Y705), which is not amenable to be detected by IF due to its low expression in HEK293T.

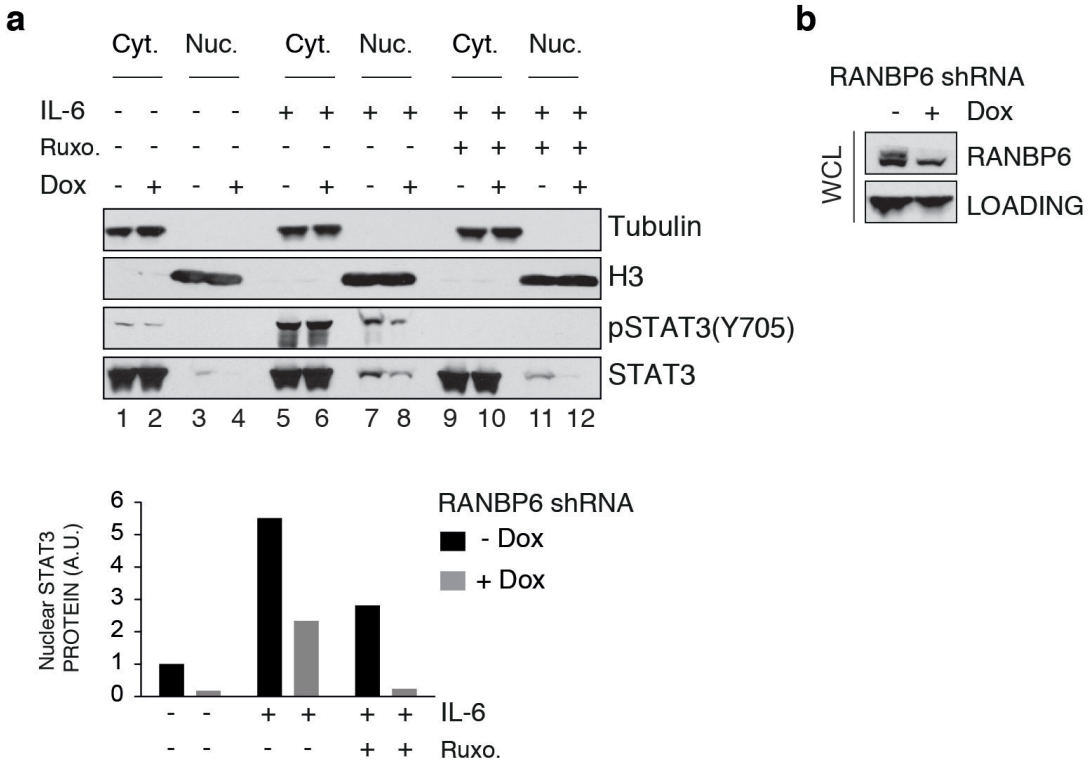

Figure 3-8. RanBP6 KD impairs IL-6 induced nuclear translocation of STAT3. **a,** Shown are immunoblots (upper panel) and densitometric quantification (lower panel) of fractionated cell lysates from HEK-293T cells treated with the indicated reagents. Note that the IL-6 induced nuclear localization of STAT3 and p-STAT3 is reduced by ruxolitinib (lane 11 *versus* lane 7). This effect is phenocopied by RanBP6-shRNA (lane 8 *versus* lane 7). **b,** immunoblot confirms Dox-induced RanBP6 knockdown in the whole cell lysate. Cyt.=cytoplasm. Nuc.=nucleus.

We next examined whether RanBP6 interacts with STAT3 since both our subcellular fractionations and IF results suggested that STAT3 could be a cargo of RanBP6. GST-RanBP6 fusion protein binds to both STAT3 and phosphorylated STAT3 (Y705) in the whole cell lysates from HEK293T (Fig 3-9).

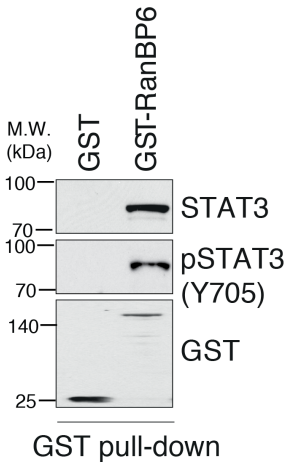

Figure 3-9. STAT3 and p-STAT3 (Y705) bind to GST-RanBP6. Immunoblot showing GST-RanBP6 interacts with STAT3 or phosphorylated STAT3 (Y705) from HEK-293T whole-cell lysates.

We next examined the effect of RanBP6 on STAT3-regulated gene expression. We transient transfected HEK293T cells expressing Dox-inducible RanBP6 shRNA with an engineered STAT3-reporter gene. We observed reduced expression of STAT3-responsive luciferase activity following RanBP6 knockdown, while in HEK293T parental cells, the luciferase activity remained unchanged (Fig. 3-10).

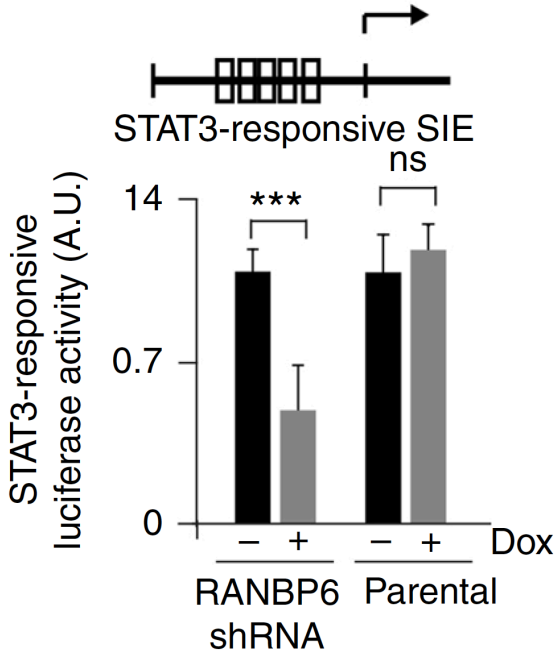

Figure 3-10. RanBP6 KD decreases transcription of STAT3 reporter gene. SIE sis-inducible elements. Data are represented as mean ± SD (n ≥ 3). Student's t test: ***p < 0.001; **p < 0.01; ns not significant.

To evaluate the effects of RanBP6 on the expression of endogenous STAT3 target genes, we analyzed HEK293T cells expressing Dox-inducible RanBP6 shRNA using Affymetrix gene expression arrays and single-sample gene set enrichment analysis (ssGSEA). Gene sets that have been reported to be activated by STAT3 (MsigDB, http://www.broadinstitute.org/gsea/msigdb/) showed lower enrichment scores in RanBP6 knockdown cells whereas gene sets that are negatively regulated by STAT3 (Dauer-STAT3-targets-DN) showed higher enrichment scores in RanBP6 knockdown cells (Fig. 3-11).

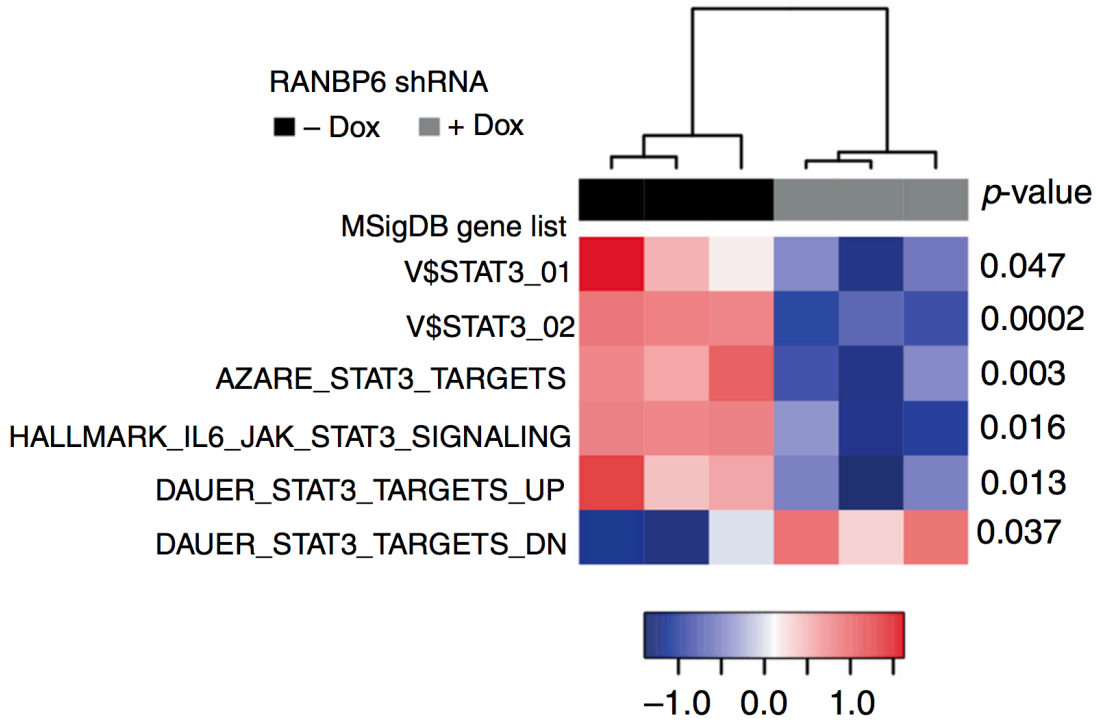

Figure 3-11. Gene expression profiling showing the effect of RanBP6 KD on endogenous STAT3 target genes. Heatmap represents the enrichment scores from single-sample gene set enrichment analysis (ssGSEA) of three biological replicates. Student's t test p-values (DOX- *versus* DOX+) for each gene sets are indicated.

We confirmed these results by quantitative PCR for several of the genes that have been reported to be activated (*PTGS2*, *MAFF* and *EFNB2*) or repressed (*IFIT1* and *CPS1*) by STAT3. These genes showed similar changes in expression following RanBP6 and STAT3 knockdown, respectively (Fig. 3-12).

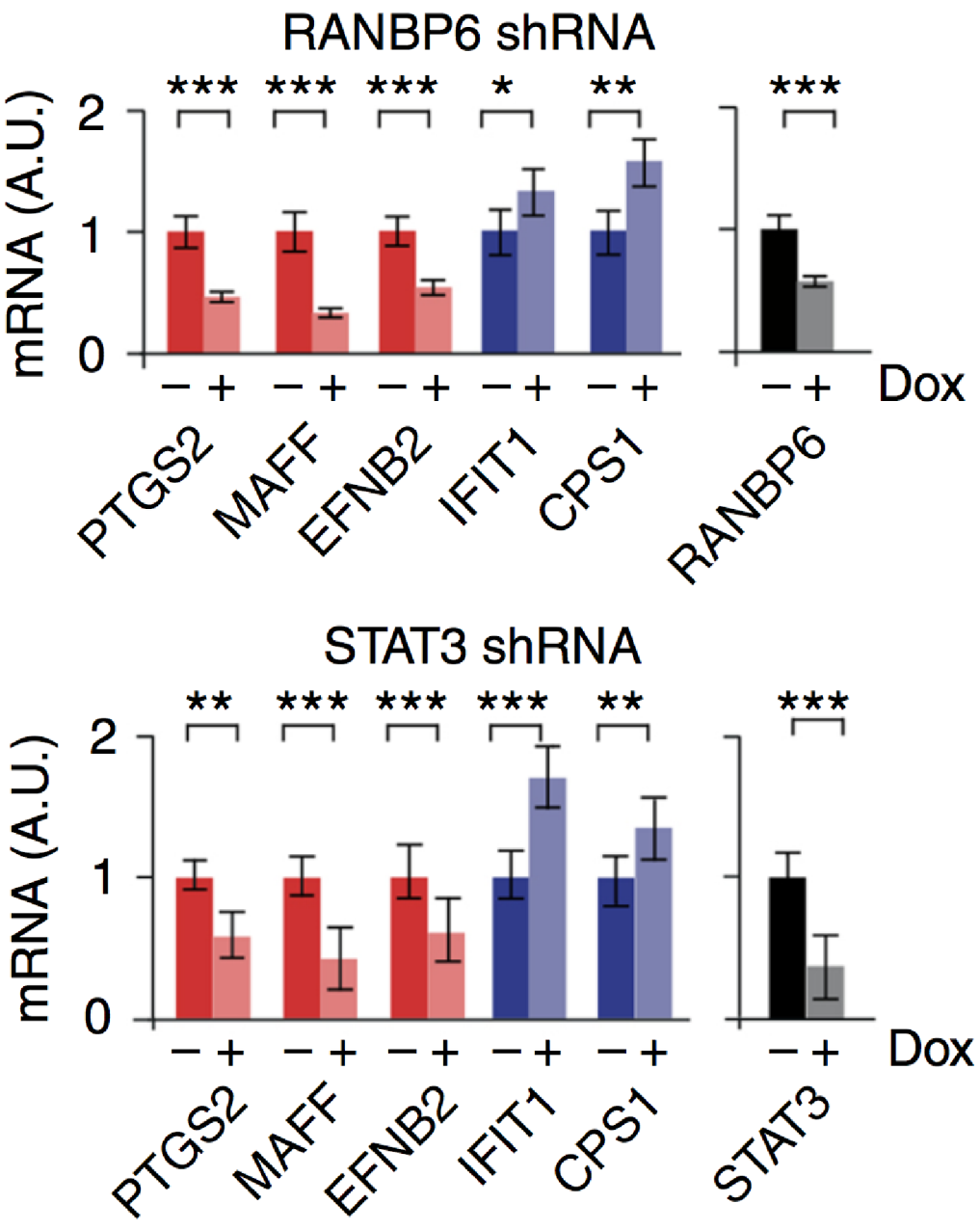

Figure 3-12. RanBP6 regulates STAT3-targeted genes. Quantitative PCR analysis of the expression of some RanBP6-regulated genes selected from ssGSEA (top panel) confirmed to be regulated by STAT3 (bottom panel). Data are represented as mean ± SD ($n \geq 3$). Student's t test: ***$p < 0.001$; **$p < 0.01$; ns not significant. Data provided by Dr. Oldrini.

3.5 RanBP6 represses EGFR transcription through activated STAT3

Given our findings that RanBP6 regulates nuclear translocation of STAT3 and STAT3-dependent transcription, we wondered whether RanBP6 mediates transcriptional repression of EGFR through STAT3. We first examined the effect of STAT3 knockdown on *EGFR* mRNA levels using HEK293T cells expressing Dox-inducible STAT3-shRNA. We observed increased EGFR mRNA and protein levels following STAT3 knockdown (Fig. 3-13).

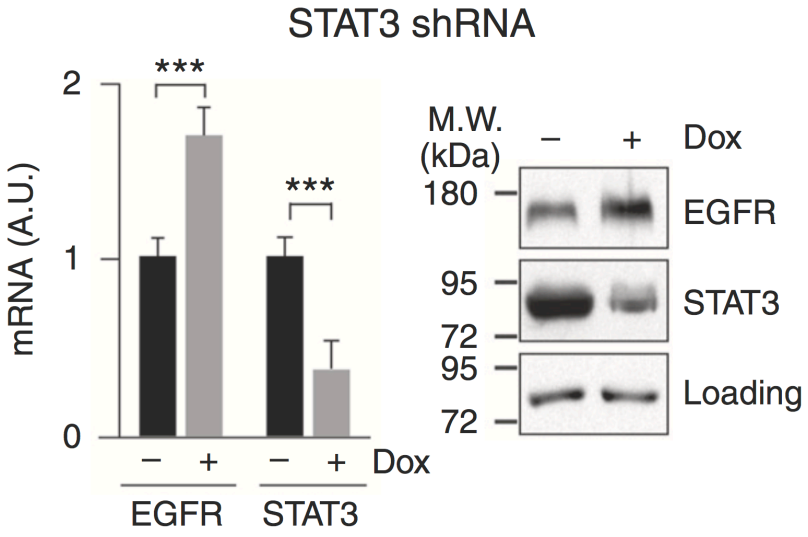

Figure 3-13. STAT3 KD increases EGFR at both protein (right panel) and mRNA levels (left panel) in HEK293T. HEK293T cells were transfected with Dox-inducible STAT3 hairpin. Data are represented as mean ± SD ($n \geq 3$). Student's t test: ***$p < 0.001$. Data provided by Dr. Oldrini.

We next examined whether EGFR might be a direct target of transcriptional repression by STAT3. Using the Jaspar transcription profile database (http://jaspar.genereg.net) (Mathelier et al., 2016), we identified multiple putative STAT3 binding sites in a 1.5 kb region upstream to the transcription starting site (TSS) of the *EGFR* gene. We selected two regions, a proximal and a distal (EGFR_1, -1340:-1111; EGFR_2, -223:-

117), for further analysis. By performing an anti-STAT3 ChIP assay in LN18 GBM cell line, we found that STAT3 protein is recruited to these two specific regions and that the binding is lost upon RanBP6 silencing (Fig. 3-14). Similar binding was observed for *PTGS2*, a known STAT3 target gene, but not for the negative control *HPRT*.

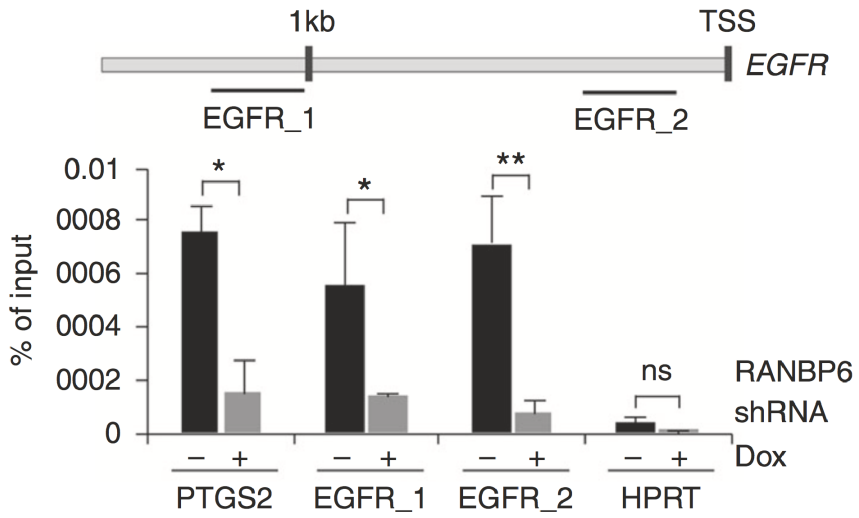

Figure 3-14. STAT3 binding to the EGFR promoter is decreased by RanBP6 KD. Bottom panel, CHIP experiments on the promoter indicated genes with STAT3 antibody in LN18 cells with Dox-inducible shRanBP6. Plotted values are relative enrichments to % input, measured for two regions (EGFR_1 and EGFR_2) in 1.5kb upstream of *EGFR* transcriptional start site (TSS) (see top panel). Binding to the *PTGS2* and *HPRT* promoter was used as positive and negative control, respectively. Data are represented as mean ± SD ($n \geq 3$). Student's t test: ***$p < 0.001$; **$p < 0.01$; ns not significant. Data provided by Dr. Carro.

Since RanBP6 associated with both STAT3 and phosphorylated STAT3 (tyrosine 705)(Fig. 3-9), we explored whether transcriptional repression of EGFR might be mediated by activated STAT3. Expression of a STAT3 mutant with constitutive activation (STAT3C) was sufficient to lower EGFR mRNA levels (Fig. 3-15) whereas inhibition of STAT3 phosphorylation with the JAK kinase inhibitor ruxolitinib raised EGFR levels in HEK293T and LN18 (Fig. 3-16).

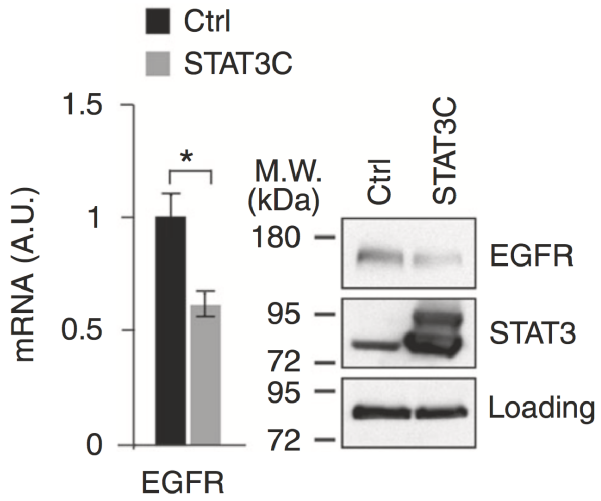

Figure 3-15. Expression of a constitutive active STAT3 mutant decreased EGFR levels. Shown is the mRNA level (left panel) and protein level (right panel) of EGFR and STAT3 in HEK293T. Data provided by Dr. Oldrini.

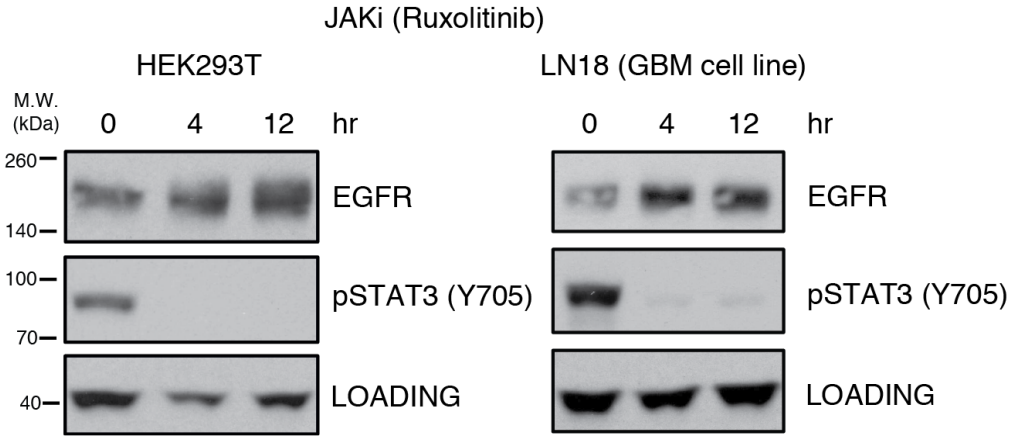

Figure 3-16. Inhibition of STAT3 activation by JAK kinase inhibitor ruxolitinib raised EGFR protein levels. HEK293T and LN18 cells were pretreated with 1 μM of ruxolitinib for the indicated time points.

Lastly, we wondered whether blockade of activated STAT3 was sufficient to mitigate the effect of RanBP6 KD on EGFR. We treated the HEK293T cells expressing Dox-inducible RanBP6 shRNA with either DMSO (vehicle) or 1 μM of ruxolitinib in a

time course manner. Consistent with what we have shown in Fig 3-16, we observed that ruxolitinib treatment raised EGFR basal levels (Fig 3-17) (compare EGFR ratios lane 5 *versus* lane 1). Furthermore, RanBP6 silencing lost its ability to raise EGFR levels in the setting of sustained (12 hours) pharmacological p-STAT3 blockade by ruxolitinib (compare EGFR ratios lane 6:lane 5 *versus* lane 2:lane 1), suggesting that RanBP6 represses EGFR transcription through activated STAT3.

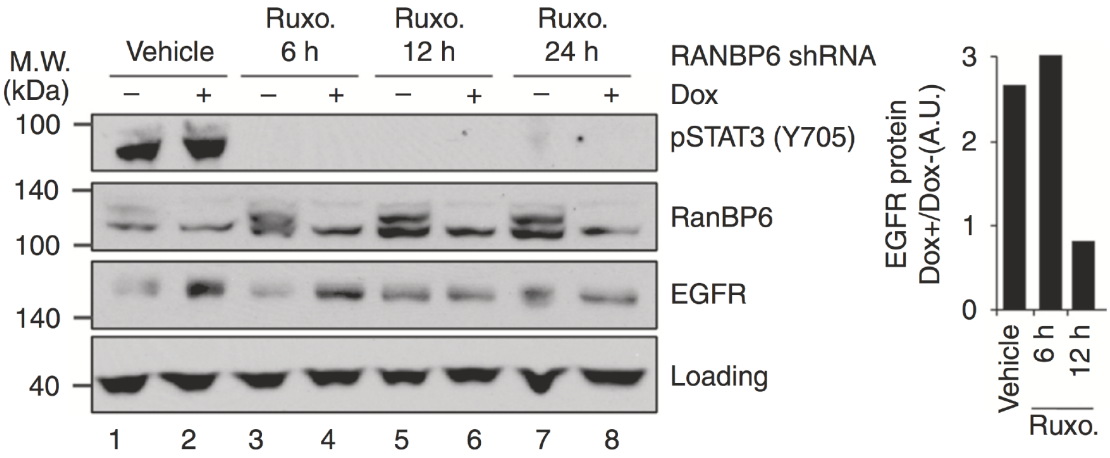

Figure 3-17. Pharmacological blockade of JAK-STAT with ruxolitinib mitigates the effect of RanBP6 KD on EGFR protein levels in HEK293T. Left panel, HEK293T cells expressing Dox-inducible RanBP6 shRNA were pretreated with 1 μM of ruxolitinib for the indicated time points. Right panel, densitometric analysis of EGFR ration between Dox+ *versus* Dox- samples for each treatment.

3.6 The effect of CRM1 inhibition on RanBP6, acetylated STAT3 or STAT3 levels

Our EGFR interactome study suggested that exportin-1 (XPO1/CRM1) also associates with EGFR, which is in line with other EGFR interactome study (Foerster et al., 2013). Furthermore, we also conducted a RanBP6 interactome and substrate screen (Chapter 6), and we found that RanBP6 is also associated with XPO1, with a preferential binding in the absence of RanQ69L (a non-hydrolyzable form of

RanGTP). In addition, a recent proteomic study on the analyses of interactors and cargoes of XPO1 showed that RanBP6 is associated with XPO1 (Kirli et al., 2015). These data suggested that XPO1 is in the same complex of EGFR-RanBP6.

Moreover, XPO1/CRM1 inhibition has been shown to repress STAT3 activation in triple-negative breast cancer cell lines (Cheng et al., 2014) and that inhibition of XPO1 using different selective inhibitors of nuclear export (SINE) perturbs cancer cell or tumor growth in multiple cancer types, including inhibition of glioma cell growth by inducing cell cycle arrest at G1 phase (Liu et al., 2016). Therefore, we further explored a potential contribution of exportin-1 (XPO1/CRM1) in our model.

It has been shown that XPO1 blockade by selinexor (KPT330), a CRM1 inhibitor that covalently binds to C528 of CRM1 and triggers CRM1 degradation, repressed the oncoprotein Survivin transcription by lowering levels of total STAT3 and STAT3 acetylation in a triple negative breast cancer cell line (MDA-MB-468) (Cheng et al., 2014). Therefore, we examine the effects of pharmacological XPO1 inhibition on acetylated STAT3 and total STAT3 levels in HEK-293T cells, as well as the GBM cell lines LN18 and SF268. XPO1 inhibition with KPT330 lowered levels of Survivin and XPO1 in all examined experimental models, which is line with other published reports (Cheng et al., 2014; De Cesare et al., 2015; Liu et al., 2016). However, we did not observe any reduction in total STAT3 or acetylated STAT3 at 48 hours (Fig 3-18a) or at any of the examined earlier time points (Fig 3-18b).

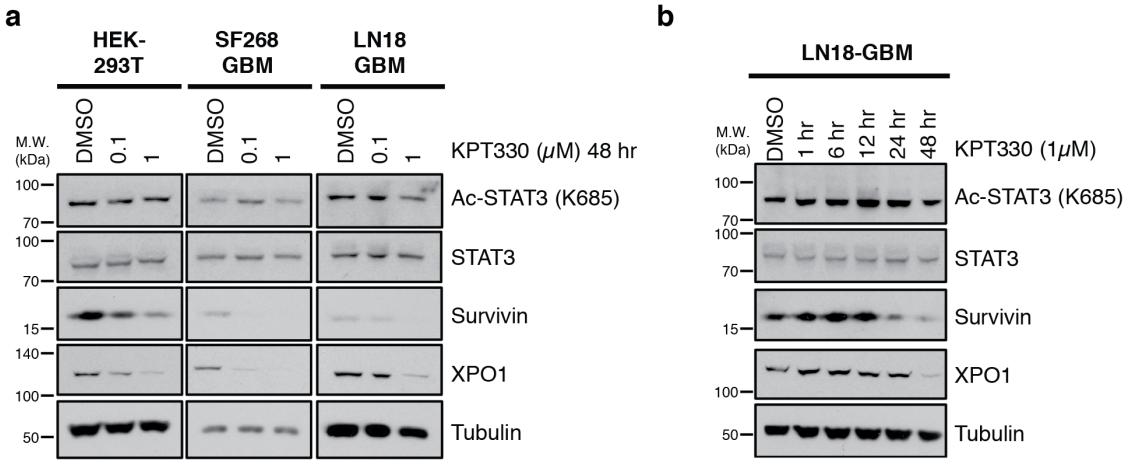

Figure 3-18. XPO1 inhibition does not reduce protein levels of total STAT3 or acetylated STAT3. a, immunoblots of whole cell lysates from the indicated cell lines treated for 48 hours with either DMSO or XPO1 inhibitor selinexor (KPT-330). **b,** immunoblots of whole cell lysates from LN18 cell lines treated with KPT-330 (1 μM) and lysed at the indicated time points.

We next examined the effects of XPO1 inhibition on RanBP6 levels using two different XPO1 inhibitors- KPT185 and KPT330. Like KPT330, KPT185 covalently binds to C528 of CRM1 and induces CRM1 degradation. Treatment of HEK293T cells with these two different SINEs does not affect RanBP6 expression, while we did observe dose-dependent reductions of XPO1 and Survivin (Fig. 3-19a). This result is also consistent with the treatments in two different GBM cell lines- SF268 and LN18 (Fig. 3-19b).

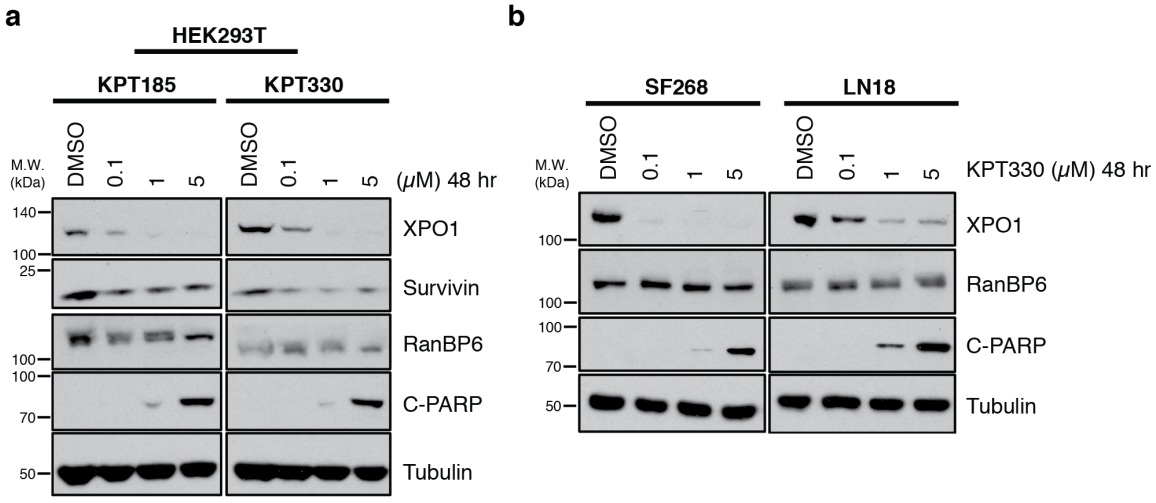

Figure 3-19. XPO1 inhibition does not affect protein levels of RanBP6. a, immunoblots of whole cell lysates from HEK293T cells treated for 48 hours with the indicated concentrations of two second generation SINEs- KPT185 (left panel), and KPT330 (right panel). **b,** immunoblots of whole cell lysates from SF268 and LN18 GBM cell lines incubated for 48 hours with indicated concentrations of KPT-330.

Lastly, we further examined the relationship between EGFR and XPO1 in the GBM-TCGA dataset. This analysis showed that: 1) XPO1 is overexpressed in GBM (Fig 3-20a), which is line with previous discovery (Green et al., 2015); 2) there was also no relationship between XPO1 mRNA levels and XPO1 gene dosage (Figure 3-20b); 3) there was no relationship between XPO1 and EGFR mRNA levels, unlike the inverse relationship between RanBP6 and EGFR in cancer cell lines and in primary human GBM tumor samples (Figure 3-20c).

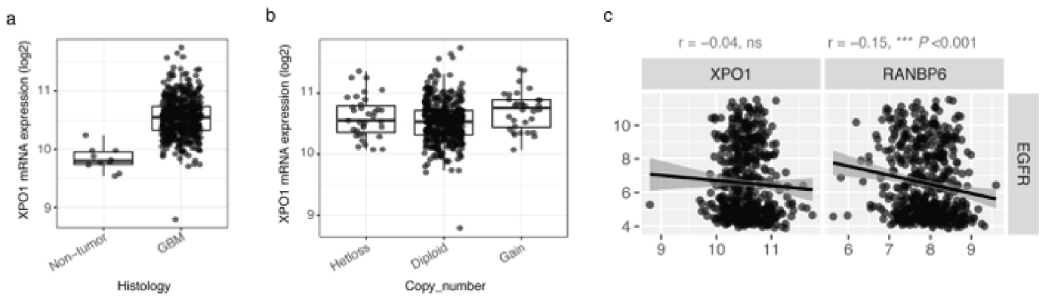

Figure 3-20. XPO1 expression in human GBM. a, and **b,** mRNA expression of XPO1 in GBM samples of the TCGA dataset stratified according to histology and XPO1 gene copy number, respectively. **c,** *RANBP6* mRNA, but not *XPO1* mRNA, negatively correlates with *EGFR* mRNA levels in GBM. Pearson's product-moment correlation is indicated.

3.7 Discussion

In the first part of this Chapter, we showed that RanBP6 negatively regulates EGFR transcription. Our data suggested that RanBP6 might possess similar functions as MIG6, which encodes a cytosolic protein that directly binds and inhibits ErbB-family receptors through their tyrosine kinase domains (Ferby et al., 2006; Maity et al., 2015). Since the protein MIG6 can binds to the tyrosine kinase domain of ERBB family members except ERBB3, we also examine whether RanBP6 regulates other ERBB family members and other receptor tyrosine kinases. Interestingly, we found that RanBP6 regulates *EGFR* and *Axl* mRNA levels, but not other RTKs including ERBB2 and ERBB3 (Fig 3-21).

The Axl has been shown to modulate acquired resistance to EGFR-targeted therapies in breast, lung and GBM (Heideman and Hynes, 2013; Meyer et al., 2013; Vouri et al., 2016). Studies have revealed that Axl could heterodimerize with the kinase domain of EGFR in cancer cells, and the activation of Axl through EGFR signaling could be ligand-independent transactivation at the cell membrane.

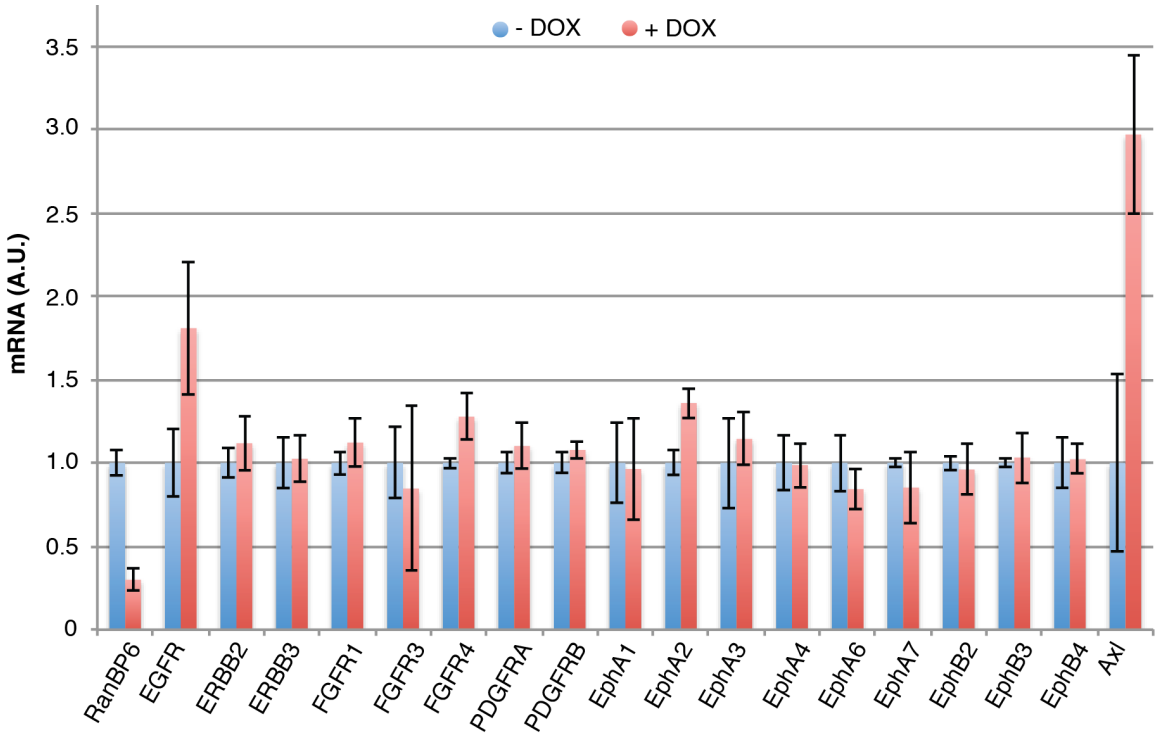

Figure 3-21. RanBP6 regulates EGFR and Axl but not other RTKs. Dox-inducible RanBP6 shRNA was stably transduced into LN18 cells (GBM cell line). Data in bar graphs are represented as mean ± SD (n=3).

We further discovered that this feedback regulation of EGFR by RanBP6 is through nuclear import of STAT3, and this STAT3 pool is more likely to be phosphorylated STAT3 (Y705), as pharmacological inhibition of p-STAT3 restores the effects of RanBP6 on EGFR.

Activation of STAT3 has been shown to promote oncogenesis in a variety of tissues, leading to intense efforts to develop STAT3 inhibitors for many cancers (Leong et al., 2003; Song et al., 2005), including highly malignant GBM. However, de la Iglesia et al. reported a PTEN-dependent tumor-suppressor function of STAT3 in glioblastoma pathogenesis (de la Iglesia et al., 2008a; de la Iglesia et al., 2008b), and its tumor suppressor function has been shown in other types of cancer, including colorectal

cancer (Musteanu et al., 2010), thyroid tumorigensis (Couto et al., 2012) and intestinal epithelial tumors (Lee et al., 2012). Our observation that STAT3 is a direct transcriptional repressor of EGFR, which has not previously been reported, is consistent with the recent report of increased EGFR signaling following JAK-STAT inhibition (Gao et al., 2016), and may have implications for targeting STAT3 for cancer therapies. Further studies are needed to determine how RanBP6-facilitated nuclear transport of STAT3 affects the substantial repertoire of STAT3 associated cellular functions and dissect transcriptional programs regulated by STAT3 and phosphorylated STAT3.

Furthermore, XPO1 is in the same complex with RanBP6 and EGFR, and XPO1 has been shown to regulate STAT3 (Cheng et al., 2014). Our observation that XPO1 did not lower total STAT3 or acetylated STAT3 in GBM cell lines is consistent with the findings (De Cesare et al., 2015), who also observed no effect of XPO1 inhibition on total or acetylated STAT3 in diffuse malignant peritoneal mesothelioma. Therefore, it is less likely that XPO1 plays a role in EGFR regulation by RanBP6.

Lastly, RanBP6 appears to regulate some other EGFR-related transcription factors in the nucleus. We showed that knockout of RanBP6 decreases nuclear cMyc and p-ERK levels but increases sp1 protein expression. It will be worth to investigate whether RanBP6 associates with these proteins, or the regulations by RanBP6 might occur through the interactions with other co-factors. Given the importance of cMyc in tumorigenesis and the undruggable properties of cMyc (Soucek and Evan, 2010), it might be interesting to examine whether and how RanBP6 regulates this transcription factor.

CHAPTER 4

THE ROLE OF PTEN IN RANBP6-EGFR INTERACTION AND REGULATION

4.1 Introduction

The tumor suppressor phosphatase and tensin homolog (PTEN) is an antagonist of phosphoinositide 3-kinase (PI3K) signaling, and it is frequently inactivated in many cancers (Chalhoub and Baker, 2009). Alterations or loss of PTEN result in activation of PI3K, which phosphorylates PIP2 to PIP3. As a consequence, excessive PIP3 localizes at the cell membrane, recruiting proteins containing PH domains, including the AKT, PDK1, and PHLPP (Soucek and Evan, 2010).

It has been shown that PTEN loss is associated with resistance to EGFR inhibitors clinically (Mellinghoff et al., 2005). Our laboratory further made a discovery that silencing of PTEN raises EGFR protein levels, in part by interfering CBL-mediated EGFR ubiquitylation and degradation (Vivanco et al., 2010).

Our discoveries that the interaction between EGFR and RanBP6 is decreased after acute EGF-stimulation (5 min, 100 ng/mL) in HEK293T cells (Fig 2-4a and Fig 2-6c). Acute EGF stimulation increases PIP3 level, which is reminiscent of PTEN loss. This raises a question whether PTEN plays an important role in RanBP6-EGFR interaction. In addition, whether the negative regulation of EGFR by RanBP6 is also PTEN-dependent.

4.2 RanBP6 and EGFR interaction is disrupted in PTEN-deficient cells

To examine whether the interaction between RanBP6 and EGFR is PTEN-dependent, we treated HEK-293T cells with EGF and then the allosteric AKT kinase inhibitor MK-2206 (Fig 4-1a). We then performed GST pulldown assays with these conditionally treated cell lysates from HEK-293T. In consistent with our previous discovery (Fig. 2-4a and Fig. 2-6c), we found a decrease association between EGFR and RanBP6 upon EGF stimulation. Addition of MK2206 (2 μM for 4 hours) on top of the EGF-stimulated cells restored the interaction of EGFR and RanBP6. (Fig. 4-1b, lane 6 *versus* lane 4). This suggested that RanBP6 might be part on an auto-regulatory mechanism where suppression of EGFR transcription by RanBP6 is temporarily inactivated following EGFR activation, perhaps to allow restoration of EGFR protein levels following ligand-induced receptor degradation.

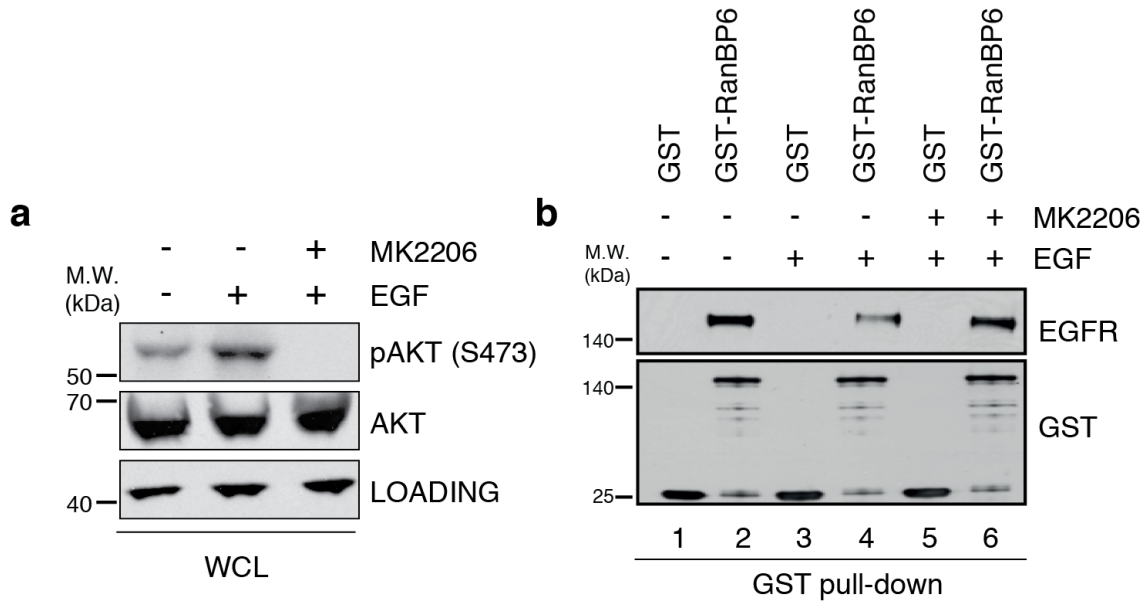

Figure 4-1. Interaction of RanBP6 and EGFR is Akt dependent. a, immunoblot of whole cell lysates (WCL) with indicated treatments, either with DMSO, 100 ng/ml of EGF (5 minutes), or 2 μM of MK2206 (4 hours). **b,** 30 μg of GST or GST-RanBP6 fusion protein were incubated with 500 μg of the pretreated HEK293T lysates from a.

In addition, we also examined the effect of PTEN knockout on the interaction between EGFR and RanBP6. We used the PTEN isogenic mouse embryonic fibroblasts (MEFs) for GST pulldown assays. GST- RanBP6 associated with endogenous EGFR in lysates from mouse embryonic fibroblasts (MEFs) but not PTEN knockout MEFs (Fig. 4-2). Taken together, these data suggest that RanBP6 and EGFR interaction is indeed PTEN-dependent.

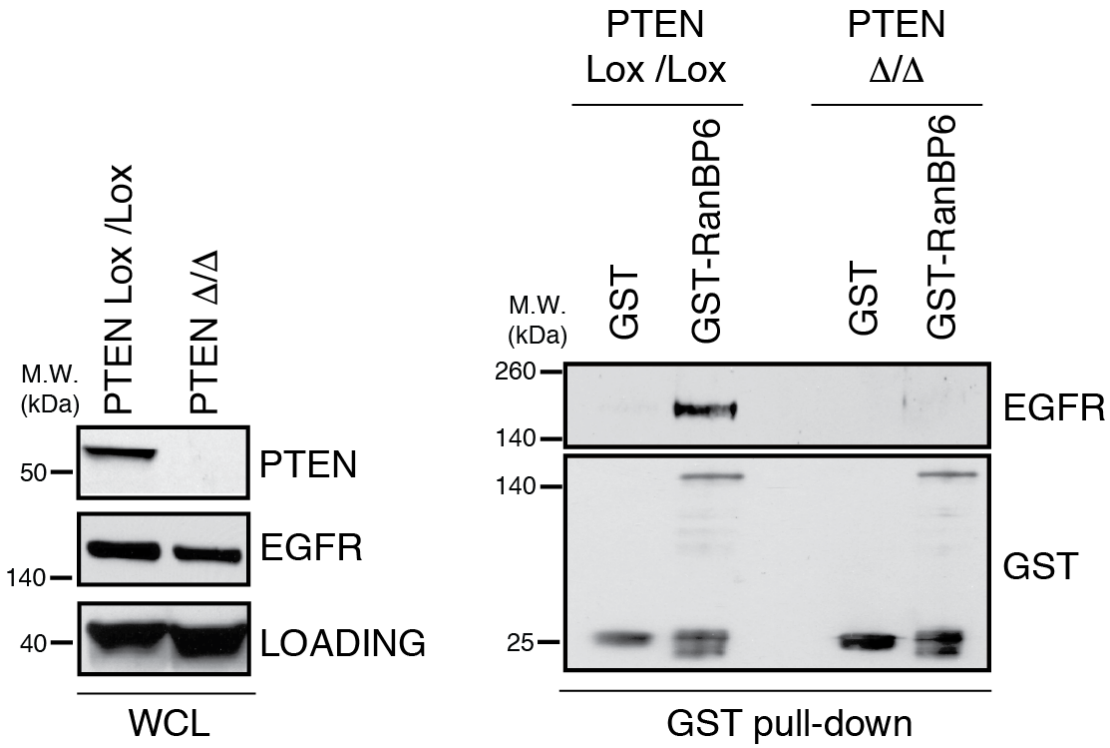

Figure 4-2. Interaction of RanBP6 and EGFR is PTEN-dependent. Left panel, immunoblot of whole cell lysates (WCL) from PTEN isogenic MEFs. Right panel, GST-RanBP6 fusion protein interacts with EGFR in PTEN $^{lox/lox}$ but not PTEN $^{\Delta/\Delta}$ MEFs.

4.3 EGFR regulation by RanBP6 is disrupted in PTEN-deficient cells

To further examine whether EGFR regulation by RanBP6 is also PTEN-dependent, we knocked down RanBP6 with Dox-inducible RanBP6 shRNA. RanBP6 only negatively

regulates EGFR in the presence of PTEN but not in PTEN null MEFs. Loss of PTEN not only impairs the interaction between EGFR and RanBP6, but also abrogates the effects of RanBP6 knockdown on *EGFR* mRNA levels (Fig. 4-3), demonstrating that both RanBP6 functions are PTEN-dependent.

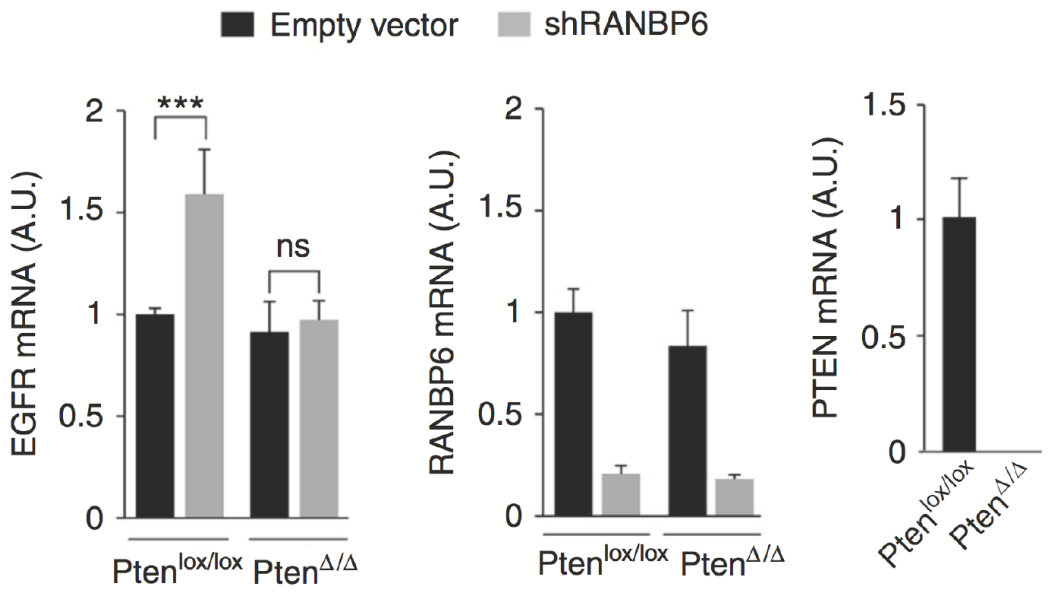

Figure 4-3. EGFR regulation by RanBP6 is PTEN-dependent. Left panel, *Ranbp6* KD raises *Egfr* mRNA level in *Pten* $^{lox/lox}$ but not *Pten* $^{\Delta/\Delta}$ MEFs; middle panel, *Ranbp6* mRNA level; right panel, *Pten* mRNA level. Data in bar graphs are represented as mean ± SD (n>=3). Student's *t* test: ***$P < 0.001$; ns, not significant. Data acquired from Dr. Oldrini.

We next examine wether PTEN status affects the relationship between *EGFR* and *RANBP6* mRNA levels in human cancer cell lines. We examined this question across a panel of 877 genetically annotated human cancer cell lines included in the publically available Cancer Cell Line Encyclopedia (CCLE) (Barretina et al., 2012). Consistent with our findings in isogenic models, we observed an inverse correlation between *RANBP6* and *EGFR* mRNA levels (Fig. 4-4, left panel). When cell lines where stratified by PTEN status, the inverse correlation between *RANBP6* and *EGFR* mRNA

levels was only present in cancer cell lines without PTEN alteration (Pearson product-moment correlation r = −0.22, p value = 2e−09) but not in cell lines with PTEN alteration (Pearson product-moment correlation r = −0.066, p value = 0.43)(Fig. 4-4, right panels). Taken together, our findings suggest that EGFR regulation by RanBP6 is disrupted in the setting of acute (e.g., EGF stimulation) or sustained (e.g., PTEN loss) PI3K pathway activation.

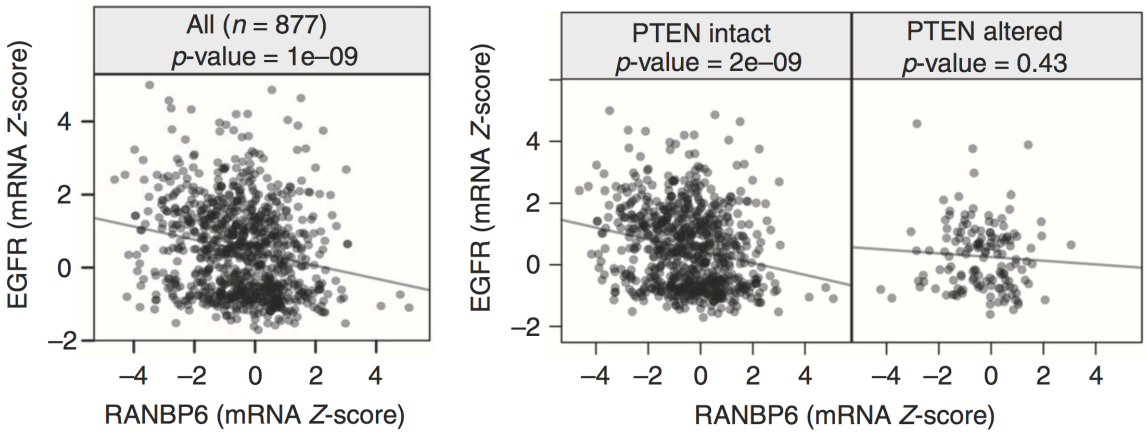

Figure 4-4. Inverse correlation between *RANBP6* and *EGFR* mRNA levels on in PTEN-intact cancer cell lines. *Left panel*, negative correlation between *RANBP6* and *EGFR* mRNA Z-score in the Cancer Cell Line Encyclopedia (n = 877, Pearson product-moment correlation r = −0.203, p value = 1e−09). *Right panels*, cancer cell lines were stratified accordingly to PTEN status. Inverse correlation between *RANBP6* and *EGFR* mRNA levels only in PTEN-intact cancer cell lines (n = 734, Pearson product-moment correlation r = −0.22, p value = 2e−09) but not PTEN altered cell lines (n = 143, Pearson product-moment correlation r = −0.066, p value = 0.43).

4.4 Discussion

In this chapter, we demonstrated that RanBP6 and EGFR interaction is dependent on the activation state of the PI3K pathway. However, it is unlikely that RanBP6 is phosphorylated by AKT or other AGC kinases because the interaction between RanBP6 and EGFR also occurs with bacterially purified GST-RanBP6, which is not amenable for posttranslational modification.

Therefore, there might be an adaptor protein or a protein complex that associates with both RanBP6 and EGFR, and these two interfaces must contain at least one association that is PTEN-dependent. For instance, phosphorylation of the adaptor protein by PI3K might result in the binding to either RanBP6 or EGFR.

Alternatively, we cannot exclude the possibility that there is a direct interaction between RanBP6 and EGFR, and the phosphorylation state of EGFR is regulated by PI3K-AKT axis. De-phosphorylation of EGFR increases the binding of EGFR and RanBP6 whereas phosphorylation of EGFR impairs this interaction. To further study the direct interaction between EGFR and RanBP6, we could purify the intracellular domain of EGFR with a tag, and incubate the purified protein with the full-length GST-RanBP6. If the direct interaction exists, we can pull down EGFR with glutathione beads and visualize both EGFR and RanBP6 bands by western blot.

CHAPTER 5

THE TUMOR SUPPRESSOR-LIKE ACTIVITY OF RANBP6 IN GLIOBLASTOMA

5.1 Introduction

Aberrant activation of EGFR in human cancer typically occurs through alterations in the *EGFR* gene, but can also be the consequence of defects in physiologic EGFR feedback regulation (Avraham and Yarden, 2011). For instance, it has been reported that *MIG6* gene is deleted in cancer and has been implicated as a tumor suppressor in experimental cancer models (Anastasi et al., 2005; Ferby et al., 2006; Maity et al., 2015).

The gene encoding *MIG6* is localized on human chromosome 1p36, a region that is known for allelic loss in human lung cancer. This suggests a prominent tumor-suppressor gene presents on this genomic locus. Although the tumor-suppressor gene *TP53* homolog, *TP73*, is located on 1p36, but no mutations have been identified in human cancers, pointing toward that *MIG-6* could be a candidate tumor-suppressor gene.

Since RanBP6 not only binds to intracellular EGFR, but also negatively regulates EGFR, which is reminiscent of MIG6, we therefore examined whether RanBP6 exhibits a tumor suppressor-like activity.

5.2 The genomic landscape of *RANBP6*

We examined this question in experimental models of glioblastoma (GBM) because we had observed in several GBMs focal deletions of the *RANBP6* gene locus on chromosome arm 9p (9p24.1). These deletions occurred independently of deletions in

CDKN2A (Fig. 5-1), suggesting that they represented two independent events with selective pressure for the loss of each gene independently. Overall, approximately 40% of GBMs in the TCGA datasets showed loss of at least one *RANBP6* allele.

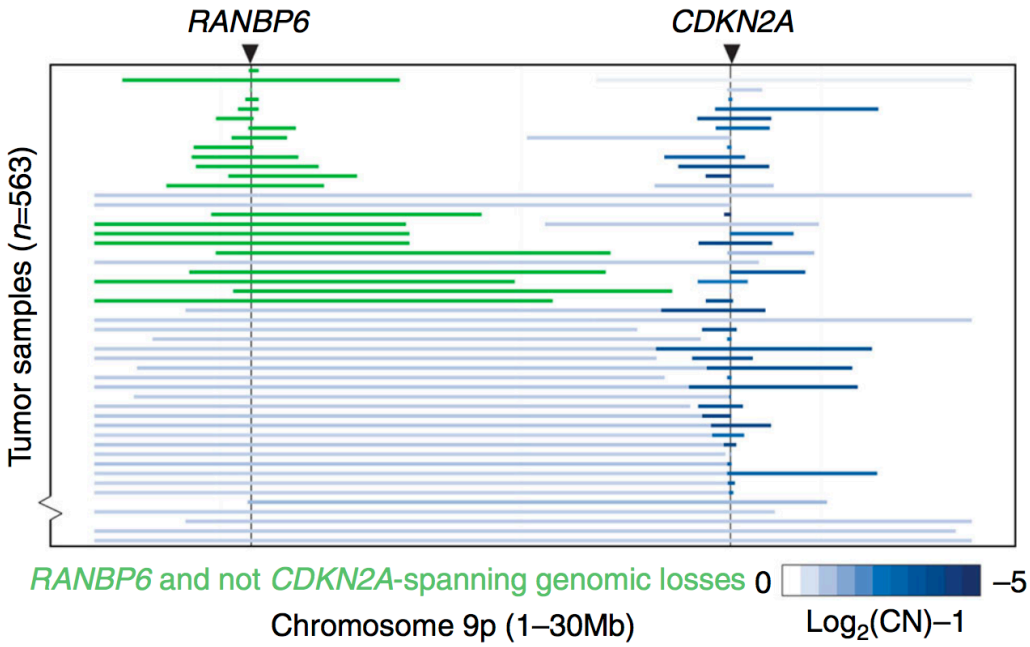

Figure 5-1. Focal deletions of the *RANBP6* (left) and *CDKN2A* (right) loci in GBM. TCGA GBM dataset analyses provided by Craig Bielski.

Copy loss at the *RANBP6* gene locus was correlated with reduced *RANBP6* mRNA levels (Fig. 5-2). *RANBP6* was lower in tumor tissue compared to adjacent normal brain tissue (Fig. 5-3).

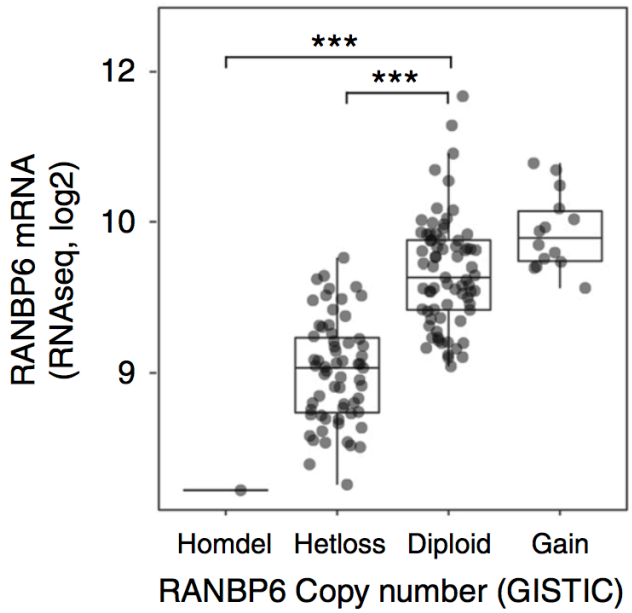

Figure 5-2. *RANBP6* copy number is correlated with *RANBP6* mRNA level. Relationship between RANBP6 copy number and mRNA levels in GBM (n = 151); Tukey's Honest Significant Difference: ***$P < 0.001$

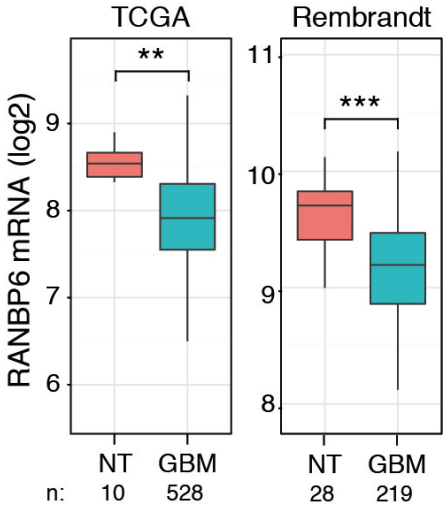

Figure 5-3. RanBP6 RNA levels in glioblastoma compared to normal brain. RANBP6 is down regulated in GBM versus non-tumoral brain control in the TCGA and Rembrandt datasets. ***$P < 0.001$; **$P < 0.01$; Tukey's Honest Significant Difference

5.3 Ectopic expression of RanBP6 suppresses EGFR and glioma growth

We next examined the relationship between RanBP6 and EGFR expression in GBM cell lines. RanBP6 knockdown upregulated EGFR expression in the PTEN-intact human GBM cell lines LN18 and LN229 (Fig. 5-4), consistent with earlier results in HEK-293T cells (Fig. 3-1).

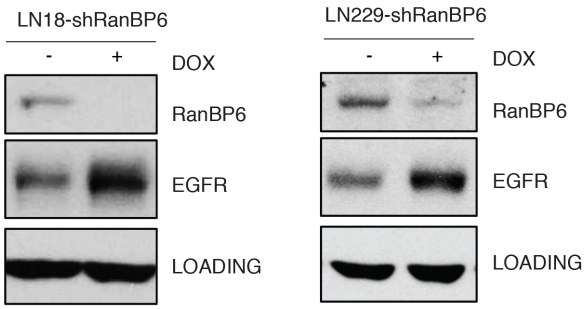

Figure 5-4. RanBP6 represses EGFR protein levels in LN18 and LN229. RanBP6 KD with Dox-inducible shRNA increases EGFR protein levels in both LN18 and LN229, two PTEN-intact GBM cell lines.

We further performed a rescue experiment by transfecting LN18 with either an empty vector (MIGR1) or RanBP6 cDNA containing three silent mutations that is resistant to human RanBP6 hairpin (Fig 5-5a). RanBP6 KD increases *EGFR* mRNA levels with control vector but not the vector containing hairpin-resistant alleles (Fig 5-5b).

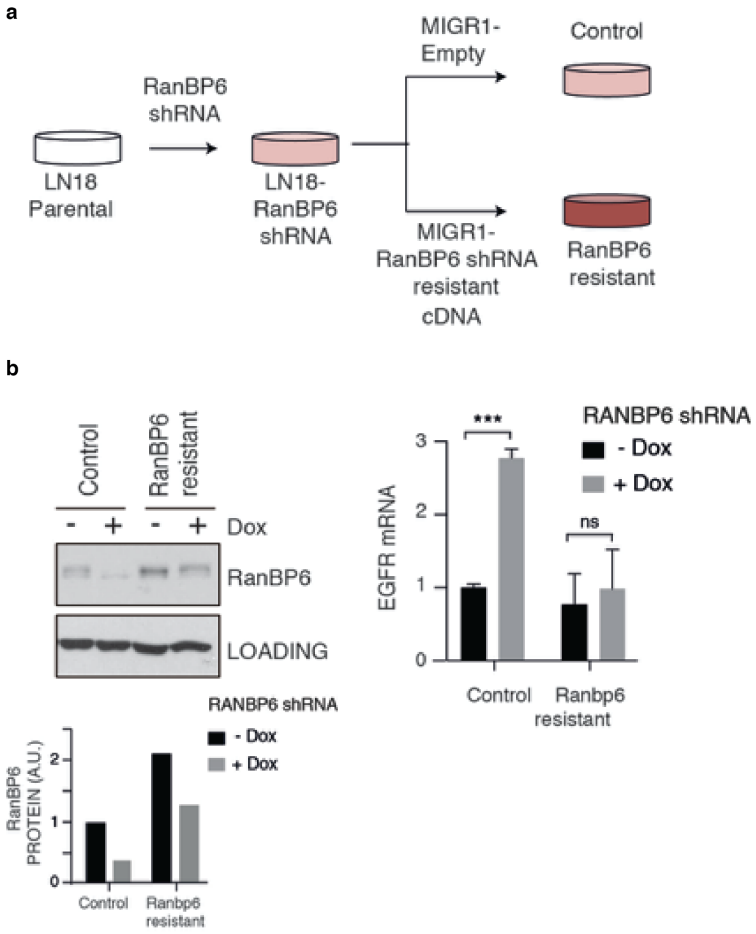

Figure 5-5. The effect of RanBP6 KD on EGFR was restored by expressing hairpin-resistant alleles. a, Cartoon showing the generation of RanBP6 shRNA resistant cDNA in LN18 cells. **b,** RanBP6 KD increases EGFR transcript levels in LN18 cells and restores of RanBP6 expression through shRNA-resistant cDNA, re-establishing normal EGFR mRNA levels. Upper left panel, immunoblot showing RanBP6 protein levels; lower left panel, densitometric analysis of RanBP6 western blot; right panel, showing is the RT-QPCR result of *EGFR* mRNA levels.

Western blotting of five patient-derived GBM tumor spheres showed markedly decreased RanBP6 protein levels in one of the five tumor sphere lines (TS516 cells) (Fig. 5-6a). We stably transduced TS516 cells with a Dox-inducible RanBP6-V5 construct and observed a reduction of colony formation in 3D soft agar assay (Fig. 5-6b). We also observed reduced EGFR protein levels upon Dox treatment (Fig. 5-6c).

Induction of RanBP6-V5 also reduced tumor growth and EGFR expression in subcutaneous TS516 xenografts (Fig. 5-6d).

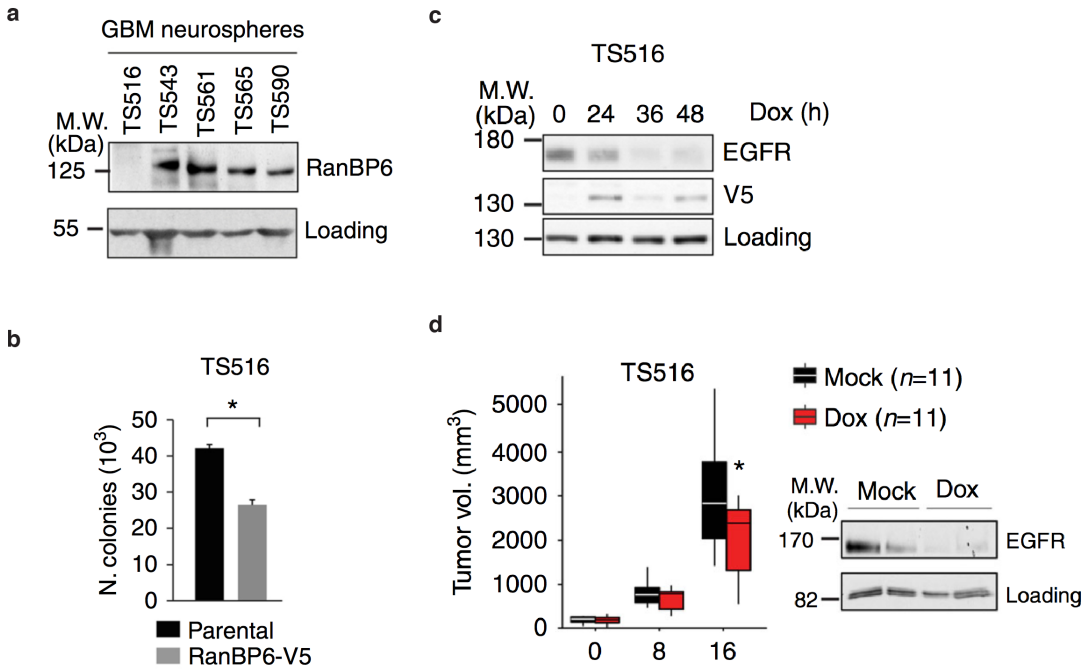

Figure 5-6. Ectopic expression of RanBP6 in TS516 decreases colony formation and tumor volume in vivo. a, RanBP6 protein levels in a panel of established patient-derived GBM tumor spheres. The immunoblots of whole-cell lysates are shown. **b,** Ectopic expression of RanBP6-V5 in RanBP6-low TS516 GBM neurosphere reduces anchorage-independent growth (left panel) and EGFR expression in a TS516 xenograft model (right panel). Student's t test: * $p < 0.05$. **c,** Ectopic expression of RanBP6-V5 reduces EGFR protein levels in a time-dependent manner. **d,** RanBP6 overexpression reduces tumor growth (left panel) and EGFR expression in a TS516 xenograft model (right panel). Student's t test: * $p < 0.05$.

RanBP6 reconstitution similarly reduced soft agar growth in RanBP6-low SF268 GBM cells (Fig. 5-7).

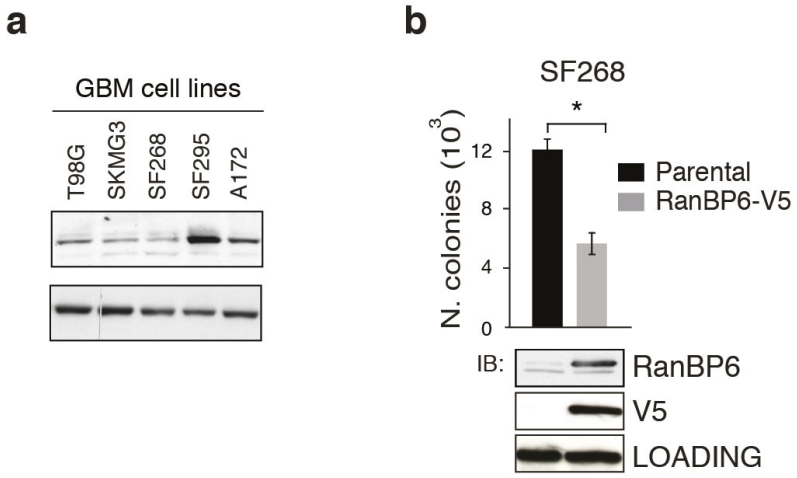

Figure 5-7. RANBP6 restoration retards growth of SF268 GBM cells. a, Immunoblot showing RanBP6 protein expression level in a panel of GBM adherent cell line. **b,** Ectopic expression of RanBP6-V5 in RanBP6-low SF268 GBM cells reduces anchorage-independent growth and lowers EGFR protein levels. Immunoblots from whole cell lysates are shown below the bar graphs. Data in bar graphs are represented as mean ± SD (n=3). Student's *t* test, $*P < 0.05$.

Lastly, we examined the effect of RanBP6 silencing on *in vivo* glioma growth using the RCAS-TVA mouse glioma model. The name RCAS stands for Replication-Competent ASLV long terminal repeat (LTR) with a Splice acceptor. For gene delivery, the avian sarcoma-leukosis virus (ASLV) requires tumor virus A (TVA) receptor to be present on the surface of target cells. Transgenic targeting of TVA to specific cell types or tissues in mice renders these cells uniquely susceptible to infection by ASLV-based RCAS viruses, making it a powerful tool for effectively modeling human tumors, including gliomas (Squatrito et al., 2010). We injected newborn *N-TVA* mice, which express the *TVA* under the control of the Nestin promoter, a well-known marker of neural stem and progenitor cells, with cells

producing the RCAS retroviruses carrying the platelet-derived growth factor-B (PDGFB) in combination with either a mouse RanBP6 shRNA or an shRNA for Luciferase as control. RanBP6 knockdown decreased survival, with mice injected with the RanBP6 shRNA living an average of 189 days (n = 10) and control mice living 275.5 days (n = 14)(p = 0.047, log rank test)(Fig. 5-8a) and promoted the development of higher grade gliomas (Fig. 5-8b and 5-8c). Cells derived from RanBP6 knockdown tumors showed increased *EGFR* mRNA levels (Fig. 5-8d).

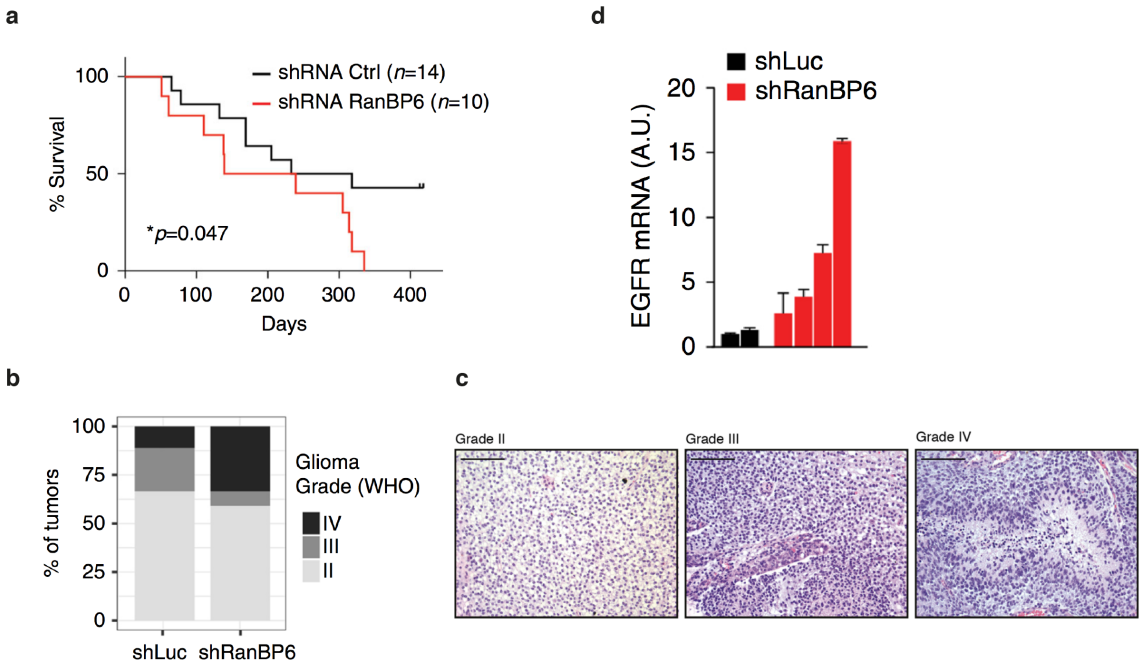

Figure 5-8. RANBP6 KD in reduces survival rate in an orthotopic glioma mouse model, increases high grade glioma and showed an enrichment of *Egfr* mRNA from the tumors. a, RanBP6 KD reduces survival in RCAS-tva mouse glioma model. Kaplan-Meier survival curves of PDGFB-induced gliomas generated in Nestin-tva mice injected with either RCAS-RanBP6 shRNA or RCAS-Luciferase shRNA as a control. **b,** Tumor grade (WHO classification) of gliomas in the RCAS-tva model. **c,** RANBP6 silencing increases GBM frequency. Representative H&E images of tumors from the RCAS-PDGF injected mice. Tumors were classified using the World Health Organization (WHO) grading system. Glioblastoma (GBM) are Grade IV. **d,** RanBP6 KD increases *Egfr* mRNA in samples from the RCAS-tva mice. Data in bar graphs are represented as mean ± SD (n ≥ 3). Data provided by Dr. Oldrini and Dr. Squatrito.

5.4 Deletion of RanBP6 in glioma cell lines increases resistance to EGFR tyrosine kinase inhibitors (TKIs)

EGFR gene is frequently amplified in GBM (approximately 40% of GBM cases), rendering it a prime target for GBM treatment (Vivanco and Mellinghoff, 2010). The two most common gain-of-function mutations are both within the extracellular domain, including 1) an in-frame deletion of exon 2-7 that is unable for ligand-binding and therefore constitutively activation of EGFR (referred to EGFRvIII), and 2) several missense mutations that cluster in extracellular domains I, II and IV. However, inhibition of EGFR by tyrosine kinase inhibitors (TKIs) has been disappointing in GBM because most of GBMs with EGFR alterations also present PTEN inactivation, an event that has been shown to confer resistance (Mellinghoff et al., 2005). We previously showed that PTEN loss confers EGFR TKI resistance, at least in part by raising EGFR levels (Vivanco et al., 2010). Since RanBP6 binds to EGFR in a PTEN-dependent manner and downregulation of RanBP6 increases EGFR signal output, we hypothesized that RanBP6 alters the sensitivity of GBM cell lines to EGFR TKIs.

We first examined the effect of RanBP6 knockdown (KD) on EGFR in both PTEN-intact and PTEN-altered glioma cell lines. In line with our previous data in LN18 and LN229 glioma PTEN-intact cell lines (Fig. 5-4), RanBP6 KD increases EGFR protein levels in Hs683, a PTEN-intact glioma cell line, while RanBP6 depletion does not raise EGFR level in SKMG-3, a PTEN-null glioma cell line overexpressing EGFR (Fig. 5-9a). We further examined whether RanBP6 silencing would also be sufficient to confer EGFR TKI resistance, and if so, whether it is also PTEN-dependent. Consistent with this model, we observed that RanBP6 knockdown confers lapatinib (EGFR/HER2 dual kinase irreversible inhibitor) resistance in PTEN wt Hs683, but not in PTEN deleted SKMG3 (Fig. 5-9b and 5-9c). We further performed a similar dose-

responsive experiment using erlotonib (an irreversible EGFR kinase inhibitor) in PTEN wt LN229 glioma cell line. We observed increased phosphorylation of EGFR (Y1068) upon RanBP6 KD (Fig. 5-9c).

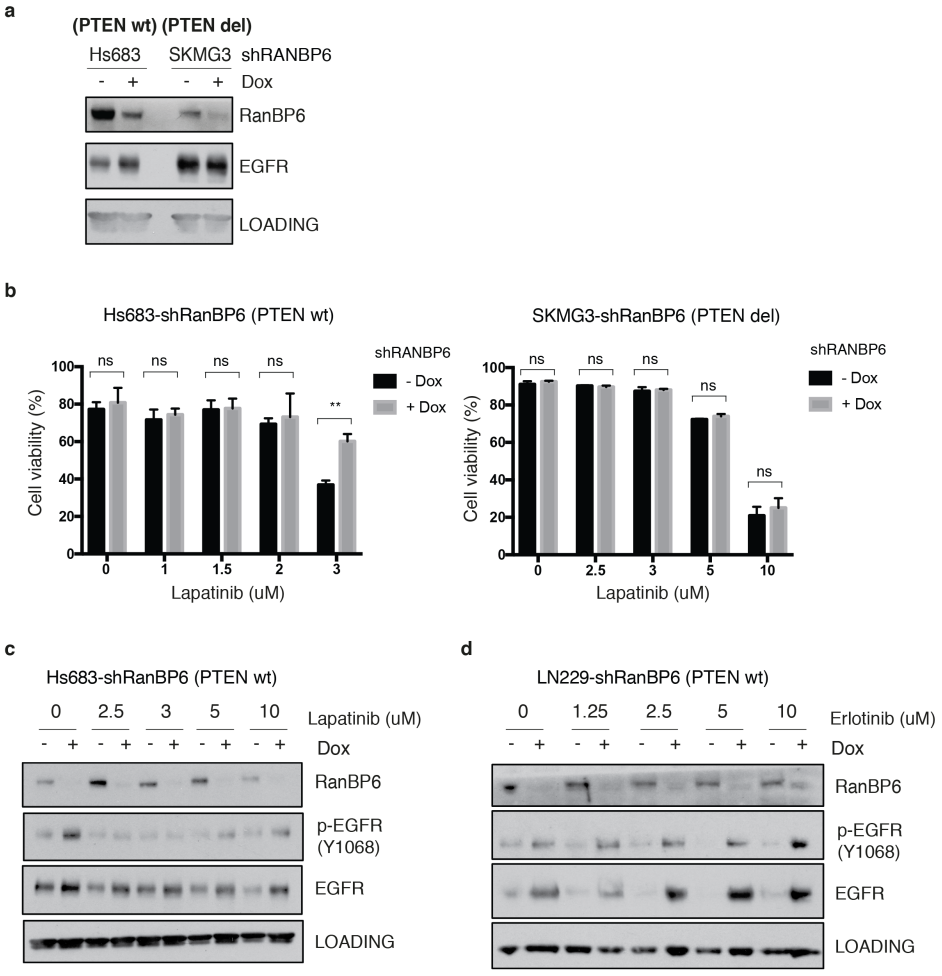

Figure 5-9. RanBP6 KD increases drug resistance to EGFR tyrosine kinase inhibitors in a PTEN-dependent manner. a, RanBP6 KD increases EGFR level in PTEN wildtype (wt) glioma cell line Hs683 but not PTEN deletion (del) glioma cell line SKMG3. **b,** shown are cell viability (%) measured by trypan blue assays. In brief, 30k cells were seeded in 6-cm dish in triplicates in 5% FBS+DMEM. Dox were pre-treated 2 days before seeding the cells. Cells were collected at day 5. Left panel, Hs683 with Dox-inducible RanBP6-shRNA; right panel, SKMG3 with Dox-inducible RanBP6-shRNA. Student's t test: ** <0.01, ns = not significant. **c,** immunoblot showing increased phosphorylation of EGFR (Y1068) in Hs683 RanBP6 KD cells at high concentrations of lapatinib. **d,** immunoblot showing increased phosphorylation of EGFR (Y1068) in LN229 RanBP6 KD cells at high concentrations of erlotinib.

5.5 Discussion

In this Chapter, we introduced a role of RanBP6 in suppressing glioma cell growth in 3D soft agar assay, as well as *in vivo* xenograft and orthotopic glioma mouse models. Our data suggested that RanBP6 possesses a tumor suppressor-like activity, at least in GBM. While we observed EGFR expression decreases upon ectopic expression of RanBP6, we could not exclude the possibility that the tumor suppressor activity of RanBP6 is mediated by other functions of RanBP6 that go beyond suppressing EGFR. Therefore, a deeper understanding of the biological functions of RanBP6 seems to be warranted.

Furthermore, we also found that RanBP6 suppresses EGFR expression preferentially in non-EGFR-amplified cancer cell lines, but not in EGFR-amplified cohorts from our CCLE analyses (data now shown), which is consistent with our *in vitro* data. When we knocked down RanBP6 in HCC827, a lung adenocarcinoma cell line overexpressing EGFR, we could not observe the effects of RanBP6 on EGFR (data now shown). These data point toward the necessity to explore the tumor suppressor function of RanBP6 in EGFR-dependent but not EGFR-overexpression cancer cell lines.

Drug resistance to EGFR TKIs has been a problem in treating EGFR-addictive cancers. Here, our preliminary data showed that RanBP6 confers resistance to EGFR TKIs in a PTEN-dependent manner. Therefore, a more thorough examination of RanBP6 KD in a panel of PTEN-dependent and non-EGFR-amplified GBM cell lines with lapatinib or erlotinib treatment could be insightful. Furthermore, we demonstrated that RanBP6 KD increases *Axl* mRNA level in a profound manner (Fig. 3-21). Taken together, these data led us to consider a possible mechanism that RanBP6 confers EGFR TKI resistance through regulating Axl, which is known for its role in

EGFR drug resistance (Heideman and Hynes, 2013; Meyer et al., 2013; Vouri et al., 2016).

CHAPTER 6

IDENTIFICATION OF RANBP6 INTERACTOME AND SUBSTRATES

6.1 Introduction

We have shown that RanBP6 is a member of the importin β superfamily and is involved in the nucleo-cytoplasmic transport. However, the substrates of RanBP6 and its biological function remain undetermined (Kimura et al., 2017). Furthermore, the tumor suppressor activity of RanBP6 may go beyond its function in regulating EGFR. It is possible that RanBP6 gains its tumor suppressor activity through its function as a transport receptor, since disruptions in the nucleo-cytoplasmic transport machinery result in tumorigenesis in many types of cancer.

Therefore, we sought to understand the fundamental biology of RanBP6 by screening its interactome and substrates. In particular, we aimed to identify RanBP6 cargoes by performing a RanGTP competition assay. It has been shown that high concentration of RanGTP competes out the substrates of the importin, and promotes the formation of exportin complexes in the nucleus (Fig. 1-4) (Guttinger et al., 2004; Jakel and Gorlich, 1998; Kimura et al., 2013a; Kimura et al., 2017; Kimura et al., 2013b; Kirli et al., 2015; Kutay et al., 2000; Mingot et al., 2004; Mingot et al., 2001). We proposed to use LC-MS/MS as a tool to identify RanBP6 interactome and substrates for this study.

Since RanBP6 preferentially binds to nuclear RanGTP (Fig. 2-8a), we considered it could function as both importin and exportin. This bi-directional function has been characterized for Importin 13 (Mingot et al., 2001).

6.2 Biochemical preparation of materials for RanGTP competition assay

To identify RanBP6 substrates, we purified RanBP6 and RanGTPase, as well as HeLa cytosolic extracts (Fig. 6-1a). We first established protocols to overexpress recombinant pCMV-HA-RanBP6 in Expi293 cells. In particular, we maximized the yield of RanBP6 protein from Expi293 by optimizing the transfection time (Fig. 6-1b).

We modified the approach that was routinely utilized for screening substrates of other members in the importin β superfamily (Mingot et al., 2001). We used the mammalian expression system instead of *E. coli* since the interactions of RanBP6 and its substrates may require certain posttranslational modifications. First, we pulled down RanBP6 using HA magnetic beads that are conjugated with a HA-antibody. Elution with 2X SDS revealed that RanBP6 is the major component besides the antibody fragments from the beads (Fig. 6-1c). These RanBP6-immobilized HA beads were later used to pulldown the cargoes of RanBP6. Of note, we also overexpressed HA-empty and performed HA-pulldown assays using the same protocol. These HA-empty-immobilized HA beads were used in the following experiments to eliminate contaminants from the HA-pulldown or any non-specific binding to the HA beads.

We then prepared the HeLa cytosolic extracts as the repertoire for the cargoes of RanBP6. The supernatant was further analyzed on western blot with histone H3 antibody, a marker for nuclear fraction. We confirmed that there was no nuclear contamination of the cytosolic extract (Fig. 6-1d).

Lastly, we followed the reported protocols to obtain recombinant His-RanQ69L, a mutant that blocks RanGTP hydrolysis and locks Ran in the GTP form from *E. coli*. We also re-charged Ran with GTP in order to obtain RanGTP. The purified His-

RanQ69L was confirmed by SDS-PAGE, and Ran was the major component in our purified samples (Fig. 6-1e).

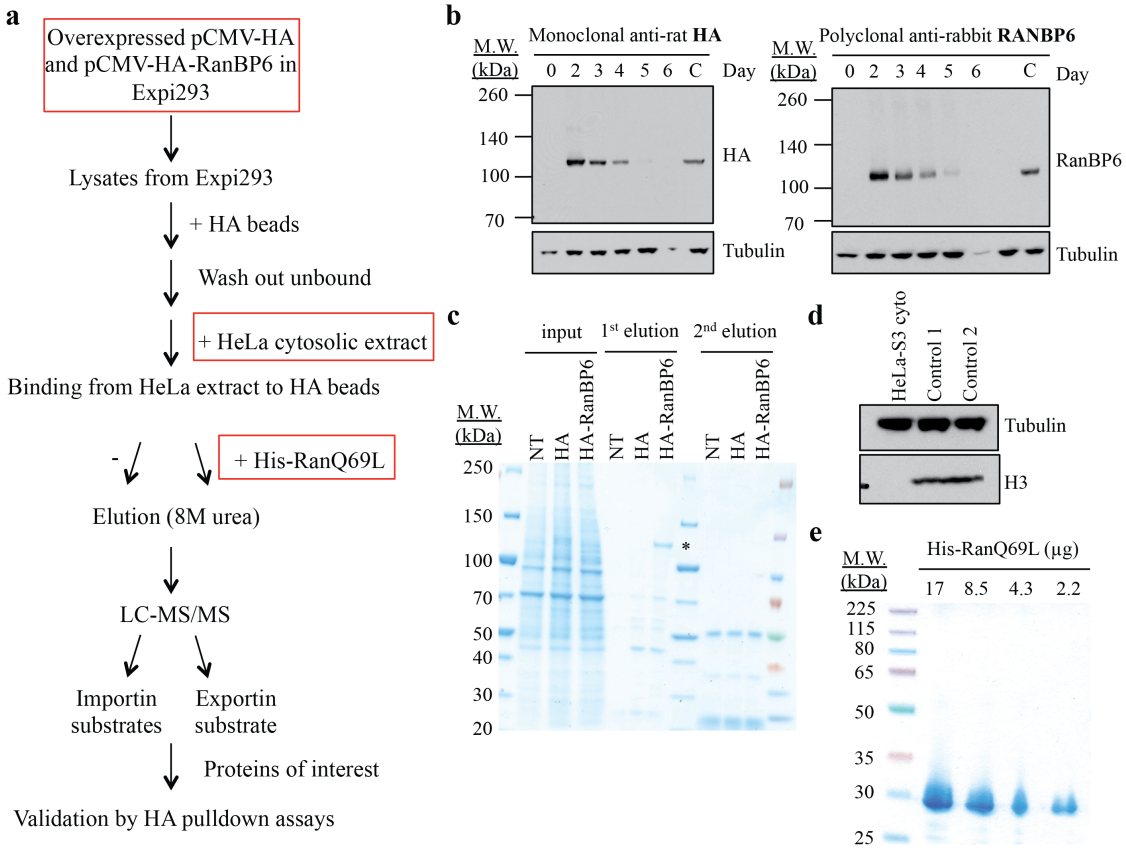

Figure 6-1. Workflow and validation of materials for identification of RanBP6 substrates by LC-MS/MS. a, Workflow utilized in this proposed study. **b**, HA-RanBP6 expression detected by monoclonal anti-rat HA (left panel) and polyclonal anti-rabbit RanBP6 (right panel) antibodies. Day= the time after transfection; C= control lysate. **c**, Shown is the HA pulldown assays with Expi293 lysates overexpressing either HA or HA-RanBP6 by CBB staining. NT= non-transfected control; *= HA-RanBP6 (126 kDa). **d**, HeLa-S3 cytosolic lysates by western blot. No nuclear contamination was detected. Control 1&2= total cellular lysates. **e**, Purified His-RanQ69L (28 kDa) by CBB staining. All the materials described above were aliquoted and snapped frozen with liquid nitrogen.

6.3 Pulldown of RanBP6 cargoes for LC-MS/MS study

To prepare samples for the MS study, HeLa cytosolic extracts were incubated with roughly 1μM of either HA or HA-RanBP6, and in the presence or absence of 5μM of His-RanQ69L, according to the workflow shown in Figure 6-1a. All samples were prepared in biological triplicates (Expi293 expressing HA or HA-RanBP6 were from three independent transfections). Therefore, a total of 12 samples with four different combinations were eluted with 8M urea for LC-MS/MS study:

1) HA-empty
2) HA-empty + His-RanQ69L
3) HA-RanBP6
4) HA-RanBP6 + His-RanQ69L.

We expected importin substrates to bind to HA-RanBP6 but to be competed out by addition of His-RanQ69L. On the other hand, we expected exportin substrates to bind to HA-RanBP6 with the presence of His-RanQ69L. Moreover, we predicted that RanBP6 interactors will not be affected by the RanGTP gradient. We expected them to be present in the HA-RanBP6 samples.

6.4 Potential RanBP6 interactors and substrates

We analyzed our MS data based on the intensity of the protein, which we identified with Proteome Discoverer software. In summary, our bait- RanBP6 was found in 6 samples (biological triplicates of HA-RanBP6 and HA-RanBP6+His-RanQ69L) but not HA-empty samples. A total of 2,200 proteins were identified, with the false discovery rate (FDR) ≤ 1%. First, we categorized these proteins into three groups: ‘empty’ (a total of 6 samples including 3 biological replicates of HA -/+ RanQ69L),

'RANBP6' (3 biological replicates) and 'RANBP6+RANQ69L' (3 biological replicates). Second, we set up a filter for proteins that were measured in at least 66% of the replicates in a group in at least one condition. This filter narrowed down the number of proteins to 1,685. Third, we performed two independent T-tests (p-value < 0.05) by comparing 'empty to RANBP6' and 'empty to RANBP6+RANQ69L.' We found that 645 proteins were significant. Fourth, we kept the proteins that were detected in either 'RANBP6' or 'RANBP6+RANQ69L,' and had more abundance over 'empty.' This filter brought down the number to 274 proteins, which we identified as RanBP6 'interactors.' Lastly, we performed a T-test (p-value <0.05) by comparing 'RANBP6' and 'RANBP6+RANQ69L.' We identified a total of 75 proteins as RanBP6 importin or exportin substrates.

We imported RanBP6 interactors (274 proteins) to STRING database (https://string-db.org) and obtained a map of interactors based on their biological processes (e.g., protein localization or intracellular protein transport) (Fig. 6-2). We also generated a volcano plot for RanBP6 substrates (75 proteins) (Fig. 6-3). These RanBP6 substrates were further narrowed down to a list of 24 proteins, based on their abundances, Log2 fold-change, and relevance to cancer development in the NCBI PubMed database (Table 6-1).

In summary, we obtained a list of 274 proteins as RanBP6 interactors, including importins, exportins, and proteins constantly bound to RanBP6 regardless of the presence or absence of RanQ69L. We further identified a list of 75 proteins as RanBP6 substrates based on their differential associations with RanQ69L. String database analyses suggested that RanBP6-associated proteins are mostly involved in macromolecule localization (GO:0033036) or metabolic process (GO:0008152),

which might not be surprising given the role of RanBP6 in the nucleo-cytoplasmic transport. For instance, our data showed that RanBP6 associates with multiple nucleoporins (Nup93 and Nup88) and the translocon Sec 61 complex (Sec61B and Sec61A1) on ER, which are involved in protein trafficking. Furthermore, RanBP6 might also play a role in mitochondrial shuttling due to its interactions with several proteins involved in mitochondrial transport (i.e., TOMM22, NDUFV1, and ATP5L).

Our top priority for this study will be to focus on the candidate substrates of RanBP6, the proteins that have shown differential associations with RanQ69L. Among these 75 substrates, we found that most of them can be categorized into three different biological functions:

1) Cell cycle, cell division or mitosis, such as cyclin-dependent kinase 1 (CDK1), and protein arginine N-methyltransferase 1 (PRMT1)

2) Intracellular trafficking, such as Exportin-1 (XPO1), Ras-related protein Rab-35

3) Mitochondrial transport, such as Mitochondrial import receptor subunit TOM70 (TOMM70A) and the apoptosis regulator BAX

Of note, most of the substrates we discovered were importin substrates, consistent with the nomenclature of RanBP6 as importin-6 (Fig. 6-3). Importantly, Ran was highly enriched with a negative value of the Log2 fold difference of RANBP6 *versus* RANBP6+RANQ69L (X-axis), suggesting that our RanGTP was indeed bound to RanBP6.

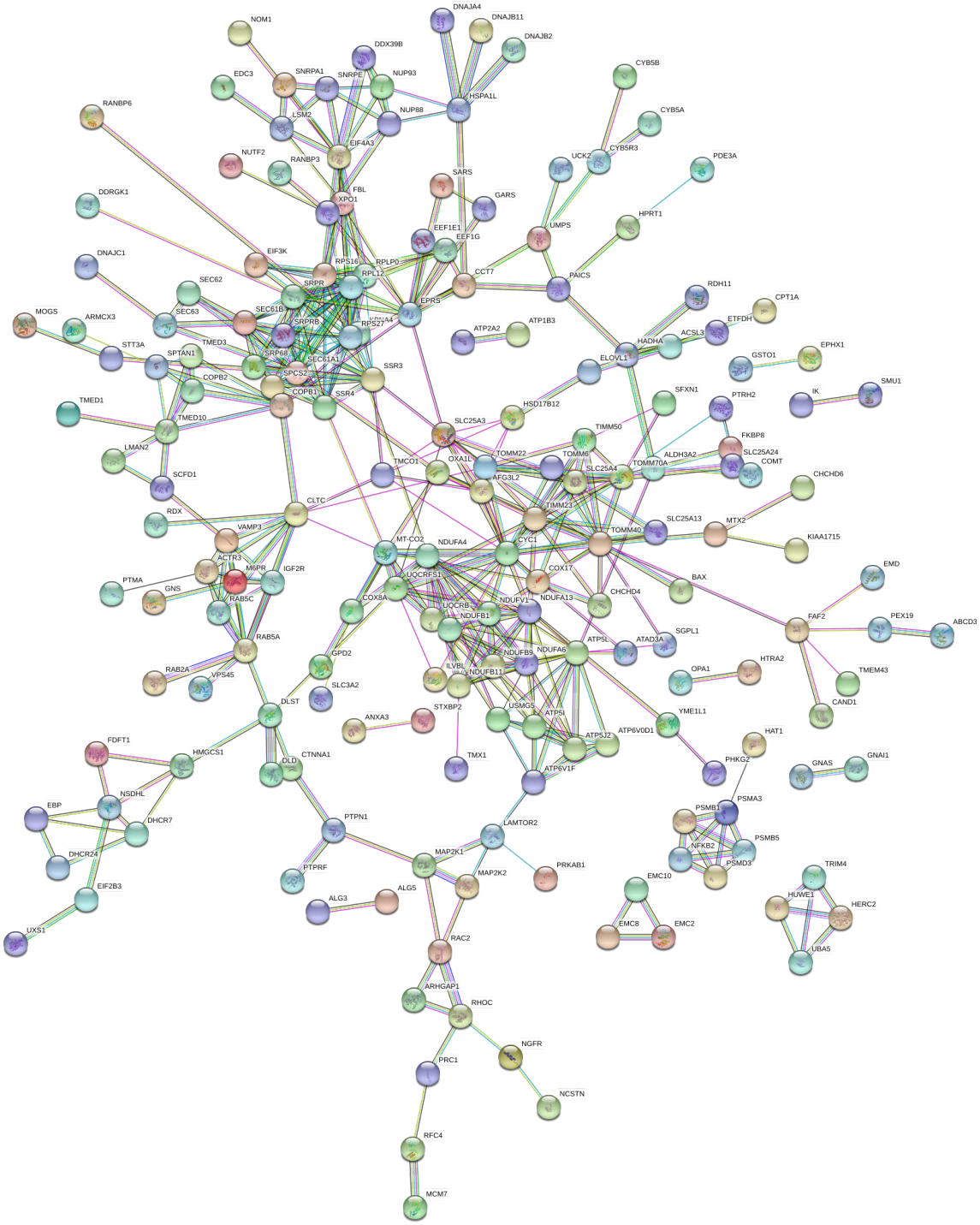

Figure 6-2. RanBP6 interactome map (274 proteins) from STRING database. Shown is a map of protein-protein interactions based on their biological processes.

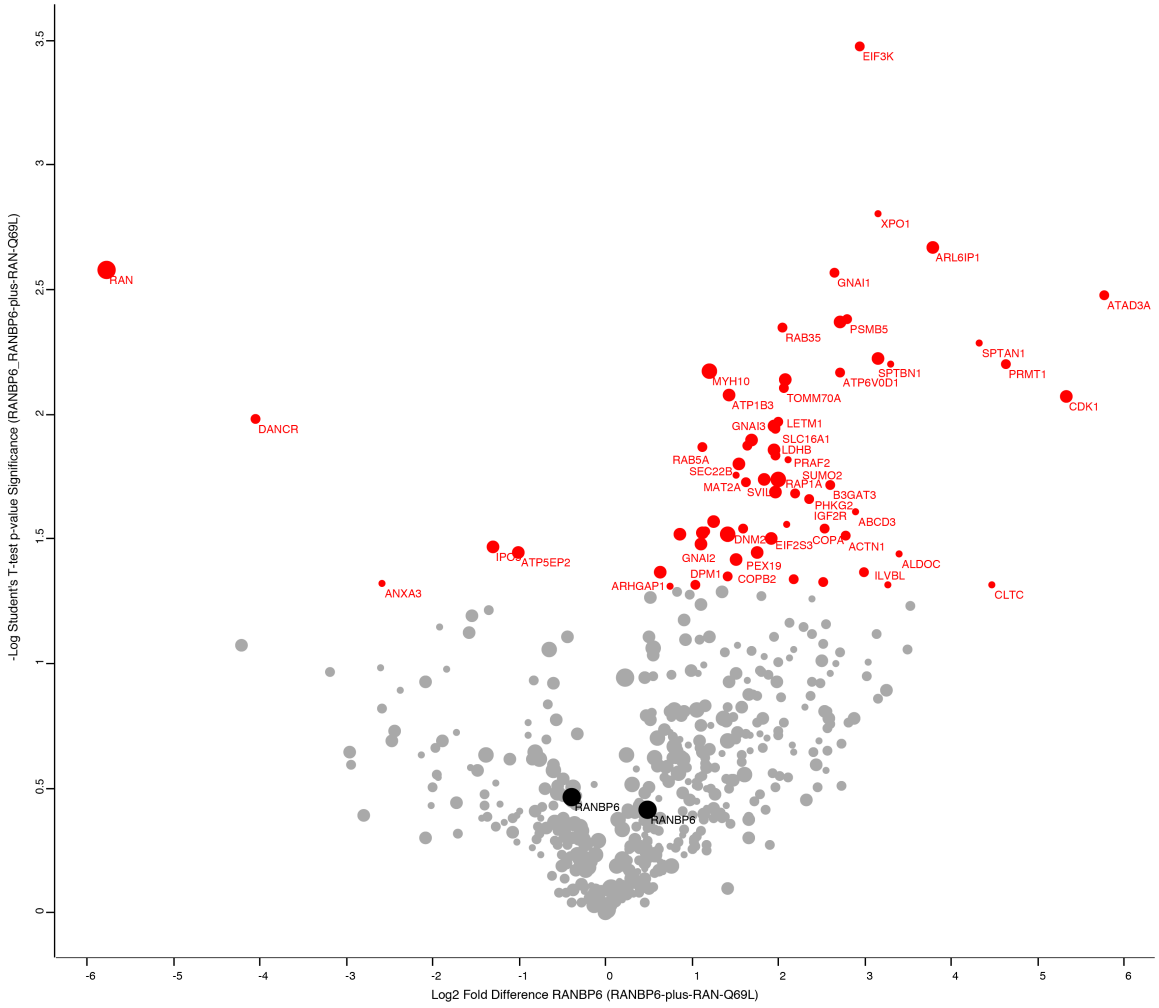

Figure 6-3. Volcano plot for RanBP6 substrates
X-axis, Log2 fold difference by comparing 'RANBP6' *versus* 'RANBP6+RANQ69L.' Y-axis, T-test significance by comparing 'RANBP6' *versus* 'RANBP6+RANQ69L. Red dots: Significant substrates. Grey dots: non-significant substrates. Noted that there are two RanBP6 (black dots), one of which is the proteolytic form of RanBP6. Red dots that have Log2 fold difference greater than 0.5 are importin substrates, while those ones are lower than -0.5 are exportin substrates. The diameters of the circles represent the abundance of the proteins pulled down in the MS study.

Table 6-1. Cancer-associated RanBP6 substrates. A list of 24 proteins that have been shown to be associated with tumorigenesis according to NCBI PubMed database.

Protein name	gene names
Cyclin-dependent kinase 1	CDK1;CDC2
Protein arginine N-methyltransferase 1	PRMT1
Protein flightless-1 homolog	FLII
Exportin-1	XPO1
Proteasome subunit beta type-5	PSMB5
Coatomer subunit alpha;Xenin;Proxenin	COPA
Apoptosis regulator BAX	BAX
Cation-independent mannose-6-phosphate receptor (insulin-like growth factor-2 receptor)	IGF2R
Alpha-globin transcription factor CP2	TFCP2
Ras-related protein Rab-35	RAB35
Small ubiquitin-related modifier 2;Small ubiquitin-related modifier 4;Small ubiquitin-related modifier 3	SUMO2;SUMO3;SUMO4
LETM1 and EF-hand domain-containing protein 1, mitochondrial	LETM1
PRA1 family protein 2	PRAF2
Monocarboxylate transporter 1	SLC16A1
L-lactate dehydrogenase B chain;L-lactate dehydrogenase	LDHB
Ras-related protein Rap-1A;Ras-related protein Rap-1b;Ras-related protein Rap-1b-like protein	RAP1A;RAP1B
Delta(24)-sterol reductase	Nbla03646;DHCR24
S-adenosylmethionine synthase isoform type-2	MAT2A
Dynamin-2	DNM2
Transcription intermediary factor 1-beta (TIF-1B; KAP-1)	TRIM28
Ras-related protein Rab-5A	RAB5A
Serine/threonine-protein phosphatase 2A 55 kDa regulatory subunit B alpha isoform	PPP2R2A
Guanine nucleotide-binding protein G(i) subunit alpha-2	GNAI2
Rho GTPase-activating protein 1	ARHGAP1

6.5 Discussion

In this study, we sought to advance our understanding of the biological functions of RanBP6 by performing RanGTP competition assay and LC-MS/MS study. Since RanBP6 has a tumor-suppressor function in glioblastoma, we prioritized our substrate validations based on the protein abundance, Log2 fold-change of 'RanBP6' *versus* 'RanBP6+RanQ69L' and the relevance to cancer-associated studies from NCBI PubMed database. However, we could not exclude the possibility that many non-cancer-related substrates might contribute to important biological functions of RanBP6.

Interestingly, XPO1 was identified as a candidate RanBP6 substrate. In our other RanBP6 interactome study with a different design in A431 cells (data not shown), we also observed that RanBP6 associates with XPO1. Furthermore, a recent study revealed that RanBP6 was pulled down in a screen of XPO1 interactome (Kirli et al., 2015). Although the mechanism by which XPO1 forms a trimeric complex with RanGTP and exportin cargoes for nuclear export is well-characterized, it remains unclear how XPO1 shuttles back from cytoplasm to the nucleus. Our study suggests that RanBP6 may be the importin for XPO1. Since high XPO1 expression has been correlated with tumorigenesis, it will be interesting to examine whether the tumor suppressor function of RanBP6 is through modulating the subcellular localization of XPO1. In addition to XPO1, several candidate substrates of RanBP6 have been reported as oncoproteins in different types of cancer. For instance, CDK1, PRMT1, RAB35 and Transcription intermediary factor 1-beta (TRIM28).

Moreover, The method that I have developed for the substrate screening in this project is an improvement to the field of nucleo-cytoplasmic transport. I expressed RanBP6

from a mammalian cell line instead of *E. coli*, since *E. coli* is not amenable for studying posttranslational modifications. This method can also be applied for studying other Ran-binding proteins in the importin β superfamily, as well as for other interactome studies of patient-derived RanBP6 mutations. Additionally, we can screen other cancer repertoires by swapping the HeLa cytosolic extracts for the specific cell lines in which we are interested.

Taken together, our study identified RanBP6 as an importin receptor, and its candidate importin substrates that are involved in tumorigenesis. Further validations are needed to decipher precisely how RanBP6 contributes to tumorigenesis through its interactions with these cargoes.

CHAPTER 7

CONCLUSION AND FUTURE DIRECTIONS

7.1 Conclusion

Our laboratory had previously identified Ran binding protein 6 (RanBP6), a protein of hitherto unknown functions, as a novel EGFR-associating protein from EGFR immunoafffinity purification and LC-MS/MS. In this work, I have characterized the biological function of RanBP6 as an EGFR negative regulator. RanBP6 silencing impairs nuclear translocation of STAT3, reduces STAT3 binding to the EGFR promoter, results in transcriptional derepression of EGFR, and increases EGFR pathway output. Focal and broad deletions of the *RANBP6* locus on chromosome 9p were found in a subset of glioblastoma (GBM) and silencing of RanBP6 promotes glioma growth *in vivo*. These results provide an example of EGFR deregulation in cancer through silencing of components of the nuclear import pathway (Fig.7-1).

In addition, my study on identifications of RanBP6 interactome and substrates reveal an important function of RanBP6 as an importin in tumorigenesis, as many of the candidate substrates are overexpressed in multiple cancers. (e.g., XPO1, RAB35, CDK1, PRMT1, TIF-1β.)

Taken together, my data identify a novel link between the Ran-GTPase nuclear transport pathway and key cancer signaling pathways, which warrant further study as inhibitors targeting nuclear transporters enter clinical evaluation as cancer therapeutics.

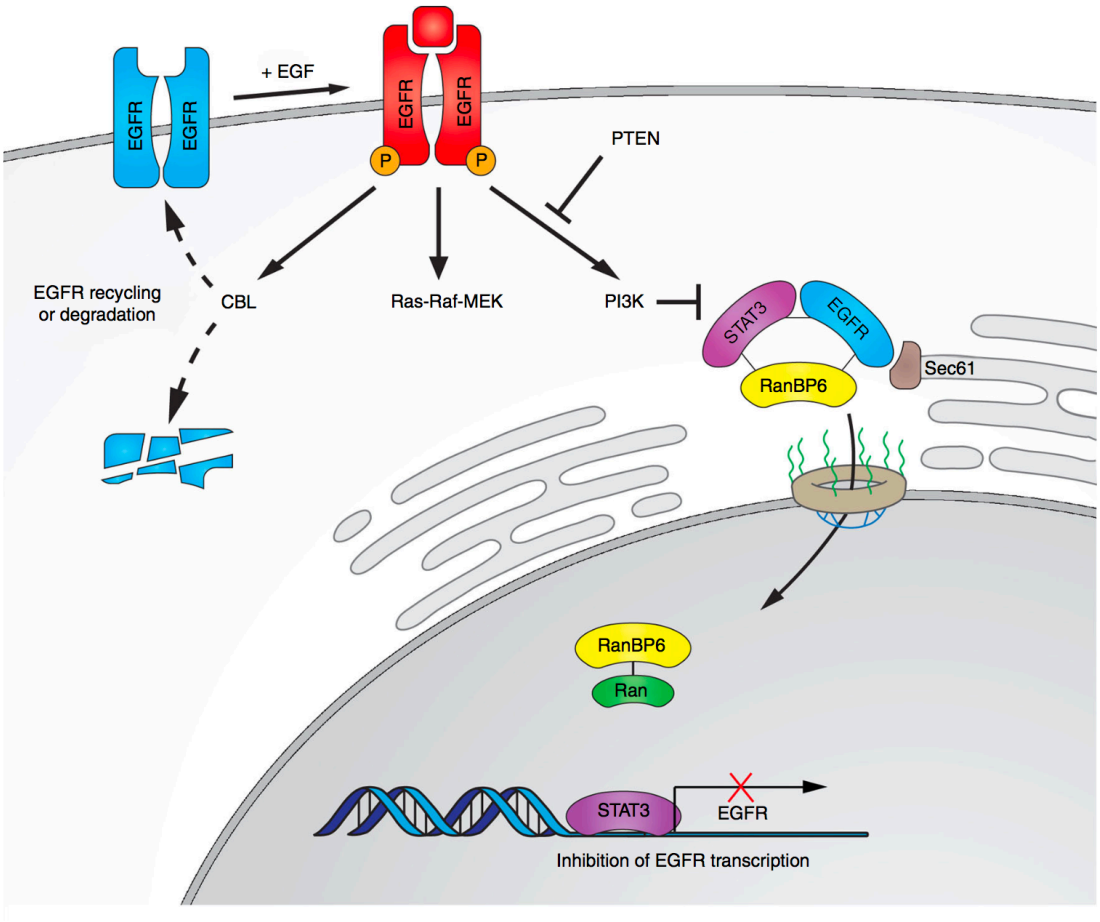

Figure 7-1. Model of EGFR regulation by RanBP6. A (small) pool of EGF receptors functions as a scaffold for RanBP6-mediated nuclear import of STAT3. Nuclear STAT3 represses *EGFR* transcription. The solid lines between EGFR-STAT3-RanBP6 and RanBP6-Ran indicate protein-protein interactions (might not be direct interactions). This mechanism of EGFR regulation serves to repress *EGFR* transcription at steady state and is inactivated when the cellular demand for EGFR transcription increases (e.g., following EGF-induced receptor protein degradation). Cancer cells inactivate this physiologic mechanism of EGFR regulation through deletion of the RANBP6 gene or silencing of PTEN (which disrupts the EGFR-RanBP6 interactions).

7.2 Future directions

Aim 1. Validation of RanBP6 substrates

Our preliminary data showed that several cancer-related proteins could be potential RanBP6 substrates (Table 6-1). I will perform HA pulldown assays to validate the interactions between these candidates and HA-RanBP6. Next, I will examine the subcellular localizations of these candidates in two models- 1) HEK293T cells expressing CRISPR/Cas9 single-guided RanBP6 RNA, and 2) HeLa cells expressing Dox-inducible RanBP6 shRNA. Depletion of RanBP6 should reduce the protein expressions of these candidates in the nucleus. Once I confirm the interactions and changes of subcellular localization upon RanBP6 KD, I will perform the import assays with confocal microscope as described in other literatures (Jakel et al., 1999; Jakel and Gorlich, 1998; Kimura et al., 2017; Kirli et al., 2015; Kutay et al., 2000; Mingot et al., 2004; Mingot et al., 2001).

Aim 2. Examination of the tumor suppressor function of RanBP6 in an EGFR-dependent cancer model- pancreatic cancer

It has been shown that the development from intraepithelial neoplasia lesions (PanIN) to pancreatic ductal adenocarcinoma **(**PDAC) is dependent on EGFR signaling (Ardito et al., 2012; Navas et al., 2012; Perera and Bardeesy, 2012). RanBP6 depletion upregulates EGFR and its downstream signaling. Recent studies revealed that 3D culture of murine pancreatic organoids successfully recapitulates the pathogenesis of PDAC (Boj et al., 2015) and identifies the nuclear transport as a crucial pathway involved in pancreatic cancer progression. This raises a question whether RanBP6 plays an important role in EGFR-mediated pancreatic cancer progression. In addition, inactivation of the CDKN2A tumor suppressor gene is observed in at least 40% of

PanIN lesions. Furthermore, we showed that the gene encoding *RANBP6* is frequently silenced along with its genomic neighbor *CDKN2A* on chromosome 9p in multiple cancers, including pancreatic adenocarcinoma. Based on these observations, I hypothesized that depletion of RanBP6 accelerates transformation in the PanINs and PDACs due to their dependence on EGFR signaling.

I obtained 8 different murine pancreatic organoids (2 normal, 3 PanIN and 3 PDAC) and the culture techniques from Dr. Steven Leach's laboratory. I 3D-cultured murine normal pancreatic organoids, and also the organoids expressing either $Kras^{LSL\text{-}G12D/+}$; *Pdx-Cre* or $Kras^{LSL\text{-}G12D/+}$; $Trp53^{LSL\text{-}R172H/+}$; *Pdx-Cre* that recapitulate features of PanIN and PDAC respectively (Fig. 7-2a). I expanded these organoids and examined RanBP6 mRNA and protein expression in these organoids. RanBP6 appeared to be low-expressed in PanINs comparing to normal organoids both at the mRNA and protein levels (Fig. 7-2b and 7-2c).

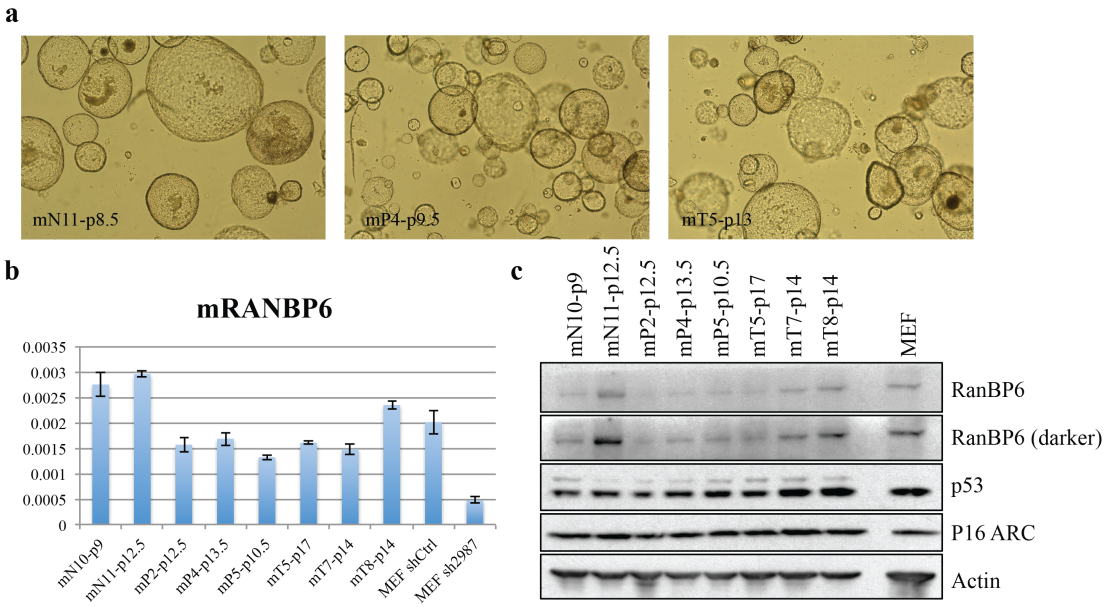

Figure 7-2. Accessing RanBP6 expression in the murine pancreatic organoids. **a**, Shown are images of 3D cultured murine pancreatic organoids. Left panel- normal organoids; middle panel- PanIN organiods; right panel- PDAC organoids. N= normal; P= PanIN; T= PDAC. **b**, RanBP6 mRNA expression levels in a panel of organoids comparing to MEF-shCtrl and MEF-shRanBP6 2897. **c**, RanBP6 protein expression levels in a panel of organoids comparing to MEF

I further engineered two murine RanBP6 hairpins to an shRNA construct that has Dox-inducible GFP (Fig. 7-3a), and stably transduced these two hairpins in KPC4662, a murine PDAC cell line. Dox treatment induced RanBP6 knockdown with either hairpin (Fig. 7-3a and 7-3b).

Next, I stably transduced 8 different organoids with these two RanBP6 hairpins, and observed GFP expression under fluorescent microscope upon treatment of Dox (Fig. 7-3c). Examination of the knockdown efficiency of RanBP6 by RT-QPCR showed an efficient knockdown of RanBP6 in normal organoids (Fig. 7-3d, left panel), but not PanINs or PDACs after several trials (data now shown). Interestingly, in the normal

organoids where RanBP6 were knocked down, I observed an increase of *Egfr* mRNA levels (Fig. 7-3d, right panel).

Given the low mRNA expressions of *Ranbp6* in PanINs and PDACs compared to normal organoids (Fig. 7-2b), perhaps the better strategy for studying the role of RanBP6 in these organoids will be ectopic expression of RanBP6 instead of depletion of RanBP6. I will overexpress HA-RanBP6 in these organoids for *in vitro* growth assays or *in vivo* orthotopic injections for tumor growth study.

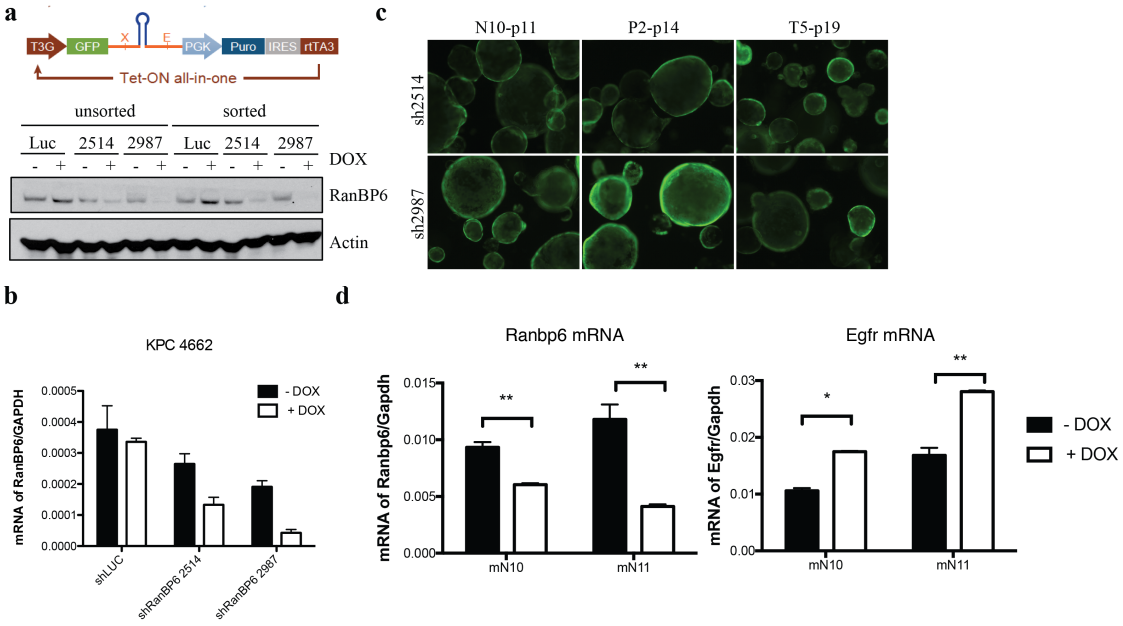

Figure 7-3. Validating RanBP6 KD efficiency in 2D murine PDAC cell line and 3D murine pancreatic organoids. **a**, Upper panel- shown is the shRNA construct that contains doxycycline-inducible GFP. Lower panel- two RanBP6 shRNA (2514 and 2987) were able to KD RanBP6 in both unsorted or GFP-sorted KPC2662 (murine PDAC cell line). Shown are the results from western blot (**a**) and RT-QPCR (**b**). **c,** Addition of Dox successfully induced GFP expression in 3 different murine pancreatic organoids transfected with the two hairpins (sh2514 and sh2987). (**f**) Left panel, accessing the KD efficiency by RT-QPCR showed efficient knockdown of RanBP6 in normal organoids. Right panel, *Egfr* mRNA levels were increased in Ranbp6 KD organoids. Of note, cells or organoids were treated with 2µg/mL of doxycycline for 96 hours.

Aim 3. Characterization of RanBP6 patient mutations

Our preliminary data have shown that two of the mutations (I984L and N973Kfs, a frameshift mutation that causes truncated RanBP6) in RanBP6 are recurrent in multiple cancers from cBioPortal database (Fig. 7-4a) (Cerami et al., 2012), and that reconstitution of RanBP6 in RanBP6-low cancer cell lines reduces cell growth, while these two mutations revert the effect of RanBP6 on cell growth (Fig 7-4b). These two mutations map to a HEAT domain that is closed to the C-terminus of RanBP6. Since the HEAT domains are important for cargo binding (Vetter et al., 1999), I hypothesized that mutations of RanBP6 might abolish its interaction with the candidate substrates that I identified from Aim 1. Furthermore, given the importance of RanBP6 in regulating EGFR signaling, I hypothesized these patient-derived mutations will alter EGFR signaling in the pancreatic cancer model.

For a more comprehensive analysis, I have included other reported RanBP6 patient mutations with more than four entries in the cBioPortal database (Fig. 7-4a). I overexpressed HA, HA-RanBP6 wt, HA-RanBP6 mutants (mt), including I984L, N973Kfs, R949C, E636K, D437Y and E174Q in the floating Expi293 and performed HA-pulldown assays with the lysates from Expi293. The purified HA-tagged proteins were further analyzed on the SDS-PAGE (Fig. 7-4c). I will investigate whether these mutants will impair the interactions between RanBP6 and the candidate substrates from Aim 1.

To further investigate whether the patient-derived mt might alter cancer signaling, I examined a panel of PDAC cell lines and found that two of them have low RanBP6 expression (AsPC-1 and Panc-1) (Fig. 7-4d), which is consistent with our analyses from Cancer Cell Line Encyclopedia (CCLE) (Fig. 7-4e). I further reconstitute pCMV-

HA-RanBP6 wt and mt to these two cell lines (Fig. 7-4f), and I will perform RNA-sequence to analyze the alterations of cancer signaling pathways.

In summary, RanBP6 is a novel negative regulator of EGFR signaling pathway, but the tumor suppressor function of RanBP6 remains unclear. The aims I described here will shed light on molecular-based study of RanBP6 in EGFR-dependent cancer types.

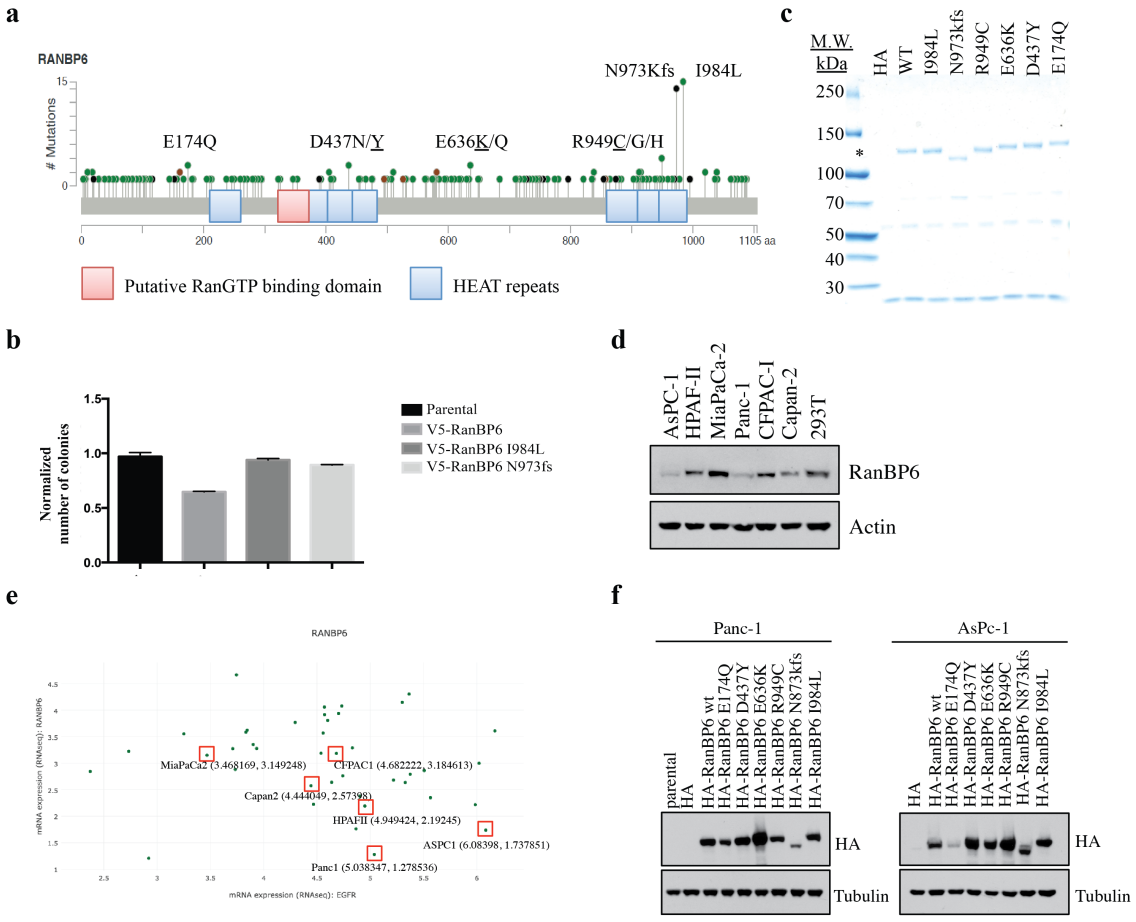

Figure 7-4. Characterization of RanBP6 patient mutations. a, Shown are RanBP6 patient mutations that haven been reported in cBioPortal. **b**, The most two common mutations (I984L and N973fks) of RanBP6 revert its tumor suppressor function in colony formation assays. **c,** Shown is purified HA, HA-RanBP6 wt and mt from floating Epxi293 by CBB staining. **d**, immunoblot showing RanBP6 protein expression level in a panel of PDAC cell lines. **e**, The mRNA expression levels of *RanBP6* (x-axis) and *EGFR* (y-axis) from cell lines examined in **d**. Data are acquired from Cancer Cell Line Encyclopedia (CCLE). **f,** Reconstitution of pCMV-HA-RanBP6 wt and mt to RanBP6-low expression PDAC cell lines (Panc-1 and AsPc-1).

APPENDIX A
MATERIALS AND METHODS

Cell Lines and Reagents

Epidermoid carcinoma cell line A431, Human Embrionic Kidney HEK-293T, DF1, Human Glioma cell lines LN18, T98G, A172, and HeLa-S3 were purchased from ATCC. SF268 and SF295 were obtained from NCI. Expi293 was purchased from Invitrogen. *SKMG*-3 cells were a gift of Hans Skovgaard (Rigshospitalet, Oslo). GBM tumor spheres were derived at the MSKCC Brain Tumor Center according to MSKCC IRB guidelines. MEF PTEN $^{lox/lox}$ were kindly provided by Hong Wu (UCLA). Antibodies to RanBP6 (ab74448), RanGAP1 (ab92360) and Nup93 (ab168805) were purchased from Abcam. Antibodies to EGFR (#2085), pEGFR Tyr1068 (#3777), Gab1 (#3232), pGab1 Tyr627 (#3231), pErk1/2 Thr202/Tyr204 (#9101), Akt (#9272S), pAkt Ser473 (#4051), S6 (#2317S), pS6 Ser240/244 (#5364), PTEN (#9556), STAT3 (# 12640S), pSTAT3 Tyr705 (#9145S) and H3 (#4499S) were purchased from Cell Signaling. Antibodies to GST (G7781), V5 agarose affinity gel (A7345), Importin α (I1784) Importin β (I2534), Ran (R4777), Vinculin (V9131) were purchased from Sigma. Antibody to V5 (P/N 46-1157) is from Invitrogen. Nup93 (SC-374399), RCC1 (SC-55559, STAT3 (SC-482), p16 (SC-468) Tubulin (SC-23948) and EGFR (SC-101) were purchased from Santa Cruz. The AKT inhibitor MK2206 is purchased from Selleckchem, and the JAK inhibitor Ruxolitinib (Novartis) was kindly provided by Ross Levine.

To generate the RANBP6 expressing lentiviral construct, RanBP6 was PCR amplified using pBluescriptR- human RanBP6 (Open Biosystems, clone ID 30347107) as template and the primers pLenti6.3-RanBP6-V5 Forward and Reverse listed in

Supplementary Table S7. The amplified product was then transferred into a lentiviral expression plasmid (pLenti6.3/V5-DEST, Invitrogen) with the Gateway recombination technology using the pDONR221 vector as an intermediate vector. Construct was Sanger sequence verified. GST-RanBP6 was generated by sub-cloning the amplified PCR product of human RanBP6 to a digested GST vector (pGEX6.2, GE healthcare). TRIPZ RanBP6 inducible shRNAs from Open Biosystem (V3THS_374866 and V3THS_374867) were used to knockdown human RanBP6. Mouse specific RanBP6 hairpin was designed and cloned into the mir30 based retroviral MLP vector (kindly provided by Scott Lowe) and subsequently into the RCAS vector (Supplementary Table S7). RanBP6 cDNA that is resistant to the human hairpin V3THS_374867 was generated by PCR cloning of human RanBP6 cDNA to MSCV-MIGR1-GFP plasmid (Addgene #27490). Three codons inside the hairpin sequence were swapped to generate silence mutations by site-directed mutagenesis kit (Agilent Technologies, catalog #210519-5). TRIPZ STAT3 inducible shRNAs is from Open Biosystem (V3THS_376017).

Cell line Transfections and Infections

Adherent lines were grown in DMEM 10% FBS (Omega scientific, FB-11). Neurospheres were grown in NeuroCult NS-A Proliferation Kit (Stem Cell Technology) supplemented with Heparin (2mg/ml), human EGF and bFGF (20ng/ml each). Lentivirus and retrovirus were generated by co-transfection of retro or lentiviral plasmids and the packaging VSVg for retrovirus and pMD2G and psPAX2 for lentivirus in Gp2-293 using Calcium Phosphate. High titer virus was collected at 36 and 60 hours following transfection and used to infect cells for 12 hours. TS516 was spin-infected for 2 hours at 1000rpm. Transduced cells were selected after 48 hours from the last infection with blastidicin (2-5μg/ml), G418 (500-800μg/ml) and

puromycin (3μg/ml) according to the plasmid antibiotic resistance. DF1 cells were grown at 39°C in DMEM (ATCC) containing 10% FBS (SIGMA, F7524). DF1 cells were transfected with the RCAS viral plasmids, using Fugene 6 Transfection reagent (Roche), accordingly to manufacturer's protocol. EGF time course experiments were carried out in cells serum starved for 16 hours and then stimulated with 100ng/ml EGF for the indicated time. EGF and Doxycycline were from SIGMA.

Immunoprecipitation and Immunoblotting

A431 PTEN isogenic-Dox-inducible RanBP6 V5 cells were induced or not with 1μg/ml Dox and were lysed 36 hours later in JS lysis buffer (50mM HPES, 150mM NaCl, 1% Glycerol, 1% Triton X-100, 1.5mM $MgCl_2$, 5mM EGTA). Lysates were precleared by incubation for 1 hour at 4°C with Protein G/A (Calbiochem) blocked in 5% BSA and then incubated with the V5 antibody (Invitrogen) for 2 hours followed by 1 hour incubation with Protein G/A. The immunoprecipitates were washed 4 times with JS lysis buffer and bound proteins were eluted in Laemmli Buffer. Proteins for immunoblot analysis were run either on 4-12% Bis-Tris SDS-PAGE gels (Invitrogen) or on house-made SDS-PAGE gels and transferred to nitrocellulose membrane (Amersham). Membranes were incubated in blocking buffer (5% milk 0.1% Tween, 10 mM Tris at pH 7.6, 100 mM NaCl) and then with primary antibody either 1 hour at room temperature or overnight at 4°C according to the antibody. Anti-mouse or rabbit-HRP conjugated antibodies (Jackson Immunoresearch) were used to detect desired protein by chemiluminescence with ECL (Amersham).

GST fusion protein expression, purification and pull down assay

BL21 cells transformed with pGEX6p2-RanBP6 were grown in 200 ml of LB medium at 37°C to an A_{600} of 0.4-0.7. Protein was induced by culturing in the presence of

1mM of isopropyl-thio-D-galactopyranoside (IPTG) at 20°C for 16 hours. Bacterial pellets were collected by centrifugation at 7700xg for 10 minutes at 4°C. Pellets were resuspended in 10 ml of cold lysis buffer (1% Triton X-100, 1mM of dithiothritol, 1X protease inhibitor cocktail I and 1X phosphatase inhibitor cocktail in 1X PBS). Resuspended bacterial lysates were sonicated (41% amplitude, 4 pulses of 10 seconds/cycle) and centrifuged at 12,000 rpm for 15 minutes at 4°C. The supernatants were transferred to 15 ml falcon tube and incubated with 50% GST beads slurry at 4°C for 2-4 hours. Supernatants with beads were then sedimented at 500 xg at 4°C for 5 minutes, and washed twice with ice-cold wash buffer, and washed again with 1X PBS without detergent. Beads were finally resuspended in 1-2 bed volumes of GST maintenance buffer (50mM Tris, 100mM NaCl 1mM EDTA, 10% glycerol, 1mM dithiothritol, and 1X protease and phosphatase inhibitors). The proteins were aliquoted, snap frozen with liquid nitrogen, and stored at -80°C. 25 µg of GST empty vector and pGEX-RanBP6 beads were incubated with 500 µg of cell lysates on a rotator in the cold room for 2-4 hours. Lysates from HEK-293T were from cells either serum starved for 12 hours and stimulated with EGF (100ng/ml) or grown in full media. The beads were sedimented, washed three times with cold lysis buffer (Cell signaling, catalog #9803S) with 5 minutes incubation at 4°C in between washes, and then lysed with 2X SDS sample buffer (Bio-rad, #161-0737).

His-RanQ69L protein extraction, purification and re-charging with GTP

BL21 cells transformed with His-RanQ69L were grown in 2 liters of LB medium at 37°C to an OD_{600} of 0.6-0.8. Protein was induced by culturing in the presence of 0.5 mM of isopropyl-thio-D-galactopyranoside (IPTG) at 18°C for 16~18 hours. Bacterial pellets were collected by centrifugation at 6000 x.g. for 10 minutes at 4°C. For cells from 1L culture, pellets were resuspended in 25 ml of ice-cold lysis buffer (50 mM

Tris, pH = 7.5, 20 mM Imidazole, 150 mM NaCl, 1 mM $MgCl_2$, 0.35 µl beta-ME/mL lysis buffer, 1x protease inhibitor cocktail, 10 µl benzonase, and 10 mg lysozyme). Resuspended bacterial lysates were sonicated (50% amplitude, six 1 minute rounds with 1 second pulse and 1 second pause) and centrifuged the lysate at 25,000 rpm for 40 minutes at 4°C. The supernatants were transferred to 50 ml falcon tube and incubated with Ni-NTA beads slurry (1.5 ml of beads per 1L of culture) at 4°C for 1 hour. The resin was washed with 50-100 ml of ice-cold Ni-Wash Buffer (50 mM Tris, pH = 7.5, 20 mM Imidazole, 150 mM NaCl, 1 mM $MgCl_2$, and 0.35 µl beta-ME/mL lysis buffer). The His-RanQ69L-immobolized Ni-NTA beads were eluted with 10 ml of Ni-Elution Buffer (20mM Tris, pH = 7.5, 300 mM Imidazole, 150 mM NaCl, 1 mM $MgCl_2$, 0.35 µl beta-ME/mL lysis buffer and 1X protease inhibitor cocktail), and the peak fractions were pooled, and diluted with lysis buffer for two times of dialysis (3 hours) with Dialysis Buffer (20 mM Tris, pH =7.5, 100 mM NaCl, 1 mM $MgCl_2$, 0.35 µl beta-ME/mL lysis buffer). The proteins were further re-charged with GTP in the following order: 4 mM of EDTA was added to chelate Mg^{2+} from the RanGDP/GTP binding pocket, buffer exchanged, and 100 mM GTP was added to His-RanQ69L at 4°C overnight. The next day, the dialyzed proteins were concentrated with protein concentrator (cut-off: 10k) and injected to Superdex 75 5/150 GL (size exlusion chromatography). The fractions from the trace were analyzed on CBB-stained gel. The fractions contained Hi-RanQ69L (M.W.~ 30 kDa) were aliquoted, snap frozen with liquid nitrogen, and stored at -80°C.

Expression of HA-empty and HA-RanBP6 from Expi-293 and HA-pulldown

Expi-293 cells were grown in 300 mL of suspension and transfected with either pCMV-HA or pCMV-HA-RanBP6 according to the manufacturer's protocol (Invitrogen). The transfected cells were collected, washed with PBS and lysed at Day

2 (48 hours) post-transfection with 5 times of the pellet volume with the Lysis Buffer (20 mM Tris-HCl, pH = 7.5, 150 mM NaCl, 1 mM EGTA, 1.5 mM $MgCl_2$, 1% glycerol, 1% triton X-100, 0.5 mM 2ME, 1X protease inhibitor cocktails, and 1X phosphatase inhibitor cocktail). The lysates were then sonicated 4 rounds (41% amplitude, six 1 minute rounds with 1 second pulse and 1 second pause), and ultracentrifuged at 45,000 rpm for 45 minutes. The Expi293-expressing HA-empty or HA-RanBP6 proteins were aliquoted, snap frozen with liquid nitrogen, and stored at -80°C.

Collection of HeLa-S3 cytosolic extract

5 x 10^9 HeLa-S3 cells were grown, collected (viability > 95%), washed with 1X PBS, and lysed with 50 ml of Cytosolic Extract Buffer (60 mM KCl, 10 mM HEPES, 1 mM EGTA, 1 mM MgCl2, 0.1% (1mg/mL) of digitonin, 1 mM 2ME, 1X protease inhibitor cocktail, and 1X phosphatase inhibitor cocktail) on ice for 10 minutes. The extract was pelleted at 1000 x.g. for 4 minutes at 4°C, and the supernatant was removed to a clean tube for ultracentrifugation at 50,000 rpm for 90 minutes. The final supernatant was added with glycerol (1% final concentration), aliquoted, snap frozen with liquid nitrogen, and stored at -80°C.

TCGA, CCLE and GBM datasets

CCLE data were downloaded from the cBio Portal using the "cgdsr" package. TCGA GBM and REMBRANDT data were downloaded from the GlioVis data portal (http://gliovis.bioinfo.cnio.es). All code used to analyse the data and generate the plots is available at: https://github.com/squatrim/oldrini2016.

Evaluation of glioma growth *in-vivo*

For the TS516 xenograft model, SCID mice were injected subcutaneously with 10^6 glioma cells, which were suspended in 100μL of a 50:50 mixture of growth media and Matrigel (BD #356237). Ntv-a mice, and procedures for RCAS-mediated gliomagenesis have been described previously. Ntv-a pups were injected with a total of 200,000 DF1 cells transfected with various constructs: 100,000 RCAS-PDGFB plus 100,000 RCAS-shRanBP6 or RCAS-shLuc. After injection of the DF1 cells during the newborn period, mice were aged until they developed symptoms of disease (lethargy, poor grooming, weight loss, macrocephaly). Samples in panel 5H are derived from tumors generated in a Ntv-a; Ink4a/Arf null background. RCAS-shRanBP6 and RCAS-shLuc constructs express a EGFP reporter that allowed to isolate the tumor cells by FACS. Samples were prepared by enzymatic dissociation and low-speed centrifugations as previously described.

Statistical analysis

Data are presented throughout as mean and SD, except otherwise indicated. Results were analyzed by unpaired two-tailed Student's *t*-tests unless otherwise noted and were considered statistically significant if $P < 0.05$. Kaplan–Meier survival curve was produced with GraphPad Prism; *P* value was generated using the Log-Rank statistic.

Gene ontology analysis

The gene ontology enrichment was performed using the Gene Ontology Consotrium website (www.geneontology.org), through the analysis tools from the PANTHER Classification System, by uploading the list of the Uniprot_IDs of the proteins identified in the mass spectrometry experiments. The enrichment results were filtered to reduce the number of redundant GO classes, by using the “Clusterprofiler” and “GOSemSim” packages in R (Yu et al., 2010; Yu et al., 2012). All code used to

analyze the data and generate the plots is available at: https://github.com/squatrim/oldrini2016.

CRISPR/Cas9-mediated knockout of RanBP6

RanBP6 CRISPR constructs were generated with guided RNAs that target human RanBP6 sequence (Table S9) and pX330 CRISPR/Cas9 vector (Addgene #42230) (Cong et al., 2013). pX330 vector was digested with BbsI and ligated with annealed oligonucleotides. HEK-293T cells were transfected with three different sgRanBP6 constructs. Clonal isolations were performed by serial dilutions (0.5 cells/well). Genomic DNA extractions were performed with the cell lines that are recovered from single cells. Each of the clones was examined by SURVEYOR nuclease assays. The PCR products that were amplified from SURVEYOR primers (Table S9) were further validated by Sanger sequence to confirm the indels. Out of all the clones that were generated by three independent sgRNAs, we selected the one that has the best knockout efficiency for further experiments.

Subcellular fractionation assay

Cytoplasmic and nuclear fractions of HEK-293T cells serum starved for 12 hours and treated either with EGF (100ng/ml) for 15 minutes or IL6 (10ng/ml) for 30 minutes were prepared with nuclear extract kit (Active Motif, #40010.) The cytoplasmic fractions were extracted with hypotonic buffer. The nuclear pellets were stringently washed 4 times before addition of nuclear lysis buffer, vortexed, and briefly sonicated (10% amplitude for 5 seconds) before 30 minutes incubation on a rotator at 4°C. For subcellular analysis of STAT3, the lysates were normalized to protein concentration. For GST-RanBP6 pulldown with Ran and RCC1, the fractionated lysates were normalized to the cell number (cytoplasm:nuclear = 50:1).

Reverse Transcription Quantitative PCR

RNA was isolated with TRIzol reagent (Invitrogen) according to the manufacturer's instructions. For reverse transcription PCR (RT-PCR), 500ng of total RNA was reverse transcribed using the High Capacity cDNA Reverse Transcription Kit (Applied Biosystems). The cDNA was used for quantitative PCR using SYBR® Green ERTM kit (Invitrogen) according to the manufacturer's instructions. Quantitative PCRs were run and the melting curves of the amplified products were used to determine the specificity of the amplification. The threshold cycle number for the genes analyzed was normalized to GAPDH and HPRT. Sequences of the primers used are listed in Table S9 and primers for human RanBP6 are from Qiagen (PPH13358B).

Luciferase assay

The promoter constructs of EGFR and Actin (ACTB) were purchased from SwitchGear Genomics (Product ID: #S714178 and #S717678). For measuring EGFR promoter activity, HEK-293T cells expressing Doxycycline inducible shRanBP6 were either treated with or without Doxycycline for 72 hours, and were further serum starved for 16 hours. 50 ng of Actin or EGFR promoter construct and 10 ng of cypridina control were co-transfected to the cells with Fugene. The luciferase activities of renilla and cypridina were measured 48 hours after transfection by following the manufacturer's protocol (LightSwitch Dual Assay System, SwitchGear Genomics #DA010). STAT3 reporter for measuring the transcriptional activity of STAT3 was purchased from Qiagen (#CCS-9028L). For STAT3 reporter assay, both HEK-293T and HEK293T-RanBP6 cell lines were treated with or without Doxycycline for 72 hours. Both of the cell lines were transfected with 100 ng of STAT3 reporter construct. The luciferase assay was developed by using Dual-Glo

Luciferase Assay System from Promega (Catalog #E2920). The cells were seeded at a concentration of 15,000 cells/well in the 96-well plate, and were transfected at 60-80% confluence. Each measurement was done in biological triplicates with SpectraMax M5 multi-mode microplate readers (Molecular Devices).

Gene expression array and ssGSEA

HEK-293T cells expressing Doxycycline inducible RanBP6 hairpins were either treated with or without Doxycycline for 72 hours, and further serum starved for 16 hours. Total RNA was extracted with Qiagen RNeasy Mini Kit. The quality of the RNA was evaluated using Agilent BioAnalyzer RNA nano assay, and the high quality RNA samples were processed for microarray at the Integrated Genomics Operation (IGO) at MSKCC. In summary, 500 ng of the RNA was reverse transcribed to double-stranded cDNA. The cDNA was used as a template for in vitro transcription with biotin-labelled uridine triphosphate at 37°C for 16 hours. The biotin-labelled cDNA was fragmented, and processed to hybridization cocktail to be hybridized to the GeneChip Human Genome U133 Plus 2.0 arrays (Affymetrix) according to the Affymetrix GeneChip protocol. Each sample was done in biological triplicates. Expression array analysis was completed in R (version 3.2.2) using the Bioconductor suite. The 'affy' package was used for robust multi-array average normalization followed by quantile normalization. For genes with several probe sets, the median of all probes had been chosen. Data are available online at NCBI GEO, Accession Number GSE76943. Single-sample Gene Set Enrichment Analysis (ssGSEA) has been performed in R using the 'gsva' function of the 'gsva' package. STAT3-related gene lists were downloaded from the Molecular Signatures Database (MSigDB) at the Broad institute (http://software.broadinstitute.org/gsea/msigdb). All code used to

analyze the data and generate the plots is available at: https://github.com/squatrim/oldrini2016.

Chromatin Immunoprecipitation

ChIP was performed as described in Frank et al. (Frank et al., 2001). LN18 cells were treated with or without doxycycline and starved overnight with DMEM without serum. Cells were fixed with 1% formaldehyde for 15 min, stopped with 0.125 M glycine for 5 min, and washed twice with PBS. Cell pellets were sonicated for 6 min at 20% amplification (15 sec on followed by 60 sec off) followed by 2 min sonication at 40% (15 sec on followed by 60 sec off) with a Branson 450 Sonifier. Lysates were precleared with Protein A/G beads (Santa Cruz) and incubated at 4°C overnight with 5 µg of polyclonal antibody specific for STAT3 (sc-482, Santa Cruz), or normal rabbit immunoglobulins (Santa Cruz). DNA was eluted in 100 µl of water and 5 µl were analyzed by qRT-PCR with SYBR Green (Applied Biosystems). The amplification product was expressed as a percentage of the input for each condition. The HPRT gene promoter was used as negative control (Jahani-Asl et al., 2016). Primers used to amplify sequences surrounding predicted binding sites were designed using the Primer3 software (http://frodo.wi.mit.edu/cgi-bin/primer3/primer3_www.cgi) based on STAT3 binding site prediction using the the Jaspar transcription profile database (http://jaspar.genereg.net)(Mathelier et al., 2015) and the MatInspector software (http://www.genomatix.de).

Immunofluorescence

HEK-293T cells were seeded at 10,000 cells/well on 12mm poly-D-lysine and fibronectin coated rounded coverslip in 24-well plate and cultured in presence of 2 µg/ml of Doxycycline for 4 days with the last 16-18 hours in serum-starved condition.

1 μM of Ruxolitinib was applied to the culture for 4 hours and 10 ng/ml IL-6 for 30 min. Cells were fixed in 3.2% PFA in PBS for 20 min, washed three times in PBS, incubated for 20 min in blocking solution (10% Donkey or Goat serum in 0.1% Triton-X PBS), incubated for 2 hours with 1:100 Rabbit anti-STAT3 (Santa Cruz, sc-842) in blocking solution, washed three times in PBS, incubated for 1 hour with 1:500 anti-rabbit A488 (Invitrogen) in 0.1% Triton-X PBS, washed three times in PBS and mounted with Vectashield HM- DAPI (Vector Laboratories, H-1500). Cultures were imaged with Leica TCS SP5-II microscope and analyzed using a standardized Metamorph macro. STAT3 signal was first threshold to select the signal over the background, then the DAPI image was used to subdivide the threshold STAT3 signal into nuclear and cytoplasmic and ratio was calculated.

Soft agar assay

TS516 cells were seeded in triplicates at 300,000 cells/well in Neurocult media containing 0.4% Noble agar (SIGMA A5431) and growth factor supplements (20ng/mL EGF, 10ng/mL bFGF) and SF268 at 50,000cells/well in DMEM 10% FBS. Cells were plated between two layers of Neurocult media and growth factors or DMEM and FBS containing 0.65% Nobel agar. Noble agar layers were containing Dox at 1.2μg/ml. Colonies were stained 3/4 weeks after plating with either crystal violet (0.005%) (SIGMA V5265) and quantified using imagine software (Oxford Optronix) and an image processing algorithm (Charm algorithm, Oxford Optronix).

APPENDIX B

LIST OF PRIMERS USED IN THIS WORK

Primer Sequences for PCR cloning and mutagenesis:

ID	Sequence (5' -> 3')
pGEX6p-RanBP6-Forward	ATTCCCGGGATGGCGGCAACCG
pGEX6p-RanBP6-Reverse	CGATGCGGCCGCTCAAGCAAAATTTAGCAACTCG
RanBP6-MIGR1-Forward	GAATTAGATCTACCATGGCGGCAACC
RanBP6-MIGR1-Reverse	GTTAACCTCGAGTCAAGCAAAATTTAGC
RanBP6-867 hairpin resistant cDNA sense	GAGAACTGTATCTCAGCAATAGGGAAAATTTTAA AGTTTAAACCTAACTGTGTAAATGTAGATG
RanBP6-867 hairpin resistant cDNA antisense	CATCTACATTTACACAGTTAGGTTTAAACTTTAA AATTTTCCCTATTGCTGAGATACAGTTCTC
pLenti6.3-RanBP6-V5 Forward	GGGGGACAAGTTTGTACAAAAAAGCAGGCTCCA CCATGGCGGCAA
pLenti6.3-RanBP6-V5 Reverse	GGGGACCACTTTGTACAAGAAAGCTGGGTAAGC AAAATTTAG

Short-hairpin RNA target site sequences:

ID	Sequence (5' -> 3')
TRIPz sh Human RanBP6_1	TTAATTCCAAAACTCTGCT
TRIPz sh Human RanBP6_2	TAAACTTCAAAATCTTCCC
RCAS sh Mouse RanBP6	CCAGGTTGAAATGTCTCTTCA
RCAS sh Luciferase	TTAATCAGAGACTTCAGGCGGT
TRIPz sh Human STAT3	AAGTTTCTAAACAGCTCCA

Single-guided RanBP6 target site sequences:

ID	20nt sequence (5' -> 3')	PAM	Strand
1	ATGGCGGCAACCGCGTCTGC	AGG	+

Surveyor primers for PCR amplifying U6-sgRNA fragments:

ID	Sequences (5’ -> 3’)
RanBP6_S7F	CCAAAACCTAGCTCGCAGCC
RanBP6_S7R	GAAACTTCAGACCTTCCGGC
RanBP6_S8F	CACGGCTCTCACCTCTCTCC
RanBP6_S9R	GCCAGAAAACGTGAAGTGCAA

Primer for checking the indels of the PCR product:

ID	Sequences (5’ -> 3’)
Human U6	ACTATCATATGCTTACCGTAAC

Primer for qPCR analysis:

Gene symbol	Forward Primer 5’->3’	Reverse Primer5’->3’
RanBP6 (mouse)	ATGATGACTGGGTAAATGCTGA	CCAAGTCCACAAGCCAGTCT
EGFR (human)	AGTCGGGCTCTGGAGGAAA	ACATCCTCTGGAGGCTGAGA
STAT3 (human)	CAGGAGGGAGCTGTATCAGG	AGGACTTGGGCACAGAAGC
PTGS2 (human)	AGGGATTTTGGAACGTTGTG	GAGAAGGCTTCCCAGCTTTT
MAFF (human)	AGCGGAGGGGAGACTGAC	CACAGACATGTTTGCAGAAGG
EFNB2 (human)	TCTTTGGAGGGCCTGGAT	GATCCAGCAGAACTTGCATCT
ITIF (human)	AGAACGGCTGCCTAATTTACAG	GCTCCAGACTATCCTTGACCTG
CPS1 (human)	CAAGTTTTGCAGTGGAATCG	ACTGGGTAGCCAATGGTGTC
HPRT (human)	GGCCAGACTTTGTTGGATTTG	TGCGCTCATCTTAGGCTTTGT

Primer for Chip analysis

ID	Forward Primer 5’->3’	Reverse Primer5’->3’
EGFR_ STAT3_1	CAACGCACAGTGGCTGTACT	CCCTTTGCTGTCTCTGAAGG
EGFR_ STAT3_2	TTGGCTCGACCTGGACATAG	GAGGGAGGAGAACCAGCAG
PTGS2_ STAT3_1	AACCTTACTCGCCCCAGTCT	CCGCCAGATGTCTTTTCTTC
HPRT	CGGTAGGTTTGGGAATCA	CAGTTTGCAGGCTCACTA

APPENDIX C

LIST OF FIGURES CREATED BY OTHERS

BIBLIOGRAPHY

Abe, N., Inoue, T., Galvez, T., Klein, L., and Meyer, T. (2008). Dissecting the role of PtdIns(4,5)P2 in endocytosis and recycling of the transferrin receptor. J Cell Sci *121*, 1488-1494.

Anastasi, S., Lamberti, D., Alema, S., and Segatto, O. (2016). Regulation of the ErbB network by the MIG6 feedback loop in physiology, tumor suppression and responses to oncogene-targeted therapeutics. Semin Cell Dev Biol *50*, 115-124.

Anastasi, S., Sala, G., Huiping, C., Caprini, E., Russo, G., Iacovelli, S., Lucini, F., Ingvarsson, S., and Segatto, O. (2005). Loss of RALT/MIG-6 expression in ERBB2-amplified breast carcinomas enhances ErbB-2 oncogenic potency and favors resistance to Herceptin. Oncogene *24*, 4540-4548.

Ardito, C.M., Gruner, B.M., Takeuchi, K.K., Lubeseder-Martellato, C., Teichmann, N., Mazur, P.K., Delgiorno, K.E., Carpenter, E.S., Halbrook, C.J., Hall, J.C.*, et al.* (2012). EGF receptor is required for KRAS-induced pancreatic tumorigenesis. Cancer Cell *22*, 304-317.

Avraham, R., and Yarden, Y. (2011). Feedback regulation of EGFR signalling: decision making by early and delayed loops. Nat Rev Mol Cell Biol *12*, 104-117.

Barretina, J., Caponigro, G., Stransky, N., Venkatesan, K., Margolin, A.A., Kim, S., Wilson, C.J., Lehar, J., Kryukov, G.V., Sonkin, D.*, et al.* (2012). The Cancer Cell Line Encyclopedia enables predictive modelling of anticancer drug sensitivity. Nature *483*, 603-607.

Beg, A.A., Ruben, S.M., Scheinman, R.I., Haskill, S., Rosen, C.A., and Baldwin, A.S., Jr. (1992). I kappa B interacts with the nuclear localization sequences of the subunits of NF-kappa B: a mechanism for cytoplasmic retention. Genes Dev *6*, 1899-1913.

Bild, A.H., Turkson, J., and Jove, R. (2002). Cytoplasmic transport of Stat3 by receptor-mediated endocytosis. EMBO J *21*, 3255-3263.

Bischoff, F.R., and Ponstingl, H. (1991). Catalysis of guanine nucleotide exchange on Ran by the mitotic regulator RCC1. Nature *354*, 80-82.

Boj, S.F., Hwang, C.I., Baker, L.A., Chio, II, Engle, D.D., Corbo, V., Jager, M., Ponz-Sarvise, M., Tiriac, H., Spector, M.S.*, et al.* (2015). Organoid models of human and mouse ductal pancreatic cancer. Cell *160*, 324-338.

Brankatschk, B., Wichert, S.P., Johnson, S.D., Schaad, O., Rossner, M.J., and Gruenberg, J. (2012). Regulation of the EGF transcriptional response by endocytic sorting. Sci Signal *5*, ra21.

Breit, M.N., Kisseberth, W.C., Bear, M.D., Landesman, Y., Kashyap, T., McCauley, D., Kauffman, M.G., Shacham, S., and London, C.A. (2014). Biologic activity of the novel orally bioavailable selective inhibitor of nuclear export (SINE) KPT-335 against canine melanoma cell lines. BMC Vet Res *10*, 160.

Burgess, A.W., Cho, H.S., Eigenbrot, C., Ferguson, K.M., Garrett, T.P., Leahy, D.J., Lemmon, M.A., Sliwkowski, M.X., Ward, C.W., and Yokoyama, S. (2003). An open-and-shut case? Recent insights into the activation of EGF/ErbB receptors. Mol Cell *12*, 541-552.

Cerami, E., Gao, J., Dogrusoz, U., Gross, B.E., Sumer, S.O., Aksoy, B.A., Jacobsen, A., Byrne, C.J., Heuer, M.L., Larsson, E.*, et al.* (2012). The cBio cancer genomics portal: an open platform for exploring multidimensional cancer genomics data. Cancer Discov *2*, 401-404.

Chalhoub, N., and Baker, S.J. (2009). PTEN and the PI3-kinase pathway in cancer. Annu Rev Pathol *4*, 127-150.

Chen, L.F., and Greene, W.C. (2003). Regulation of distinct biological activities of the NF-kappaB transcription factor complex by acetylation. J Mol Med (Berl) *81*, 549-557.

Cheng, Y., Holloway, M.P., Nguyen, K., McCauley, D., Landesman, Y., Kauffman, M.G., Shacham, S., and Altura, R.A. (2014). XPO1 (CRM1) inhibition represses STAT3 activation to drive a survivin-dependent oncogenic switch in triple-negative breast cancer. Mol Cancer Ther *13*, 675-686.

Chook, Y.M., and Blobel, G. (2001). Karyopherins and nuclear import. Curr Opin Struct Biol *11*, 703-715.

Chuderland, D., Konson, A., and Seger, R. (2008). Identification and characterization of a general nuclear translocation signal in signaling proteins. Mol Cell *31*, 850-861.

Cimica, V., Chen, H.C., Iyer, J.K., and Reich, N.C. (2011). Dynamics of the STAT3 transcription factor: nuclear import dependent on Ran and importin-beta1. PLoS One *6*, e20188.

Cingolani, G., Petosa, C., Weis, K., and Muller, C.W. (1999). Structure of importin-beta bound to the IBB domain of importin-alpha. Nature *399*, 221-229.

Couto, J.P., Daly, L., Almeida, A., Knauf, J.A., Fagin, J.A., Sobrinho-Simoes, M., Lima, J., Maximo, V., Soares, P., Lyden, D.*, et al.* (2012). STAT3 negatively regulates thyroid tumorigenesis. Proc Natl Acad Sci U S A *109*, E2361-2370.

Cross, D.A., Alessi, D.R., Cohen, P., Andjelkovich, M., and Hemmings, B.A. (1995). Inhibition of glycogen synthase kinase-3 by insulin mediated by protein kinase B. Nature *378*, 785-789.

Dan, H.C., Cooper, M.J., Cogswell, P.C., Duncan, J.A., Ting, J.P., and Baldwin, A.S. (2008). Akt-dependent regulation of NF-{kappa}B is controlled by mTOR and Raptor in association with IKK. Genes Dev *22*, 1490-1500.

Datta, S.R., Dudek, H., Tao, X., Masters, S., Fu, H., Gotoh, Y., and Greenberg, M.E. (1997). Akt phosphorylation of BAD couples survival signals to the cell-intrinsic death machinery. Cell *91*, 231-241.

De Cesare, M., Cominetti, D., Doldi, V., Lopergolo, A., Deraco, M., Gandellini, P., Friedlander, S., Landesman, Y., Kauffman, M.G., Shacham, S.*, et al.* (2015). Anti-tumor activity of selective inhibitors of XPO1/CRM1-mediated nuclear export in diffuse malignant peritoneal mesothelioma: the role of survivin. Oncotarget *6*, 13119-13132.

de la Iglesia, N., Konopka, G., Lim, K.L., Nutt, C.L., Bromberg, J.F., Frank, D.A., Mischel, P.S., Louis, D.N., and Bonni, A. (2008a). Deregulation of a STAT3-interleukin 8 signaling pathway promotes human glioblastoma cell proliferation and invasiveness. J Neurosci *28*, 5870-5878.

de la Iglesia, N., Konopka, G., Puram, S.V., Chan, J.A., Bachoo, R.M., You, M.J., Levy, D.E., Depinho, R.A., and Bonni, A. (2008b). Identification of a PTEN-regulated STAT3 brain tumor suppressor pathway. Genes Dev *22*, 449-462.

Demory, M.L., Boerner, J.L., Davidson, R., Faust, W., Miyake, T., Lee, I., Huttemann, M., Douglas, R., Haddad, G., and Parsons, S.J. (2009). Epidermal growth factor receptor translocation to the mitochondria: regulation and effect. J Biol Chem *284*, 36592-36604.

Dougherty, M.K., Muller, J., Ritt, D.A., Zhou, M., Zhou, X.Z., Copeland, T.D., Conrads, T.P., Veenstra, T.D., Lu, K.P., and Morrison, D.K. (2005). Regulation of Raf-1 by direct feedback phosphorylation. Mol Cell *17*, 215-224.

Douville, E., and Downward, J. (1997). EGF induced SOS phosphorylation in PC12 cells involves P90 RSK-2. Oncogene *15*, 373-383.

Ekstrand, A.J., Sugawa, N., James, C.D., and Collins, V.P. (1992). Amplified and rearranged epidermal growth factor receptor genes in human glioblastomas reveal

deletions of sequences encoding portions of the N- and/or C-terminal tails. Proc Natl Acad Sci U S A *89*, 4309-4313.

Fahrenkrog, B., and Aebi, U. (2003). The nuclear pore complex: nucleocytoplasmic transport and beyond. Nat Rev Mol Cell Biol *4*, 757-766.

Fan, Q.W., Cheng, C.K., Gustafson, W.C., Charron, E., Zipper, P., Wong, R.A., Chen, J., Lau, J., Knobbe-Thomsen, C., Weller, M.*, et al.* (2013). EGFR phosphorylates tumor-derived EGFRvIII driving STAT3/5 and progression in glioblastoma. Cancer Cell *24*, 438-449.

Ferby, I., Reschke, M., Kudlacek, O., Knyazev, P., Pante, G., Amann, K., Sommergruber, W., Kraut, N., Ullrich, A., Fassler, R.*, et al.* (2006). Mig6 is a negative regulator of EGF receptor-mediated skin morphogenesis and tumor formation. Nat Med *12*, 568-573.

Flores, K., and Seger, R. (2013). Stimulated nuclear import by beta-like importins. F1000Prime Rep *5*, 41.

Foerster, S., Kacprowski, T., Dhople, V.M., Hammer, E., Herzog, S., Saafan, H., Bien-Moller, S., Albrecht, M., Volker, U., and Ritter, C.A. (2013). Characterization of the EGFR interactome reveals associated protein complex networks and intracellular receptor dynamics. Proteomics *13*, 3131-3144.

Freedman, N.D., and Yamamoto, K.R. (2004). Importin 7 and importin alpha/importin beta are nuclear import receptors for the glucocorticoid receptor. Mol Biol Cell *15*, 2276-2286.

Ganchi, P.A., Sun, S.C., Greene, W.C., and Ballard, D.W. (1992). I kappa B/MAD-3 masks the nuclear localization signal of NF-kappa B p65 and requires the transactivation domain to inhibit NF-kappa B p65 DNA binding. Mol Biol Cell *3*, 1339-1352.

Gao, S.P., Chang, Q., Mao, N., Daly, L.A., Vogel, R., Chan, T., Liu, S.H., Bournazou, E., Schori, E., Zhang, H.*, et al.* (2016). JAK2 inhibition sensitizes resistant EGFR-mutant lung adenocarcinoma to tyrosine kinase inhibitors. Sci Signal *9*, ra33.

Gorlich, D. (1997). Nuclear protein import. Curr Opin Cell Biol *9*, 412-419.

Gorlich, D., and Kutay, U. (1999). Transport between the cell nucleus and the cytoplasm. Annu Rev Cell Dev Biol *15*, 607-660.

Gorlich, D., and Mattaj, I.W. (1996). Nucleocytoplasmic transport. Science *271*, 1513-1518.

Green, A.L., Ramkissoon, S.H., McCauley, D., Jones, K., Perry, J.A., Hsu, J.H., Ramkissoon, L.A., Maire, C.L., Hubbell-Engler, B., Knoff, D.S.*, et al.* (2015). Preclinical antitumor efficacy of selective exportin 1 inhibitors in glioblastoma. Neuro Oncol *17*, 697-707.

Guttinger, S., Muhlhausser, P., Koller-Eichhorn, R., Brennecke, J., and Kutay, U. (2004). Transportin2 functions as importin and mediates nuclear import of HuR. Proc Natl Acad Sci U S A *101*, 2918-2923.

Hanson, P.I., Shim, S., and Merrill, S.A. (2009). Cell biology of the ESCRT machinery. Curr Opin Cell Biol *21*, 568-574.

Heideman, M.R., and Hynes, N.E. (2013). AXL/epidermal growth factor receptor (EGFR) complexes in breast cancer--culprits for resistance to EGFR inhibitors? Breast Cancer Res *15*, 315.

Henkel, T., Zabel, U., van Zee, K., Muller, J.M., Fanning, E., and Baeuerle, P.A. (1992). Intramolecular masking of the nuclear location signal and dimerization domain in the precursor for the p50 NF-kappa B subunit. Cell *68*, 1121-1133.

Hetzer, M., Bilbao-Cortes, D., Walther, T.C., Gruss, O.J., and Mattaj, I.W. (2000). GTP hydrolysis by Ran is required for nuclear envelope assembly. Mol Cell *5*, 1013-1024.

Hiles, I.D., Otsu, M., Volinia, S., Fry, M.J., Gout, I., Dhand, R., Panayotou, G., Ruiz-Larrea, F., Thompson, A., Totty, N.F., *et al.* (1992). Phosphatidylinositol 3-kinase: structure and expression of the 110 kd catalytic subunit. Cell *70*, 419-429.

Hofmann, K., and Falquet, L. (2001). A ubiquitin-interacting motif conserved in components of the proteasomal and lysosomal protein degradation systems. Trends Biochem Sci *26*, 347-350.

Horak, E., Smith, K., Bromley, L., LeJeune, S., Greenall, M., Lane, D., and Harris, A.L. (1991). Mutant p53, EGF receptor and c-erbB-2 expression in human breast cancer. Oncogene *6*, 2277-2284.

Hsu, S.C., and Hung, M.C. (2007). Characterization of a novel tripartite nuclear localization sequence in the EGFR family. J Biol Chem *282*, 10432-10440.

Huang, F., Kirkpatrick, D., Jiang, X., Gygi, S., and Sorkin, A. (2006). Differential regulation of EGF receptor internalization and degradation by multiubiquitination within the kinase domain. Mol Cell *21*, 737-748.

Hynes, N.E., and Lane, H.A. (2005). ERBB receptors and cancer: the complexity of targeted inhibitors. Nat Rev Cancer *5*, 341-354.

Isaacs, J.S., Hardman, R., Carman, T.A., Barrett, J.C., and Weissman, B.E. (1998). Differential subcellular p53 localization and function in N- and S-type neuroblastoma cell lines. Cell Growth Differ *9*, 545-555.

Itzhak, D.N., Tyanova, S., Cox, J., and Borner, G.H. (2016). Global, quantitative and dynamic mapping of protein subcellular localization. Elife *5*.

Jakel, S., Albig, W., Kutay, U., Bischoff, F.R., Schwamborn, K., Doenecke, D., and Gorlich, D. (1999). The importin beta/importin 7 heterodimer is a functional nuclear import receptor for histone H1. EMBO J *18*, 2411-2423.

Jakel, S., and Gorlich, D. (1998). Importin beta, transportin, RanBP5 and RanBP7 mediate nuclear import of ribosomal proteins in mammalian cells. EMBO J *17*, 4491-4502.

Jiang, X., Huang, F., Marusyk, A., and Sorkin, A. (2003). Grb2 regulates internalization of EGF receptors through clathrin-coated pits. Mol Biol Cell *14*, 858-870.

Jiang, X., and Sorkin, A. (2003). Epidermal growth factor receptor internalization through clathrin-coated pits requires Cbl RING finger and proline-rich domains but not receptor polyubiquitylation. Traffic *4*, 529-543.

Kalab, P., Pu, R.T., and Dasso, M. (1999). The ran GTPase regulates mitotic spindle assembly. Curr Biol *9*, 481-484.

Kau, T.R., Way, J.C., and Silver, P.A. (2004). Nuclear transport and cancer: from mechanism to intervention. Nat Rev Cancer *4*, 106-117.

Kimura, M., Kose, S., Okumura, N., Imai, K., Furuta, M., Sakiyama, N., Tomii, K., Horton, P., Takao, T., and Imamoto, N. (2013a). Identification of cargo proteins specific for the nucleocytoplasmic transport carrier transportin by combination of an in vitro transport system and stable isotope labeling by amino acids in cell culture (SILAC)-based quantitative proteomics. Mol Cell Proteomics *12*, 145-157.

Kimura, M., Morinaka, Y., Imai, K., Kose, S., Horton, P., and Imamoto, N. (2017). Extensive cargo identification reveals distinct biological roles of the 12 importin pathways. Elife *6*.

Kimura, M., Okumura, N., Kose, S., Takao, T., and Imamoto, N. (2013b). Identification of cargo proteins specific for importin-beta with importin-alpha applying a stable isotope labeling by amino acids in cell culture (SILAC)-based in vitro transport system. J Biol Chem *288*, 24540-24549.

Kirli, K., Karaca, S., Dehne, H.J., Samwer, M., Pan, K.T., Lenz, C., Urlaub, H., and Gorlich, D. (2015). A deep proteomics perspective on CRM1-mediated nuclear export and nucleocytoplasmic partitioning. Elife *4*.

Kudo, N., Matsumori, N., Taoka, H., Fujiwara, D., Schreiner, E.P., Wolff, B., Yoshida, M., and Horinouchi, S. (1999). Leptomycin B inactivates CRM1/exportin 1 by covalent modification at a cysteine residue in the central conserved region. Proc Natl Acad Sci U S A *96*, 9112-9117.

Kutay, U., Hartmann, E., Treichel, N., Calado, A., Carmo-Fonseca, M., Prehn, S., Kraft, R., Gorlich, D., and Bischoff, F.R. (2000). Identification of two novel RanGTP-binding proteins belonging to the importin beta superfamily. J Biol Chem *275*, 40163-40168.

Lee, J., Kim, J.C., Lee, S.E., Quinley, C., Kim, H., Herdman, S., Corr, M., and Raz, E. (2012). Signal transducer and activator of transcription 3 (STAT3) protein suppresses adenoma-to-carcinoma transition in Apcmin/+ mice via regulation of Snail-1 (SNAI) protein stability. J Biol Chem *287*, 18182-18189.

Leevers, S.J., and Marshall, C.J. (1992). Activation of extracellular signal-regulated kinase, ERK2, by p21ras oncoprotein. EMBO J *11*, 569-574.

Lemmon, M.A., Schlessinger, J., and Ferguson, K.M. (2014). The EGFR family: not so prototypical receptor tyrosine kinases. Cold Spring Harb Perspect Biol *6*, a020768.

Leong, P.L., Andrews, G.A., Johnson, D.E., Dyer, K.F., Xi, S., Mai, J.C., Robbins, P.D., Gadiparthi, S., Burke, N.A., Watkins, S.F*., et al.* (2003). Targeted inhibition of Stat3 with a decoy oligonucleotide abrogates head and neck cancer cell growth. Proc Natl Acad Sci U S A *100*, 4138-4143.

Liao, H.J., and Carpenter, G. (2007). Role of the Sec61 translocon in EGF receptor trafficking to the nucleus and gene expression. Mol Biol Cell *18*, 1064-1072.

Lin, J.R., Fallahi-Sichani, M., and Sorger, P.K. (2015). Highly multiplexed imaging of single cells using a high-throughput cyclic immunofluorescence method. Nat Commun *6*, 8390.

Lin, S.Y., Makino, K., Xia, W., Matin, A., Wen, Y., Kwong, K.Y., Bourguignon, L., and Hung, M.C. (2001). Nuclear localization of EGF receptor and its potential new role as a transcription factor. Nat Cell Biol *3*, 802-808.

Lito, P., Pratilas, C.A., Joseph, E.W., Tadi, M., Halilovic, E., Zubrowski, M., Huang, A., Wong, W.L., Callahan, M.K., Merghoub, T.*, et al.* (2012). Relief of profound feedback inhibition of mitogenic signaling by RAF inhibitors attenuates their activity in BRAFV600E melanomas. Cancer Cell *22*, 668-682.

Liu, X., Chong, Y., Tu, Y., Liu, N., Yue, C., Qi, Z., Liu, H., Yao, Y., Liu, H., Gao, S.*, et al.* (2016). CRM1/XPO1 is associated with clinical outcome in glioma and represents a therapeutic target by perturbing multiple core pathways. J Hematol Oncol *9*, 108.

Lo, H.W., Hsu, S.C., Ali-Seyed, M., Gunduz, M., Xia, W., Wei, Y., Bartholomeusz, G., Shih, J.Y., and Hung, M.C. (2005). Nuclear interaction of EGFR and STAT3 in the activation of the iNOS/NO pathway. Cancer Cell *7*, 575-589.

Lo, H.W., Hsu, S.C., and Hung, M.C. (2006). EGFR signaling pathway in breast cancers: from traditional signal transduction to direct nuclear translocalization. Breast Cancer Res Treat *95*, 211-218.

Longva, K.E., Blystad, F.D., Stang, E., Larsen, A.M., Johannessen, L.E., and Madshus, I.H. (2002). Ubiquitination and proteasomal activity is required for transport of the EGF receptor to inner membranes of multivesicular bodies. J Cell Biol *156*, 843-854.

Lu, W., Pochampally, R., Chen, L., Traidej, M., Wang, Y., and Chen, J. (2000). Nuclear exclusion of p53 in a subset of tumors requires MDM2 function. Oncogene *19*, 232-240.

Ma, X.M., and Blenis, J. (2009). Molecular mechanisms of mTOR-mediated translational control. Nat Rev Mol Cell Biol *10*, 307-318.

Madshus, I.H., and Stang, E. (2009). Internalization and intracellular sorting of the EGF receptor: a model for understanding the mechanisms of receptor trafficking. J Cell Sci *122*, 3433-3439.

Maehama, T., and Dixon, J.E. (1998). The tumor suppressor, PTEN/MMAC1, dephosphorylates the lipid second messenger, phosphatidylinositol 3,4,5-trisphosphate. J Biol Chem *273*, 13375-13378.

Maity, T.K., Venugopalan, A., Linnoila, I., Cultraro, C.M., Giannakou, A., Nemati, R., Zhang, X., Webster, J.D., Ritt, D., Ghosal, S.*, et al.* (2015). Loss of MIG6 Accelerates Initiation and Progression of Mutant Epidermal Growth Factor Receptor-Driven Lung Adenocarcinoma. Cancer Discov *5*, 534-549.

Manning, B.D., and Cantley, L.C. (2007). AKT/PKB signaling: navigating downstream. Cell *129*, 1261-1274.

Mathelier, A., Fornes, O., Arenillas, D.J., Chen, C.Y., Denay, G., Lee, J., Shi, W., Shyr, C., Tan, G., Worsley-Hunt, R.*, et al.* (2016). JASPAR 2016: a major expansion and update of the open-access database of transcription factor binding profiles. Nucleic Acids Res *44*, D110-115.

Matsuzaki, H., Daitoku, H., Hatta, M., Tanaka, K., and Fukamizu, A. (2003). Insulin-induced phosphorylation of FKHR (Foxo1) targets to proteasomal degradation. Proc Natl Acad Sci U S A *100*, 11285-11290.

Mellinghoff, I.K., Wang, M.Y., Vivanco, I., Haas-Kogan, D.A., Zhu, S., Dia, E.Q., Lu, K.V., Yoshimoto, K., Huang, J.H., Chute, D.J.*, et al.* (2005). Molecular

determinants of the response of glioblastomas to EGFR kinase inhibitors. N Engl J Med *353*, 2012-2024.

Meyer, A.S., Miller, M.A., Gertler, F.B., and Lauffenburger, D.A. (2013). The receptor AXL diversifies EGFR signaling and limits the response to EGFR-targeted inhibitors in triple-negative breast cancer cells. Sci Signal *6*, ra66.

Mingot, J.M., Bohnsack, M.T., Jakle, U., and Gorlich, D. (2004). Exportin 7 defines a novel general nuclear export pathway. EMBO J *23*, 3227-3236.

Mingot, J.M., Kostka, S., Kraft, R., Hartmann, E., and Gorlich, D. (2001). Importin 13: a novel mediator of nuclear import and export. EMBO J *20*, 3685-3694.

Moll, U.M., LaQuaglia, M., Benard, J., and Riou, G. (1995). Wild-type p53 protein undergoes cytoplasmic sequestration in undifferentiated neuroblastomas but not in differentiated tumors. Proc Natl Acad Sci U S A *92*, 4407-4411.

Moll, U.M., Riou, G., and Levine, A.J. (1992). Two distinct mechanisms alter p53 in breast cancer: mutation and nuclear exclusion. Proc Natl Acad Sci U S A *89*, 7262-7266.

Moodie, S.A., Willumsen, B.M., Weber, M.J., and Wolfman, A. (1993). Complexes of Ras.GTP with Raf-1 and mitogen-activated protein kinase kinase. Science *260*, 1658-1661.

Musteanu, M., Blaas, L., Mair, M., Schlederer, M., Bilban, M., Tauber, S., Esterbauer, H., Mueller, M., Casanova, E., Kenner, L.*, et al.* (2010). Stat3 is a negative regulator of intestinal tumor progression in Apc(Min) mice. Gastroenterology *138*, 1003-1011 e1001-1005.

Navas, C., Hernandez-Porras, I., Schuhmacher, A.J., Sibilia, M., Guerra, C., and Barbacid, M. (2012). EGF receptor signaling is essential for k-ras oncogene-driven pancreatic ductal adenocarcinoma. Cancer Cell *22*, 318-330.

Newlands, E.S., Rustin, G.J., and Brampton, M.H. (1996). Phase I trial of elactocin. Br J Cancer *74*, 648-649.

Ogawara, Y., Kishishita, S., Obata, T., Isazawa, Y., Suzuki, T., Tanaka, K., Masuyama, N., and Gotoh, Y. (2002). Akt enhances Mdm2-mediated ubiquitination and degradation of p53. J Biol Chem *277*, 21843-21850.

Parikh, K., Cang, S., Sekhri, A., and Liu, D. (2014). Selective inhibitors of nuclear export (SINE)--a novel class of anti-cancer agents. J Hematol Oncol *7*, 78.

Park, E., Kim, N., Ficarro, S.B., Zhang, Y., Lee, B.I., Cho, A., Kim, K., Park, A.K.J., Park, W.Y., Murray, B.*, et al.* (2015). Structure and mechanism of activity-based inhibition of the EGF receptor by Mig6. Nat Struct Mol Biol *22*, 703-711.

Perera, R.M., and Bardeesy, N. (2012). Ready, set, go: the EGF receptor at the pancreatic cancer starting line. Cancer Cell *22*, 281-282.

Perkins, N.D. (2000). The Rel/NF-kappa B family: friend and foe. Trends Biochem Sci *25*, 434-440.

Rayet, B., and Gelinas, C. (1999). Aberrant rel/nfkb genes and activity in human cancer. Oncogene *18*, 6938-6947.

Rodriguez-Viciana, P., Warne, P.H., Dhand, R., Vanhaesebroeck, B., Gout, I., Fry, M.J., Waterfield, M.D., and Downward, J. (1994). Phosphatidylinositol-3-OH kinase as a direct target of Ras. Nature *370*, 527-532.

Ryan, K.M., Phillips, A.C., and Vousden, K.H. (2001). Regulation and function of the p53 tumor suppressor protein. Curr Opin Cell Biol *13*, 332-337.

Scaltriti, M., and Baselga, J. (2006). The epidermal growth factor receptor pathway: a model for targeted therapy. Clin Cancer Res *12*, 5268-5272.

Sengupta, S., Peterson, T.R., and Sabatini, D.M. (2010). Regulation of the mTOR complex 1 pathway by nutrients, growth factors, and stress. Mol Cell *40*, 310-322.

Song, H., Wang, R., Wang, S., and Lin, J. (2005). A low-molecular-weight compound discovered through virtual database screening inhibits Stat3 function in breast cancer cells. Proc Natl Acad Sci U S A *102*, 4700-4705.

Soucek, L., and Evan, G.I. (2010). The ups and downs of Myc biology. Curr Opin Genet Dev *20*, 91-95.

Sousa, L.P., Lax, I., Shen, H., Ferguson, S.M., De Camilli, P., and Schlessinger, J. (2012). Suppression of EGFR endocytosis by dynamin depletion reveals that EGFR signaling occurs primarily at the plasma membrane. Proc Natl Acad Sci U S A *109*, 4419-4424.

Squatrito, M., Brennan, C.W., Helmy, K., Huse, J.T., Petrini, J.H., and Holland, E.C. (2010). Loss of ATM/Chk2/p53 pathway components accelerates tumor development and contributes to radiation resistance in gliomas. Cancer Cell *18*, 619-629.

Stang, E., Blystad, F.D., Kazazic, M., Bertelsen, V., Brodahl, T., Raiborg, C., Stenmark, H., and Madshus, I.H. (2004). Cbl-dependent ubiquitination is required for progression of EGF receptors into clathrin-coated pits. Mol Biol Cell *15*, 3591-3604.

Stokoe, D., Macdonald, S.G., Cadwallader, K., Symons, M., and Hancock, J.F. (1994). Activation of Raf as a result of recruitment to the plasma membrane. Science *264*, 1463-1467.

Strom, A.C., and Weis, K. (2001). Importin-beta-like nuclear transport receptors. Genome Biol *2*, REVIEWS3008.

Sun, Q., Carrasco, Y.P., Hu, Y., Guo, X., Mirzaei, H., Macmillan, J., and Chook, Y.M. (2013). Nuclear export inhibition through covalent conjugation and hydrolysis of Leptomycin B by CRM1. Proc Natl Acad Sci U S A *110*, 1303-1308.

Sun, Q., Chen, X., Zhou, Q., Burstein, E., Yang, S., and Jia, D. (2016). Inhibiting cancer cell hallmark features through nuclear export inhibition. Signal Transduct Target Ther *1*, 16010.

Sun, Y., Carroll, S., Kaksonen, M., Toshima, J.Y., and Drubin, D.G. (2007). PtdIns(4,5)P2 turnover is required for multiple stages during clathrin- and actin-dependent endocytic internalization. J Cell Biol *177*, 355-367.

Tebar, F., Sorkina, T., Sorkin, A., Ericsson, M., and Kirchhausen, T. (1996). Eps15 is a component of clathrin-coated pits and vesicles and is located at the rim of coated pits. J Biol Chem *271*, 28727-28730.

Thul, P.J., Akesson, L., Wiking, M., Mahdessian, D., Geladaki, A., Ait Blal, H., Alm, T., Asplund, A., Bjork, L., Breckels, L.M.*, et al.* (2017). A subcellular map of the human proteome. Science *356*.

Vetter, I.R., Arndt, A., Kutay, U., Gorlich, D., and Wittinghofer, A. (1999). Structural view of the Ran-Importin beta interaction at 2.3 A resolution. Cell *97*, 635-646.

Vivanco, I., and Mellinghoff, I.K. (2010). Epidermal growth factor receptor inhibitors in oncology. Curr Opin Oncol *22*, 573-578.

Vivanco, I., Rohle, D., Versele, M., Iwanami, A., Kuga, D., Oldrini, B., Tanaka, K., Dang, J., Kubek, S., Palaskas, N.*, et al.* (2010). The phosphatase and tensin homolog regulates epidermal growth factor receptor (EGFR) inhibitor response by targeting EGFR for degradation. Proc Natl Acad Sci U S A *107*, 6459-6464.

Vojtek, A.B., Hollenberg, S.M., and Cooper, J.A. (1993). Mammalian Ras interacts directly with the serine/threonine kinase Raf. Cell *74*, 205-214.

Vouri, M., Croucher, D.R., Kennedy, S.P., An, Q., Pilkington, G.J., and Hafizi, S. (2016). Axl-EGFR receptor tyrosine kinase hetero-interaction provides EGFR with access to pro-invasive signalling in cancer cells. Oncogenesis *5*, e266.

Wagner, M.J., Stacey, M.M., Liu, B.A., and Pawson, T. (2013). Molecular mechanisms of SH2- and PTB-domain-containing proteins in receptor tyrosine kinase signaling. Cold Spring Harb Perspect Biol *5*, a008987.

Waldmann, I., Walde, S., and Kehlenbach, R.H. (2007). Nuclear import of c-Jun is mediated by multiple transport receptors. J Biol Chem *282*, 27685-27692.

Wang, Y.N., Yamaguchi, H., Huo, L., Du, Y., Lee, H.J., Lee, H.H., Wang, H., Hsu, J.M., and Hung, M.C. (2010). The translocon Sec61beta localized in the inner nuclear membrane transports membrane-embedded EGF receptor to the nucleus. J Biol Chem *285*, 38720-38729.

Warne, P.H., Viciana, P.R., and Downward, J. (1993). Direct interaction of Ras and the amino-terminal region of Raf-1 in vitro. Nature *364*, 352-355.

Waterman, H., and Yarden, Y. (2001). Molecular mechanisms underlying endocytosis and sorting of ErbB receptor tyrosine kinases. FEBS Lett *490*, 142-152.

Whitman, M., Downes, C.P., Keeler, M., Keller, T., and Cantley, L. (1988). Type I phosphatidylinositol kinase makes a novel inositol phospholipid, phosphatidylinositol-3-phosphate. Nature *332*, 644-646.

Wood, K.W., Sarnecki, C., Roberts, T.M., and Blenis, J. (1992). ras mediates nerve growth factor receptor modulation of three signal-transducing protein kinases: MAP kinase, Raf-1, and RSK. Cell *68*, 1041-1050.

Yao, X., Chen, X., Cottonham, C., and Xu, L. (2008). Preferential utilization of Imp7/8 in nuclear import of Smads. J Biol Chem *283*, 22867-22874.

Yarden, Y., and Sliwkowski, M.X. (2001). Untangling the ErbB signalling network. Nat Rev Mol Cell Biol *2*, 127-137.

Yewale, C., Baradia, D., Vhora, I., Patil, S., and Misra, A. (2013). Epidermal growth factor receptor targeting in cancer: a review of trends and strategies. Biomaterials *34*, 8690-8707.

Yordy, J.S., and Muise-Helmericks, R.C. (2000). Signal transduction and the Ets family of transcription factors. Oncogene *19*, 6503-6513.

Zhang, C., and Clarke, P.R. (2000). Chromatin-independent nuclear envelope assembly induced by Ran GTPase in Xenopus egg extracts. Science *288*, 1429-1432.

Zhang, X., Gureasko, J., Shen, K., Cole, P.A., and Kuriyan, J. (2006). An allosteric mechanism for activation of the kinase domain of epidermal growth factor receptor. Cell *125*, 1137-1149.

Zhang, X., Pickin, K.A., Bose, R., Jura, N., Cole, P.A., and Kuriyan, J. (2007a). Inhibition of the EGF receptor by binding of MIG6 to an activating kinase domain interface. Nature *450*, 741-744.

Zhang, X.F., Settleman, J., Kyriakis, J.M., Takeuchi-Suzuki, E., Elledge, S.J., Marshall, M.S., Bruder, J.T., Rapp, U.R., and Avruch, J. (1993). Normal and oncogenic p21ras proteins bind to the amino-terminal regulatory domain of c-Raf-1. Nature *364*, 308-313.

Zhang, Y.W., Staal, B., Su, Y., Swiatek, P., Zhao, P., Cao, B., Resau, J., Sigler, R., Bronson, R., and Vande Woude, G.F. (2007b). Evidence that MIG-6 is a tumor-suppressor gene. Oncogene *26*, 269-276.